From 2D to 1D homodecoupled high-resolution proton NMR

Cotte, Axelle

UNIVERSITÉ DE GENÈVE
FACULTÉ DES SCIENCES

Section de chimie et biochimie
Département de chimie organique

Dr. Damien Jeannerat

From 2D to 1D Homodecoupled High-Resolution Proton NMR

THÈSE

présentée à la Faculté des sciences de l'Université de Genève
pour obtenir le grade de Docteur ès sciences, mention chimie

par

Axelle COTTE

de

Rosny-sous-Bois (France)

Thèse N^{o} 4785

GENÈVE

Défigraph

2015

UNIVERSITÉ
DE GENÈVE

FACULTÉ DES SCIENCES

Doctorat ès sciences
Mention chimie

Thèse de ***Madame Axelle COTTE***

intitulée :

"From 2D to 1D Homodecoupled High-Resolution Proton NMR"

La Faculté des sciences, sur le préavis de Monsieur D. JEANNERAT, docteur et directeur de thèse (Département de chimie organique), Monsieur C. MAZET, professeur associé (Département de chimie organique), Monsieur N. WINSSINGER, professeur ordinaire (Département de chimie organique) et Monsieur N. GIRAUD, professeur associé (Université Paris Sud, Institut de Chimie Moléculaire et des Matériaux d'Orsay, Orsay, France), autorise l'impression de la présente thèse, sans exprimer d'opinion sur les propositions qui y sont énoncées.

Genève, le 28 juin 2015

Thèse - 4785 -

Le Décanat

N.B. - La thèse doit porter la déclaration précédente et remplir les conditions énumérées dans les "Informations relatives aux thèses de doctorat à l'Université de Genève".

You can’t always get what you want,
But if you try sometime, you just might find,
You get what you need.

Mick Jagger & Keith Richards

Acknowledgements

First of all, I would like to thank my supervisor Dr. Damien Jeannerat for giving me the opportunity to carry out my doctoral studies in his group, from the 1st of February 2012 to the 13th of February 2015. This experience has been really instructive. I have discovered a new and important part of the NMR world.

I would like to thank Prof. Clément Mazet, from the University of Geneva, and Dr. Nicolas Giraud, from the University of Orsay, for having accepted to be part of my thesis committee and for the great discussions during the defense. I also would like to thank Prof. Nicolas Winssinger, from the University of Geneva, for his interesting remarks and encouragement during the defense.

I am thankful to Dr. Mohammadali Foroozandeh who supervised and taught me the art of pulse sequence development. Thanks for all these fascinating discussions, your kindness and support during the first year of my Ph. D and the following.

I would like to thank André Pinto, Stéphane Grass, Patrick Romanens and Marion Pupier for technical assistance on spectrometers. With their support, everything is possible, even with whimsical instruments. My thanks also go to the Bruker Biospin team met during my thesis. They worked so hard to allow me to work on the 500 MHz spectrometer in the best possible conditions.

I sincerely thank my task force, Sonya Torche and Sonia Candolfi, for their full support and all these happy times shared at and outside the university.

I am grateful to all people met at the university, for their friendship, their unbelievable stories and encouragements. In particular the fantastic Lacour group with a special mention to Stéphane, Maya, Léo, Alexandre, Joël, Daniele, Romain and Simon: do not change anything, you are awesome!!

A big thank to the New Country Smoking Boots team and in particular to Jacques, Catherine, Jocelyne, Didier and Gwendoline. Thank you for your friendship, smiles and laughs. Without you, these three Genevan years would not have been the same. I really hope this is not the end.

A special thanks to Alexandre without whom this adventure would not have taken place. Thank you so much for believing in me and supporting me all this time despite the distance. I wish you all the best in your own adventure.

Last but not least, a heartfelt thanks to my family for their unwavering support at each step, at each moment of doubt. Thank you so much for all these important and unforgettable moments with enjoyment and entertainment that you offered me in France and in Switzerland.

Abbreviations, Symbols and Units

Abbreviations

1D, 2D:	one dimension, two dimension
BBHD:	BroadBand HomoDecoupled
$CDCl_3$:	Deuterated Chloroform
COSY:	COrrelation SpectroscopY
CT:	Constant Time
D_2O:	Deuterium Oxide
d:	doublet
DIPSI:	Decoupling In the Presence of Scalar Interactions
DW:	DWell time
Expt:	Experimental time
FID:	Free Induction Decay
FM:	Frequency Modulation
FT:	Fourier Transform
HSQC:	Heteronuclear Single Quantum Coherence spectroscopy
m:	multiplet
nemo:	non-equidistant modulation
NMR:	Nuclear Magnetic Resonance
NOESY:	Nuclear Overhauser Effect SpectroscopY
SNR:	Signal to Noise Ratio
SW:	Spectral Width
t:	triplet
TOCSY:	TOtal Correlation SpectroscopY
TPPI:	Time Proportional Phase Incrementation
ZQ:	Zero-Quantum

ZS:	Zangger-Sterk

Symbols

α, β:	spin states
B_0, B_1:	static magnetic field, rotating magnetic field
δ:	related to chemical shift
E:	energy
F1, F2:	indirect dimension, direct dimension
γ:	magnetogyric ratio
G_z:	z-pulsed field gradient
h:	Planck's constant
I:	spin quantum moment
J:	related to scalar coupling
μ:	magnetic moment
ν:	frequency of resonance
ϕ:	pulse or detection phase angle
t_1, t_2:	indirect and direct detection times

Units

h:	hour
Hz, MHz:	Hertz, Megahertz
K:	Kelvin
min:	minute
mg:	milligram
ppm:	parts per million
μs, ms, s:	microsecond, millisecond, second
μL:	microliter

Résumé

La résonance magnétique nucléaire (RMN) est une technique spectroscopique devenue indispensable notamment aux chimistes organiciens. Elle permet d'obtenir des informations essentielles sur la composition, la structure et la dynamique de molécules, qu'elles fassent partie de la gamme des petites molécules ou des macromolécules.

Cependant, l'extraction de ces informations n'est pas toujours des plus aisées. En effet, les spectres RMN proton sont généralement surchargés à cause de la faible dispersion des fréquences de résonance des protons et de la présence de large structure de couplage homonucléaire qui entraîne souvent la superposition des signaux. Des expériences à deux dimensions, permettant une meilleure dispersion des signaux, ont alors été développées, la plus connue étant l'expérience COSY.

Les développements de la spectroscopie RMN conduisant à l'obtention d'informations de plus en plus complexes, il devient indispensable d'augmenter la résolution des spectres. Une approche basée sur l'encodage spatial est ainsi présentée dans ce manuscrit. L'utilisation de l'élément de découplage homonucléaire, développé par Zangger et Sterk en 1997, permet de réduire la multiplicité des signaux enregistrés. Ainsi, les expériences 2D homonucléaires sont découplées dans la dimension indirecte F1 permettant une meilleure séparation des signaux.

L'obtention de spectres proton découplés proton à une dimension représente un défi depuis de nombreuses décennies, la technique ne permettant pas d'observer et de découpler à la fois le même noyau. Ce problème a suscité un regain d'intérêt ces dernières années et de nombreuses méthodes ont été développées. Une nouvelle approche combinant une expérience 2D découplée en F1 et le repliement spectral est proposée ici. La réduction de la fenêtre spectrale en F1 conduit à l'augmentation de la résolution spectrale et à une réduction du temps d'enregistrement de l'expérience d'un facteur pouvant atteindre deux ordres de grandeur. L'application d'un simple programme de traitement permet de transformer le spectre 2D en un spectre 1D où tous les multiplets ont été réduits en singulets.

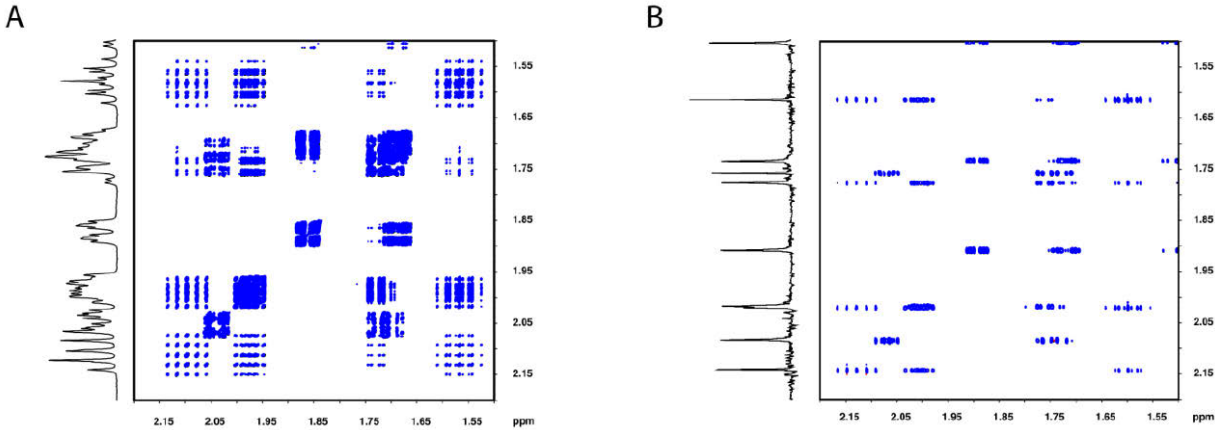

(A) Spectres 1D proton et 2D TOCSY enregistrés à haute-résolution et (B) spectres 1D et 2D homodécouplés

La modulation en fréquences de l'élément Zangger-Sterk a été développée avec succès afin de compenser la faible sensibilité de l'encodage spatial. Une solution permettant l'élimination des artefacts dus à l'irradiation simultanée de spins couplés est introduite grâce à la mise au point de la modulation non-équidistante. Les spectres découplés présentent alors une meilleure sensibilité permettant ainsi leur utilisation en routine.

Abstract

Nuclear magnetic resonance (NMR) is a spectroscopic technique that became essential in particular to organic chemists. It provides key information about the composition, the structure and the dynamic of molecules, whatever the size of molecules (including macromolecules).

However, the extraction of these data is not always easy. Indeed, proton NMR spectra are generally quite complex due to the small dispersion of proton chemical shifts and the existence of extended homonuclear coupling structures often causing signal overlap. Two-dimensional experiments have been developed, leading to a better dispersion of signals, the most known being the COSY experiment.

As development of the NMR methodology leads to more and more complex information, it becomes vital to enhance the resolution of spectra. An approach based on spatial encoding is presented in this manuscript. The use of the homonuclear decoupling element developed by Zangger and Sterk, in 1997, allows to reduce the multiplicity of signals. Thus, 2D homonuclear experiments are decoupled in the indirect F1 dimension providing a better separation of signals.

The obtention of one-dimensional proton-decoupled proton spectra has been a challenge for decades, since the related techniques did not allow to observe and decouple a nucleus at the same time. Recently, this issue has raised a renewing interest and resulted into the development of new decoupling methods. A new approach combining a 2D experiment decoupled in F1 dimension with spectral aliasing is proposed. The reduction of the F1 spectral window allows an enhancement of the spectral resolution and a reduction of the experimental time by a two magnitude order factor. The application of a simple processing program leads to the transformation of a 2D spectrum into a 1D spectrum where all multiplets are collapsed into singlets.

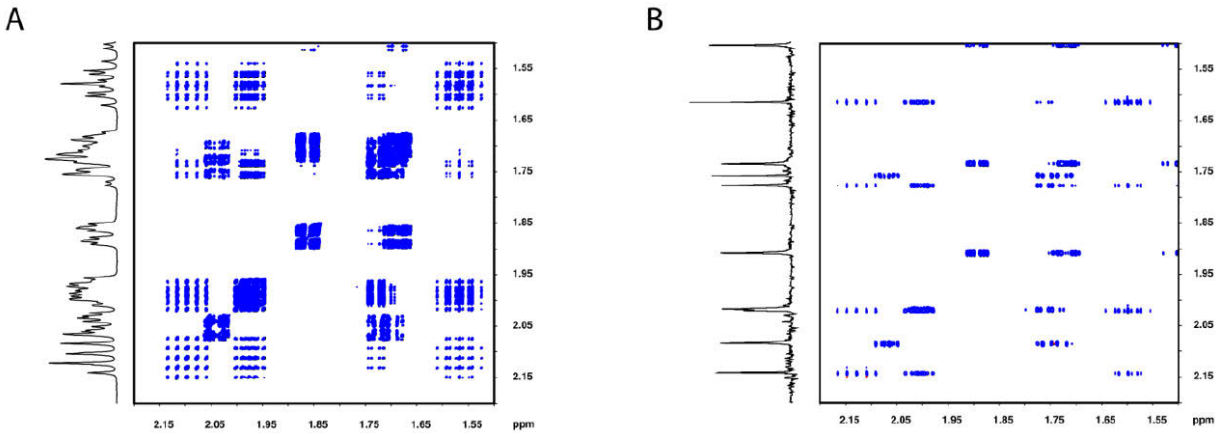

(A) Classical 1D proton and 2D TOCSY spectra recorded with high-resolution and (B) 1D and 2D homodecoupled spectra

Frequency-modulated Zangger-Sterk element has been successfully developed in order to compensate the low sensitivity of spatial encoding. A solution effectively eliminating the artifacts due to the simultaneous irradiation of coupled spins is introduced thanks to the setup of the non-equidistant frequency-modulation. Decoupled spectra are therefore showing a better sensitivity allowing a routinely use of this experiment.

List of Publications and Presentations

Publications

1. 1D NMR homodecoupled ^{1}H spectra with scalar coupling constants from aliased 2D nemoZS-DIAG spectra.
   A. Cotte, D. Jeannerat.
   Angewandte Chemie International Edition, **2015**, 54, 6016-6018.

2. Combination of homonuclear decoupling and spectral aliasing to increase the resolution in the ^{1}H dimension of 2D NMR experiments.
   A. Cotte, M. Foroozandeh, D. Jeannerat
   CHIMIA, **2012**, 66 (10), 764-769.

Oral Presentations

1. From 2D to 1D homodecoupled proton NMR spectra.
   Geneva Chemistry and Biochemistry Days 2015
   Geneva, Switzerland, January 2015

2. Proton homodecoupling with enhanced resolution and sensitivity
   EUROMAR 2014, A European Magnetic Resonance Meeting
   Zürich, Switzerland, July 2014

3. High-resolution homodecoupling
   XXth Swiss NMR Symposium
   Basel, Switzerland, January 2014

4. A new approach to separate chemical shift and scalar coupling of 1D proton NMR spectra.
   Swiss Chemical Society Fall Meeting 2013
   Lausanne, Switzerland, September 2013

Poster Presentations

1. Proton homodecoupling with enhanced resolution and sensitivity.
   Swiss Chemical Society Fall Meeting 2014
   Zürich, Switzerland, September 2014

2. Proton homodecoupling with enhanced resolution and sensitivity.
   EUROMAR 2014, A European Magnetic Resonance Meeting
   Zürich, Switzerland, July 2014

3. A new approach to separate chemical shift and scalar coupling of 1D proton NMR spectra.
   SMASH 2013, Small Molecule NMR Conference
   Santiago de Compostela, Spain, September 2013

4. A new approach to separate chemical shift and scalar coupling of 1D proton NMR spectra.
   EUROMAR 2013, A European Magnetic Resonance Meeting
   Hersonissos, Crete, July 2013

5. Broadband homodecoupling in the indirect dimension of 2D homonuclear NMR experiments.
   Swiss Chemical Society Fall Meeting 2012
   Zürich, Switzerland, September 2012

Table of Contents

Table of Figures

Once, a friend of mine told me that, for him, NMR is like the black suitcase in the great movie Pulp fiction. As a chemist, he is using it to characterize compounds he has synthesized, he can see the light shining but he does not know what is inside and how it works.

As an NMR spectroscopist and after two years and a half as a Ph. D. student in the group of Dr. Damien Jeannerat, I better understand what is in the black box.

In the next pages, I will try to explain how it works and what it is possible to do to simplify life of chemists using NMR.

Chapter 1: Introduction to the Nuclear Magnetic Resonance

The Nuclear Magnetic Resonance (herein after referred to as NMR) has been observed for the first time in 1946 by Felix Bloch[1] and Edward Mills Purcell[2] who shared a Nobel Prize for Physics in 1952.

It became an essential technique, routinely used by organic chemists, to characterize compounds, check purity of samples, monitor key parameters of reactions, … Within this first chapter, the theory of NMR spectroscopy will be reminded with an highlight on several key aspects for the understanding of the following chapters.

1) Physical principle

a) Magnetic properties of nuclei

Nuclei of atoms are composed of particles called neutrons and protons which possess an intrinsic angular momentum **I**. Its magnitude is characterized by the spin quantum number I which may take different values. For protons, neutrons and electrons, I is equal to ½.

The existence of the nuclear spin I depends on the composition of the nuclei. Nuclei containing an even number of protons and neutrons have a spin equal to zero. In this case, these nuclei are not observable by NMR. By contrast, isotopes having a nuclear spin different of zero are subject to the phenomenon of nuclear magnetic resonance and can be studied. Most of elements have an isotope with I different of zero. For example, ^{12}C nucleus has 6 protons and 6 neutrons whereas ^{13}C nucleus has a seventh neutron, allowing this nucleus to be observed by NMR.

If the angular momentum of a nucleus is not equal to zero, the nucleus has a magnetic moment **μ**. The nuclear magnetic moment is proportional to the sum of angular moments of the unpaired particles constituting the atom nucleus and therefore depends on the nucleus composition.

$$\boldsymbol{\mu} = \gamma \boldsymbol{I}$$

with γ the proportionality constant also known as the magnetogyric ratio of the nucleus. This ratio is specific to the observed nucleus. For example, the magnetogyric ratio of hydrogen atoms is about 4 times higher than the ratio of carbon nuclei.

The angular momentum is a quantized vector defined by:

$$I = m\,\frac{h}{2\pi}$$

With h the Planck's constant and m the magnetic quantic number which can take 2I+1 values. For nuclei having a spin I of ½, only two values are allowed: m = + ½ and m = - ½ corresponding to the two possible orientations of the spin.

b) Interaction with a magnetic field

In the absence of magnetic field, the two allowed states of spin ½ are characterized by a unique energy level. When a nucleus is submitted to a magnetic field, the system is acquiring some energy which is proportional to the magnetic field strength and the magnetic moment.

$$E = -\boldsymbol{\mu} . \boldsymbol{B_0}$$

By convention, the magnetic field B_0 is applied along the z-axis of the laboratory frame. The previous relation thus becomes:

$$E = -\mu B_0$$

$$E = -\gamma I B_0$$

$$E = -m \frac{h}{2\pi} \gamma B_0$$

The energy of the system is split across the two different spin states α and β (Figure 1.1).

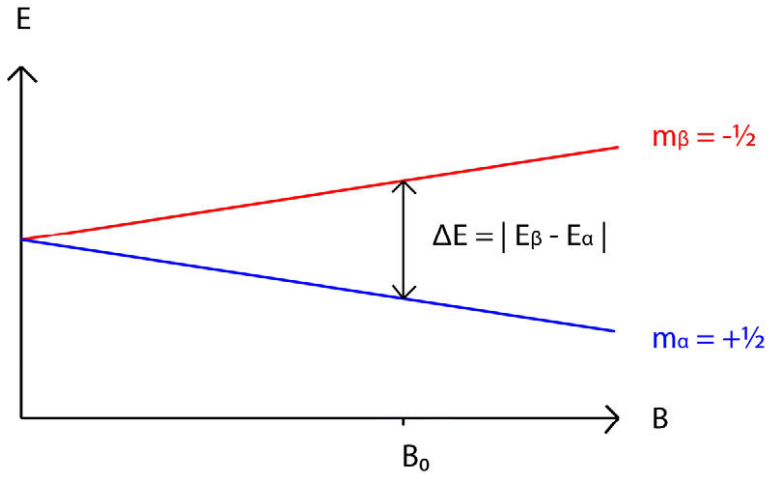

Figure 1.1: Illustration of the energy levels as a function of the magnetic field.

The transition between the two energy levels is defined by:

$$\Delta E = |E\beta - E\alpha| = \Delta m \frac{h}{2\pi} \gamma B_0$$

In the case of ½ -spins, this relation becomes:

$$\Delta E = -\frac{h}{2\pi}\gamma B_0$$

This difference of energy is also defined by:

$$\Delta E = h\nu \qquad \text{With } \nu = -\frac{\gamma B_0}{2\pi} = \frac{\omega}{2\pi}$$

The phenomenon of resonance is characterized by the frequency ν known as Larmor frequency, expressed in Hz. For a hydrogen nucleus in a magnetic field of 11.7 tesla, this frequency is equal to 500 MHz which is in the radiofrequency domain.

c) Observation of the resonance phenomenon

Spins can be represented as vectors. Without a magnetic field, they are randomly orientated. In the presence of the magnetic field B_0, spins start to precess like spinning top around the z-axis at their Larmor frequency. They are thus aligned along the field, some in the same direction, others in the anti-parallel direction (Figure 1.2). The distribution of orientations follows a Boltzmann distribution that enlightens the lowest energy level exhibiting a small excess of population compared to the higher energy level.

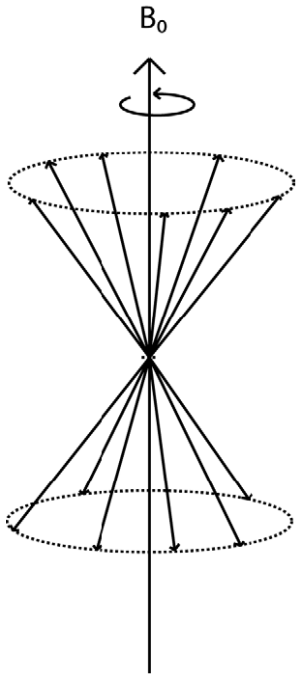

Figure 1.2: Alignment of spins in a magnetic field B_0.

In order to observe the resonance phenomenon, spins have to be moved away from their equilibrium state. A second magnetic field B_1, weaker than B_0, is thus applied perpendicular to B_0. This field will generate radiofrequencies close to the frequencies of the nuclei. Due to

this second field, magnetization is shifted away from the equilibrium and follows the B_1 field. By nature, spins are going back to the equilibrium position along the z-axis when radiofrequencies are interrupted (Figure 1.3.a). This phenomenon is called relaxation.

The x and y components of the magnetic moment induce an electric response which is detected by a receptor coil located in the xy-plane. This electrical current is modulated according to the orientation of the magnetic moment compared to the position of the coil. This current is also influenced by relaxation processes. Indeed, during relaxation, magnetic moments are leaving the xy-plane toward their equilibrium position along the z-axis. The generated current is thus decreasing through time. The detected signal is therefore an exponentially decaying sinusoid called Free Induction Decay (Figure 1.3.b). This FID is then transformed by Fourier Transform[3], a mathematical technique converting a function of time into a function of frequency. The FID is therefore transformed into a spectrum where frequencies of resonance of each spin are represented (Figure 1.3.c).

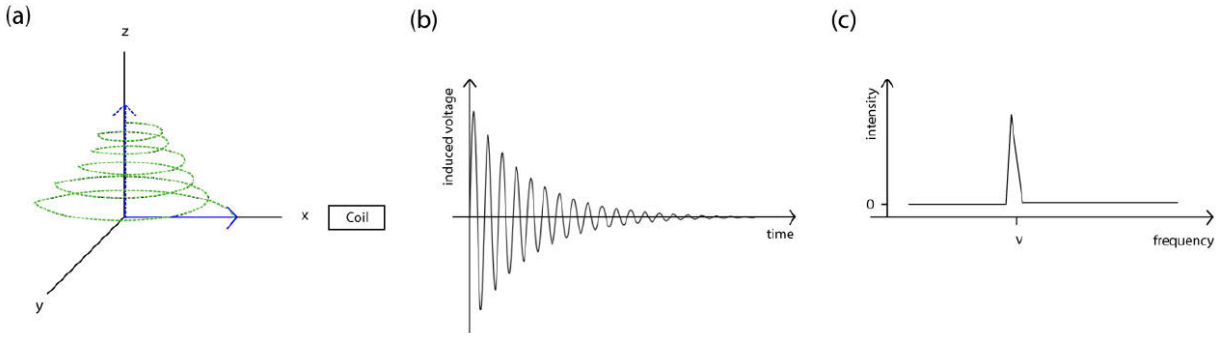

Figure 1.3: Detection of NMR signal. (a) When relaxation occurs, the magnetic moment goes back to its equilibrium position along z while precessing. (b) The voltage induced by the magnetic moment is evolves as a sinusoid decreasing with time because of the spin relaxation. (c) After FT, the signal appears in the spectrum at the frequency of resonance of the observed nucleus.

2) Notion of chemical shift

The frequency of resonance of a molecule's nuclei depends on two main parameters: the magnetic field of the spectrometer used for the analysis and the magnetogyric ratio of the observed nucleus. As an example, at 500 MHz, the proton Larmor frequency is equal to 500 MHz whereas the carbon is resonating at 125 MHz. But all proton nuclei are not exactly resonating at 500 MHz. Local variations of the magnetic field appear depending on the local electronic distribution. Nuclei are in fact resonating in a range of frequencies around the Larmor frequency. This environmental dependency allows the distinction of protons based on functional groups they are involved in (Figure 1.4).

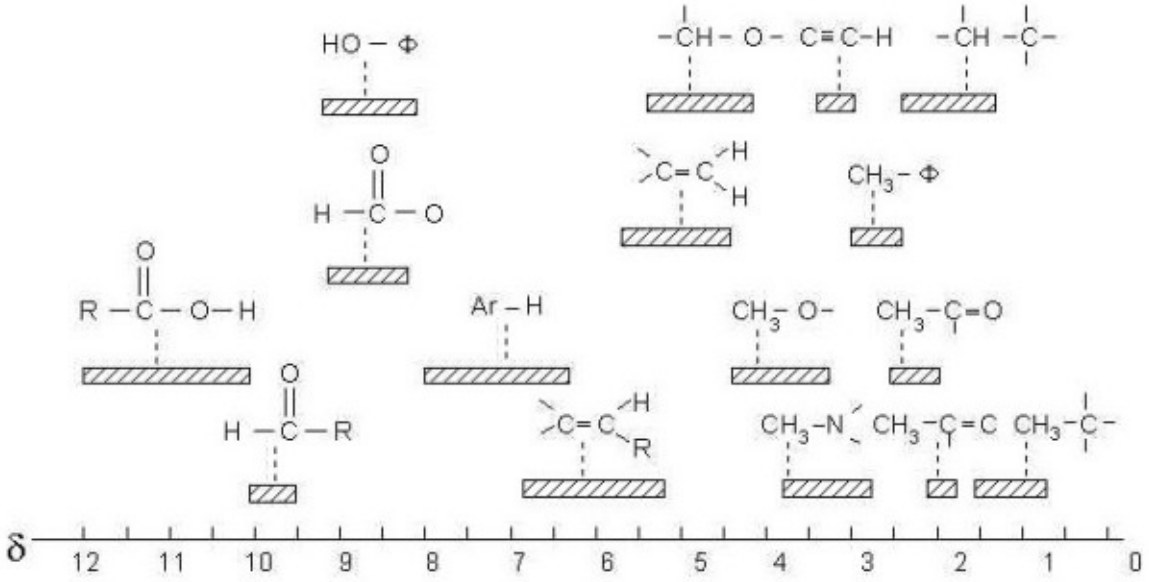

Figure 1.4: Chemical shift ranges are presented for different chemical groups.

The spectrometer magnetic field B_0 acts on electrons surrounding the observed nucleus. These electrons are moving and inducing a local magnetic field B' which affects the magnetic field felt by the nucleus (Figure 1.5). The magnetic field B is defined by the following relation:

$$B = B_0 - B' = B_0\,(1 - \sigma)$$

Where σ corresponds to the shielding constant of the nucleus. It is determined by the electronic structure of the molecule in the vicinity of the observed nucleus. The frequency of resonance of this nucleus is thus characterized by its chemical surrounding (Figure 1.5).

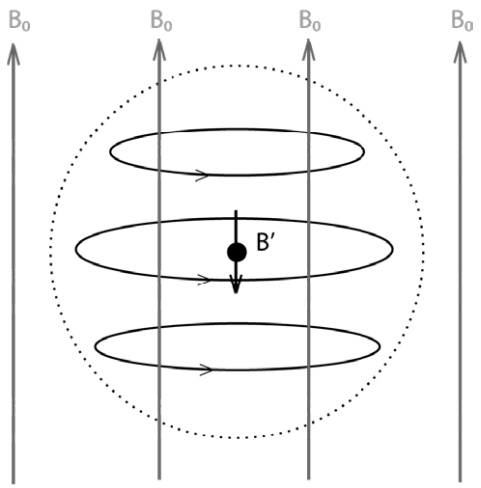

Figure 1.5: A magnetic field B_0 is applied to an atom. The magnetic field B' is induced by electrons. The magnetic field experienced by nuclei of a molecule is thus different, depending on the chemical group which atoms belong to.

The chemical shift δ of the observed nucleus is defined by :

$$\delta = 10^6 \frac{\sigma_{ref} - \sigma}{1 - \sigma_{ref}} \cong 10^6 (\sigma_{ref} - \sigma)$$

The higher the electron density of the nucleus is, the more efficient the shielding due to the electrons is. Thus the magnetic field B is felt weaker and therefore the chemical shift is low.

However, it is easier to determine the difference between the frequency of resonance of the nucleus and the frequency of reference than to determine the value of the shielding constant for each nucleus. The previous relation becomes:

$$\delta = 10^6 \frac{\nu - \nu_{ref}}{\nu_{ref}}$$

With δ expressed in ppm and ν in Hertz. Note that chemical shifts are expressed in ppm and not in Hz. This is due to the fact that the frequency differences are of the order of few hundreds of Hz which is very low compared to the Larmor frequency of the spectrometer. More importantly, values of chemical shifts have to be independent of the Larmor frequency so that they can be compared whatever the strength of the magnetic field used for the acquisition of the spectrum.

3) Notion of scalar coupling

Scalar coupling correspond to an indirect interaction between nuclei. It is mediated by electrons involved in chemical bonds. This interaction is independent of the magnetic field of the spectrometer.

Also called spin-spin coupling, they modify the appearance of NMR signals by splitting the natural lineshape into spaced lines. The gap between these lines depends on the strength of the coupling between the nucleus responsible of the signal and its neighbors. The strength of the coupling is determined by the value of the coupling constant, given in Hertz, characteristic of the interaction.

This interaction is related to the bond electrons which generate a local magnetic field interacting with nuclei. This field orientates the nuclear spin of a nearby atom. If a nucleus has a neighbor of the same nature, one can observe an interaction between the nuclear spin of the first nucleus with the nuclear spin of the neighbor. Thus, the signal will be composed of two lines, one corresponding to the interaction of the first spin with the second in the α-state, the other corresponding to the interaction with the second spin in the β-state. The spectrum will therefore exhibit a doublet as being the signal of the first nucleus. Different multiplicities (or splitting) can be observed depending on how many nuclei are interacting together (Figure 1.6).

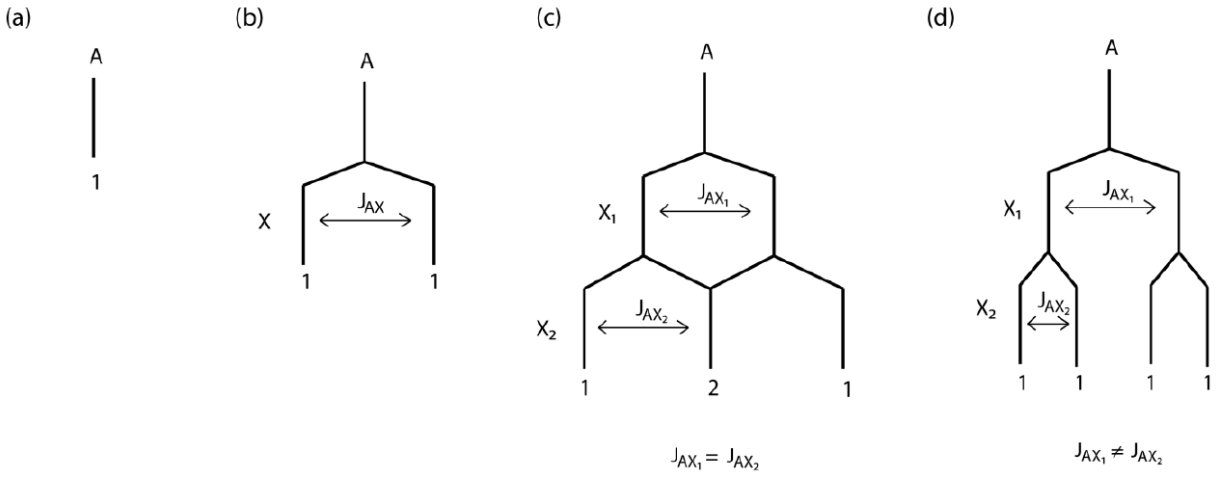

Figure 1.6: Illustration of the first-order multiplicity of signals of spin A depending on the number of neighbors X. If a nucleus has no coupling partners, the signal will appear as a singlet (a). When increasing the number of nuclei interacting together, more lines are appearing in the signal. A doublet (b) corresponds to the interaction of nucleus with another one, a triplet (c) or a doublet of doublet (d) characterize the interaction of one nucleus with two partners with identical (c) or different (d) coupling strength.

When a nucleus is interacting with two partners with the same value of coupling constant, the lines are added and a triplet is observed instead of a doublet of doublet (Figure 1.6.c and 1.6.d respectively). The addition of two lines leads to the increase of the intensity of the resulting line. The Pascal's triangle determines the line intensities of a given multiplet. In the case of a triplet, the relative intensities will be 1-2-1, the digit 2 resulting from the addition of two lines with intensity of 1.

The strength of the coupling is depending on the distance between nuclei interacting together, i.e. on the number of bonds between two nuclei. The closer the nuclei are, the stronger the coupling is. Notation for coupling is: ^{x}J where x is equal to the number of bonds. ^{1}J couplings are observed in the case of dihydrogen or for protons linked to their carbons. The value of ^{1}J depends of the hybridization level of the carbon and is generally between 100 and 250 Hz. This coupling is not observed in proton experiments. The ^{2}J coupling concerns two protons attached to the same carbon atom. The constant value varies from -23 to +42 Hz. Above three chemical bonds, coupling constants are really weak with the exception of aromatic protons presenting a W motif. ^{3}J coupling constant values are also depending on the dihedral angle θ between nuclei which is the angle between two consecutive CH bonds. This is defined by the Karplus relation[4]:

$$^{3}J = A + B \cos \theta + C \cos^{2}\theta$$

Where A, B and C are coefficients determined from models of known molecules. Figure 1.7 shows the dependence of the coupling constant on the dihedral angle θ.

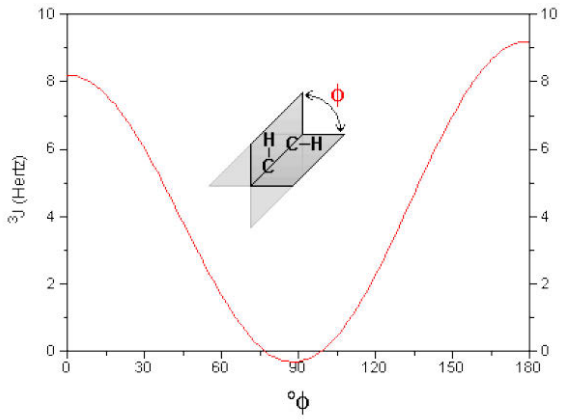

Figure 1.7: Variation of three-bond coupling constant as a function of the value of the dihedral angle θ according to the Karplus relationship.

Coupling constant values have to be determined in order to analyze the conformation of a molecule. It is mostly the case when analyzing molecules with high molecular weight such as natural products, peptides or proteins for determining their secondary structure.

4) Pulse sequences

Depending on the information that we would like to extract from a sample, it may be interesting to observe, or on the contrary to remove, contributions of chemical shift or scalar coupling of a given nucleus. Some experiments have been specially designed for this purpose.

a) Refocusing of chemical shift : example of the spin-echo pulse sequence

Different pulse sequence elements can be introduced in sequences to refocus the evolution of chemical shift. The most common element is the spin-echo motif.

α) Principle of the spin-echo

The spin-echo[5] sequence is shown in figure 1.8.

Figure 1.8: Spin-echo pulse sequence

The 90 degree pulse on x-axis allows to tilt the bulk magnetization from its equilibrium position along the z-axis to y-axis. This magnetization then precesses in the transverse plane during a delay DE. A phase shift of magnetizations appears since some spins evolve faster than others. The 180 degree pulse inverts the dephasing process. Indeed, this pulse on y-axis makes magnetizations tipping in the second half of the xy plane while keeping the rotation angle of each spin. The magnetizations spinning faster are thus behind the magnetizations spinning slowly. At the end of the second delay DE, all the magnetizations are orientated along the y-axis. The signal can then be recorded along the same axis (Figure 1.9.a).

The 180 degree pulse can be applied to one or the other axis of the transversal plan leading to the return of magnetizations along the y-axis before detection. When the pulse is applied on x, the magnetizations are refocused along –y so the detected signal will be negatively phased (Figure 1.9.b). On the contrary, a 180 degree pulse applied on y will lead to the magnetization refocusing along +y, the signal will be positively phased.

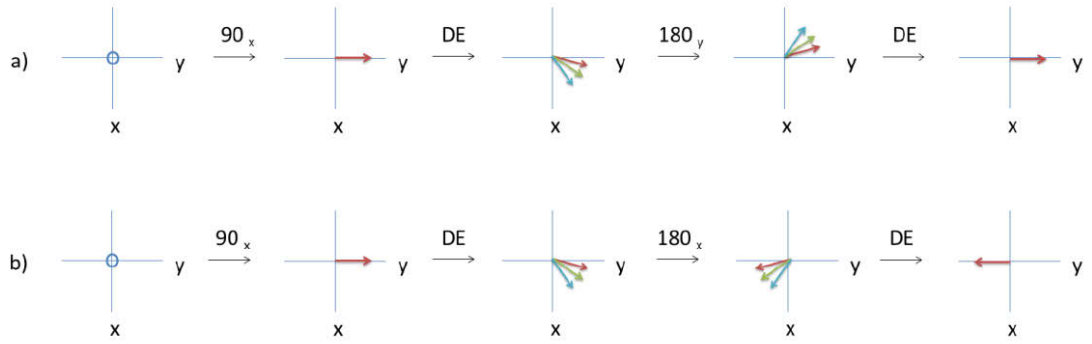

Figure 1.9: Principle of spin-echo. Chemical shift evolution is refocused after two DE time intervals whether the 180 degree pulse is applied along x- or y-axis.

β) Application of the spin-echo to a coupled system of spins

Let's observe the effect of the spin-echo on a spin A scalarly coupled to a spin X. The signal of spin A will be composed of two lines, one corresponding to the magnetization of A coupled to X in the α-state, the other to the magnetization of A coupled to X in the β-state. For the sake of clarity, we will describe the effects of the spin-echo on the chemical shift and scalar coupling separately in the case where the frequency of reference corresponds to the frequency of the spin A.

The 90 degree pulse on the x-axis tips the magnetization of spins A and X to the y-axis. There is thus creation of a transverse magnetization. During the delay DE, only the magnetization of spin X is precessing in the xy plane, the magnetization of spin A is on-resonance, lying along the y-axis. The 180 degree pulse on y-axis tips the magnetization on the second half of the

transverse plane. The magnetization of spin X is thus behind the magnetization of spin A. During the second delay DE, the magnetization of spin X precesses again and is back along the y-axis with the magnetization of spin A. At the end, no phase difference has been created between the two magnetizations; the chemical shift is said to be refocused (Figure 1.10).

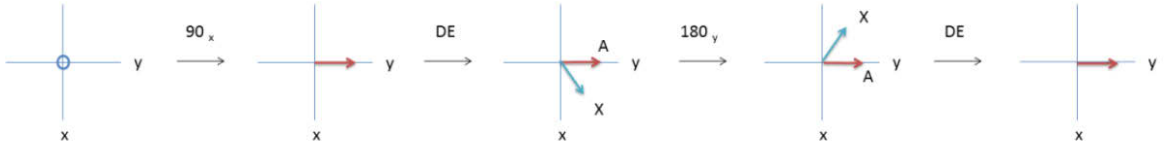

Figure 1.10: Refocusing of the chemical shift at the end of the spin-echo.

Concerning the scalar coupling between spin A and spin X, the spin dynamic is different. In this case, the corresponding signal is composed of two lines, at +J/2 and –J/2 Hz with regards to the frequency of the observed spin. During the first delay, the two vectors are precessing in opposite directions, one towards +J/2, the other towards –J/2. The 180 degree pulse switches their positions. Spins A coupled to spins X in the α-state are now coupled with spins X in the β-state as well as spins A coupled to spins X in the β-state are now coupled to spins X in the α-state. The 180 degree pulse is applied to both spins A and X. Spins X are therefore feeling the same inversion. Finally, vectors continue to precess in the same direction during the second delay. Scalar coupling is not refocused by the spin-echo pulse sequence (Figure 1.11).

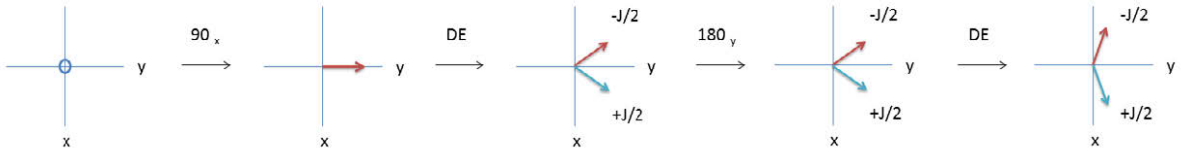

Figure 1.11: Evolution of scalar coupling during the spin-echo.

b) Refocusing of scalar coupling: example of the Zangger-Sterk element

The so-called Zangger-Sterk pulse sequence element[6] (Figure 1.12) is an ingenious motif developped by Zangger and Sterk in 1997 to remove effects of J-coupling. It is composed of a selective 180 degree pulse and a z-gradient that act on spins of the sample in a specific way.

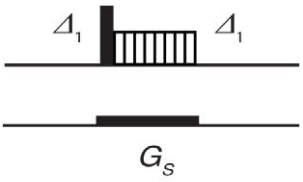

Figure 1.12: Zangger-Sterk pulse sequence element

Unlike broadband pulse, called hard pulse, which acts on all the spins of a sample, the selective pulse, or soft pulse, is a pulse that acts only on a restricted bandwidth (typically 100 Hz) i.e. on several spins depending on its selectivity, an important parameter to which a particular attention must be paid. When the selective pulse is associated to a hard 180 degree pulse, scalar interactions between spins can be suppressed. Indeed, each spin selected by the soft pulse undergoes an inversion while coupling partners are unaffected. The hard 180 degree pulse inverts all the spins, the selected ones and their partners. The active spins, that are spins selected by the shaped pulse, are affected by a rotation of 360 degrees whereas passive spins are only inverted. This difference leads to the refocusing of scalar coupling evolution without interfering with the evolution of chemical shifts. The decoupling of a signal at time τ can be achieved by inverting all its scalar coupling partners at time τ/2 [6]. Figure 1.13 shows the effects of these two pulses on spins from the point of view of chemical shift and scalar coupling evolutions.

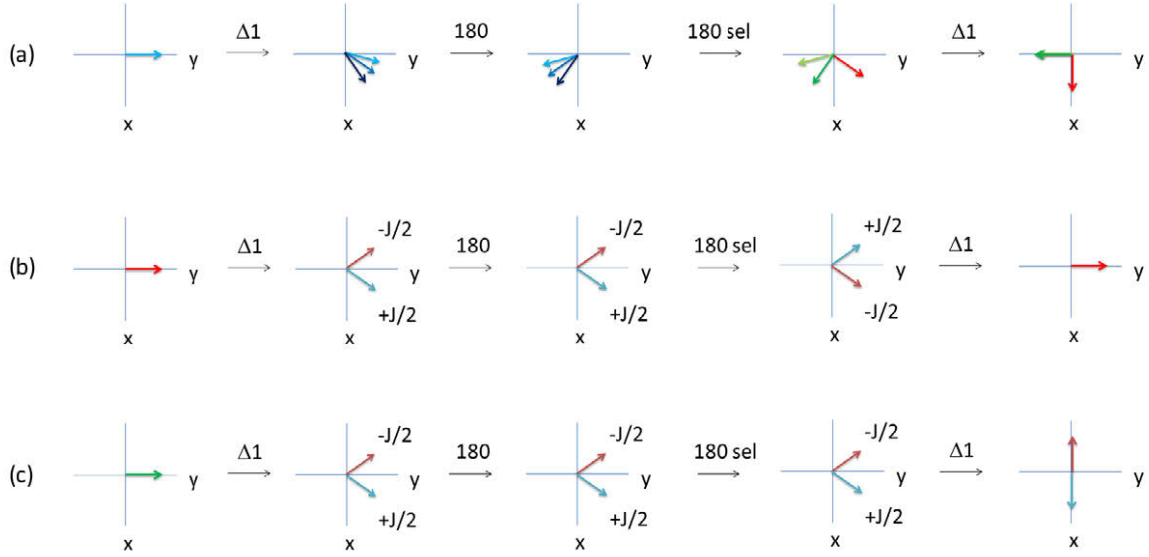

Figure 1.13: Effects of the ZS element on spins: chemical shift evolution is presented in (a) while scalar coupling evolution of active and passive spins are shown in (b) and (c) respectively. Active spins are represented by red arrows and passive spins are shown in green. In (a), spins are precessing during Δ1 and then inverted by the 180 degree pulse. The soft 180 degree pulse inverts only active spins, passive

spins are unaffected. After these two pulses, active and passive spins have experienced a 360 degree rotation and a 180 degree inversion respectively. The chemical shift continues to evolve during Δ1. Scalar coupling evolves during delays and is only affected by selective pulses. That's why scalar coupling of passive spins is unaffected (c) by this sequence while it is refocused at the end in the case of active spins (b).

It is important to use a soft pulse in this motif since a hard 180 degree pulse would lead to a 360 degree rotation of all spins leaving scalars interactions unaffected. This pulse has to be selective enough to act only on active spins without their coupling partners. However, the use of a selective pulse implies that all recorded signals correspond only to the selected spins. Thus, in order to recover all signals of the studied molecule, Zangger and Sterk had the idea to apply what is called spatial encoding: applying a z-gradient and the selective pulse at the same time.

During the application of this field gradient, different parts of the sample experience different magnetic fields. The selective pulse can excite spins at different locations based on their frequencies. A spin with a given frequency will be on-resonance at a given location in the sample volume. Each signal on the spectrum will come from a different part of the NMR tube (Figure 1.14).

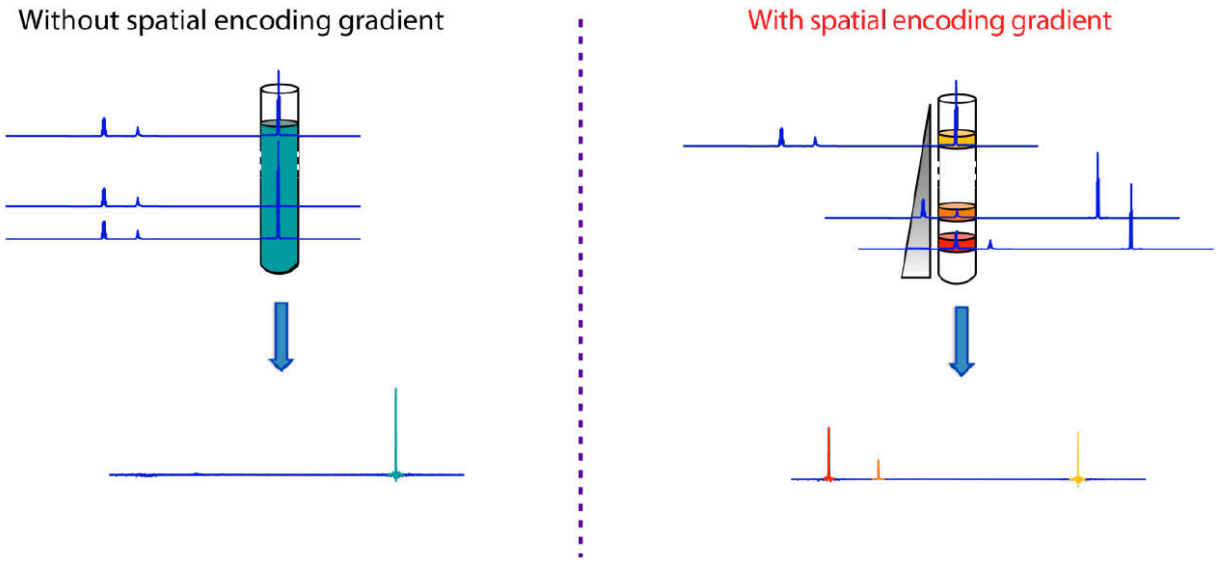

Figure 1.14: Illustration of spatial encoding. Without the gradient, the same spins are selected in all the sample leading to the decoupling of only these spins. With the spatial encoding gradient, a frequency-shift is induced; different spins are selected in different slices of the sampling leading to the decoupling of all the signals.

This spin decoupling element has been published in 1997 but has not received wide acceptance. It has been rediscovered by Morris et al.[7] and Giraud and coworkers[8-9] in the late 2000's. Several modifications have been brought to this motif (Figure 1.15), in particular the

addition of clean up gradients flanking each 180 degree pulse leading to a better elimination of the contributions of passive spins.

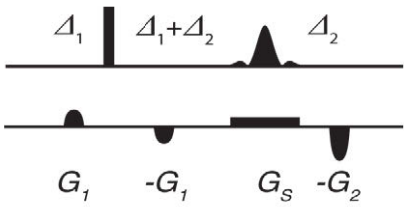

Figure 1.15: Modified Zangger-Sterk element

To insure the spin decoupling, this element has to be introduced in the middle of a stepwise incremented delay such as the t_1 evolution time of a 2D experiment.

Chapter 2: 2D BroadBand HomoDecoupling (BBHD)

Proton NMR is widely used in organic chemistry[10] because of its natural abundance in molecules and its high magnetic sensitivity. Important information related to the molecular structure of the analyzed sample can be extracted from the spin-spin coupling in 1D proton spectra. However, the splitting due to this interaction can spread a signal over several tens of hertz complicating the direct analysis of the spectrum.

Two-dimensional experiments[11] have therefore been developed to disperse resonances in space. The range of proton chemical shifts being limited compared to other nuclei, multiplets can still superimposed making difficult the analysis of a 2D map. In this case, an increase of the resolution in one or the other dimension is necessary.

In this chapter, 2D homonuclear experiments will be studied and a decoupling method will be applied in order to improve the signal separation.

1) 2D BBHD-TOCSY[12]

The TOtal Correlation SpectroscopY experiment[13] (TOCSY) is a useful method underlining scalar couplings between protons belonging to the same spin system. This experiment looks a lot like the COSY experiment. The main difference lies in the fact that the spin-spin interaction does not only exist between protons spaced by 2, 3 or 4 chemical bonds but it is relayed in all the spin system by polarization transfer from spin to spin. For example, in the case of isoleucine in which proton α is coupled to proton β which is coupled to proton γ and γ to δ, a cross-peak can be observed between protons α and β but also between protons α and γ and protons α and δ and so on for each proton belonging to this spin system. (Figure 2.1)

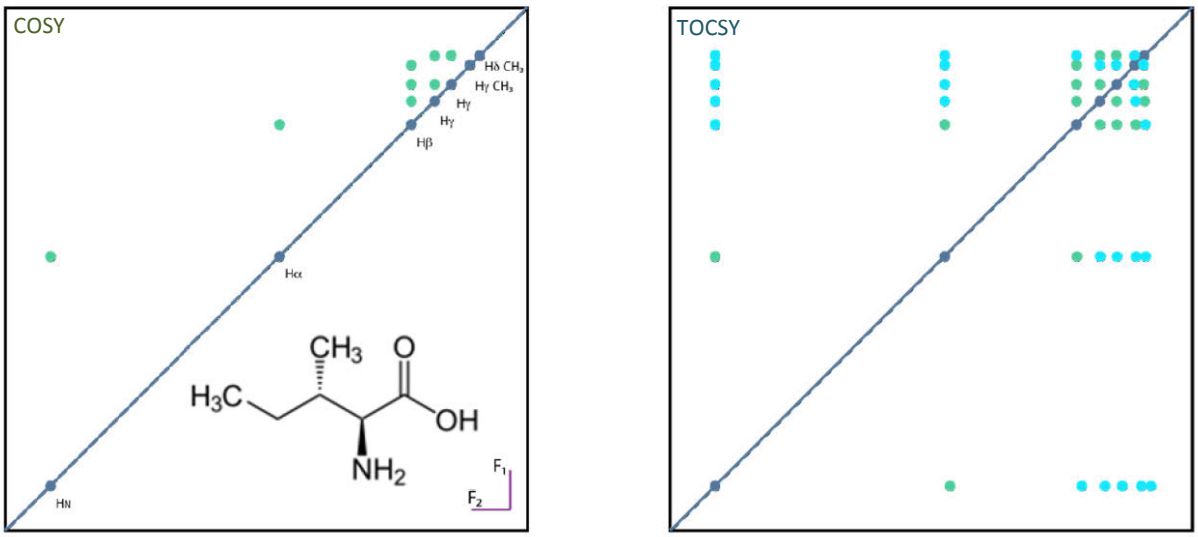

Figure 2.1: Comparison of COSY and TOCSY experiments for the aminoacid isoleucine. Dark blue dots represent diagonal peaks, green dots cross-peaks observed in COSY spectra. Light blue dots are cross-correlation observed only in TOCSY spectra.

This experiment is used to study of samples, complex by the structure of the molecule - such as small molecules synthetized by chemists, carbohydrates, oligomers, proteins …- or by the presence of several analytes in the sample. The TOCSY allows the identification of the different spin systems, independently from each other.

We will see in this section how to simplify the information obtained from this experiment.

a) 2D-TOCSY

As all pulse sequence resulting in a two-dimensional spectrum, the TOCSY pulse sequence is composed of four periods. (Figure 2.2)

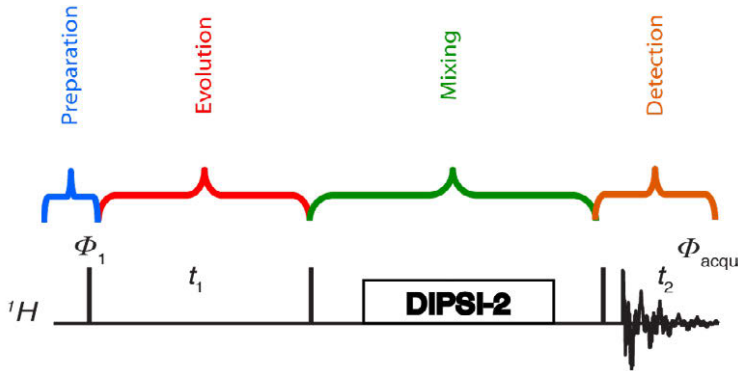

Figure 2.2: The TOCSY pulse sequence

The first period is called preparation time and generally corresponds to the initial spin excitation. Under a 90 degree pulse, spins lying at the origin along the B_0 direction (z-axis) tip into the xy plane.

The second period corresponds to the t_1 evolution time. This period is characterized by chemical shift and scalar coupling evolution.

The third time is the mixing time of the experiment. For the TOCSY, it is composed of a pulse train called spin-lock, a quick succession of short pulses keeping magnetizations in the xy plane, leading to the transfer of polarization from one spin to all spins belonging to its coupling network. There are several spin-lock sequences such as WALTZ, MLEV[14] (Malcolm LEVitt's decoupling cycle) and DIPSI[15] (Decoupling In the Presence of Scalar Interactions). For this work, we will use the DIPSI-2 sequence which has several advantages over MLEV sequences (most efficient through-bond transfer of magnetization with the least sample heating[16]). The principle is quite simple. During the mixing time, the contribution of scalar coupling remains while the differences of chemical shifts are suppressed. Spins are aligned along the z-axis. The magnetization transfer occurs between the spin 1 and the spin 2 during a delay of $1 / 2\ J_{12}$. After this, the spin 1 magnetization is transferred to the spin 3 and so on over the spin system. This transfer is done in-phase and generates cross-peaks with pure absorption.

The fourth and last time concerns the signal detection that is the acquisition of the Free Induction Decay which will be processed in a 2D spectrum by double Fourier Transform.

This experiment produces pure absorption in-phase signals, contrary to the COSY experiment which generates anti-phase signals. However, it has to be noted that the TOCSY mixing time induces the presence of zero-quantum coherence (ZQ). The ZQ signals correspond to dispersed anti-phase which are perpendicular to the desired in-phase signals (Figure 2.4.top). It can cause a decrease of the spectral resolution complicating the appearance of the desired

signals. The suppression of the ZQ coherence has now become essential. ZQ coherences behaving like z-magnetization, it is not possible to suppress them by phase cycling or the use of pulsed field gradient. Keeler et al.[17] have set up an efficient method to suppress them. It consists in a modified z-filter leading to the spatial averaging of the ZQ terms by dephasing. Indeed, a 180 degree sweep pulse is applied during a z-gradient. This pulse inverts spins at different positions of the sample at different time. Thus, spins localized at the top of the NMR tube will be inverted at the beginning of the pulse; spins at the bottom of the sample will be inverted at the end of the sweep. The pulse creates an echo that will defocus the ZQ coherence. With our experiment, the building block sweep pulse – z-gradient is applied before and after the spin-lock element (Figure 2.3). The duration of the two Chirp pulses[18] are chosen different in order to avoid any accidental refocusing of the ZQ. The second z-filter is preceded by another z-gradient, a purge gradient, allowing the passing of the desired magnetizations only. These being longitudinal they are not influenced by the z-filter and can therefore be detected. One can then observe cross and diagonal signals without phase distortion. (Figure 2.4.bottom)

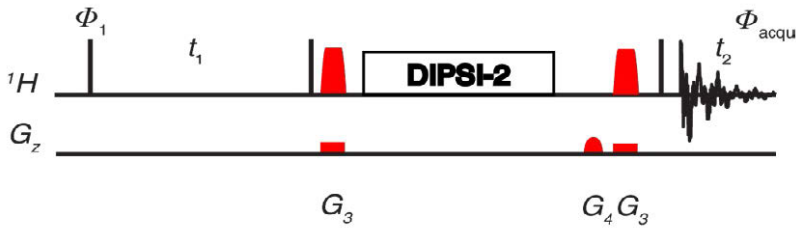

Figure 2.3: Pulse sequence of ZQ-TOCSY. The two modified z-filters are shown in red.

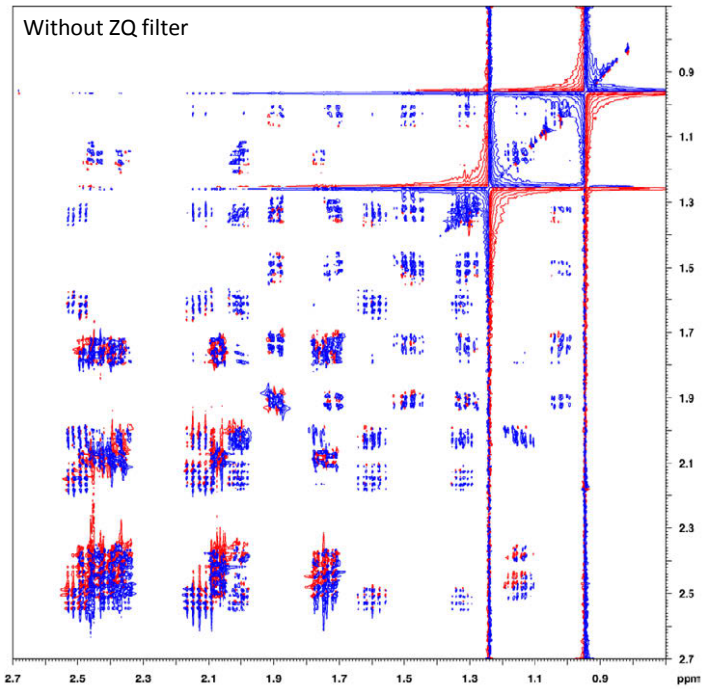

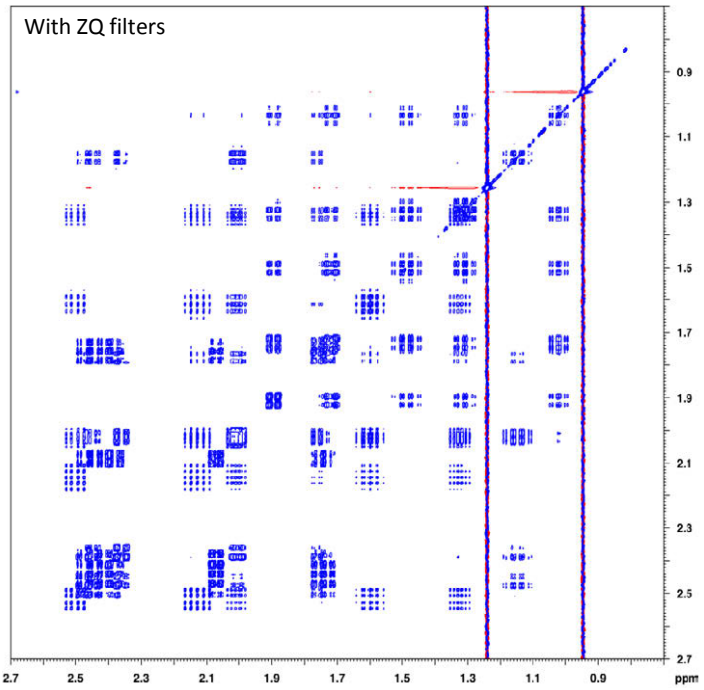

Figure 2.4: Comparison of TOCSY spectra recorded without (top) and with z-filters (bottom). Peaks are not phase-distorted after suppression of the zero-quantum coherence by z-filtration.

b) Resolution enhancement

A spectrum can be recorded in only few minutes with the acquisition of few dozens of data points at the sacrifice of the spectral resolution. (Figure 2.5.a)

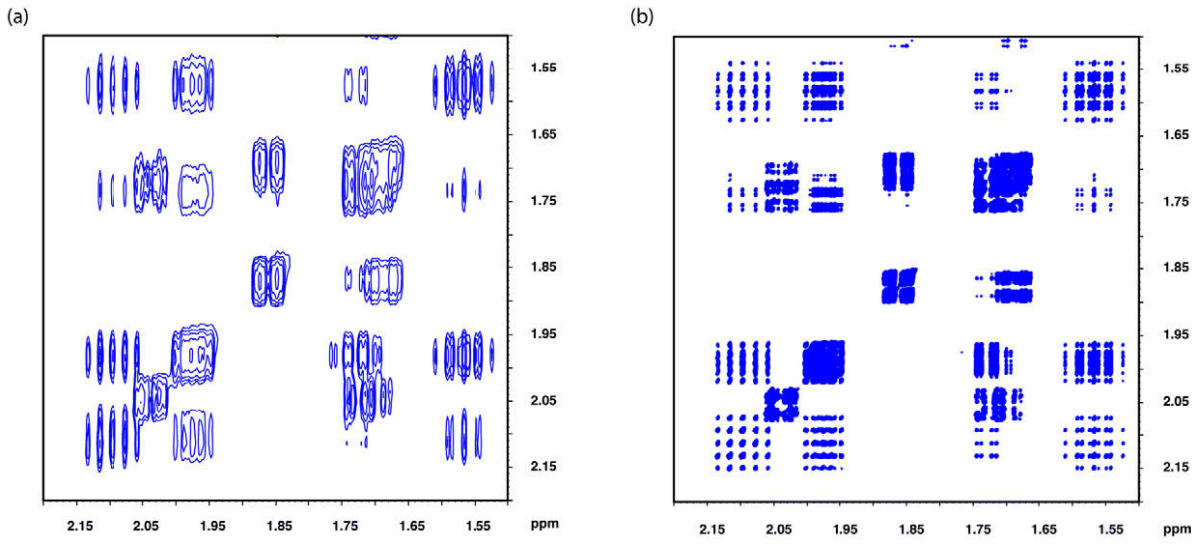

Figure 2.5: Expansions of spectra recorded with low (a) and high (b) resolution. Full coupling structures are visible in spectra recorded at high-resolution.

If a better resolution is required, one can increase the number of data points in the indirect dimension which means recording a higher number of FID in order to better define each peak. With a higher resolution each peak shows a complete coupling structure in both dimensions. (Figure 2.5.b) It is thus possible to connect each spin to its partners of coupling with a minimum of ambiguities. Indeed, the more the spectrum is said resolved, the easier it is to differentiate each signal and to highlight spectral regions where signals are overlapping.

Although the spectral resolution is limited to the number of recorded points in the indirect dimension, it is possible to enhance it without increasing the experimental time. By applying a decoupling method in the indirect F1 dimension, the spectrum presents only singlets instead of broad multiplets allowing a better identification of observable peaks. This decoupling is independent of the number of FID recorded and enables to acquire high-resolution spectra.

For this purpose, the Zangger-Sterk element[6] has been introduced in the t_1 evolution time of the ZQ-TOCSY pulse sequence (Figure 2.6). As explained in Chapter 1, the scalar coupling contribution is suppressed while chemical shift is evolving.

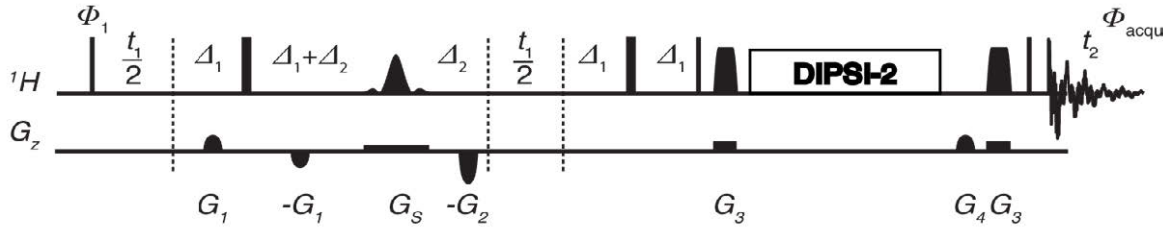

Figure 2.6: BBHD-TOCSY pulse sequence

The BBHD-TOCSY experiment results in a phase-sensitive spectrum with only singlets in the F1 dimension. The decoupling can be applied to the whole spectrum without any limitation concerning the spectral width. This spectrum is very useful when studying complex mixtures. Indeed, this experiment makes it easier to determine the exact number of signals corresponding to the analyzed molecules since this experiment permits to separate two adjacents signals less than 2 Hertz apart (Figure 2.7). Good results have been obtained on samples containing molecules of different sizes such as steroids (4-androstene-3,17-dione), alcaloids (strychnine), carbohydrates (mixtures of trioses) and even peptides (cyclosporine).

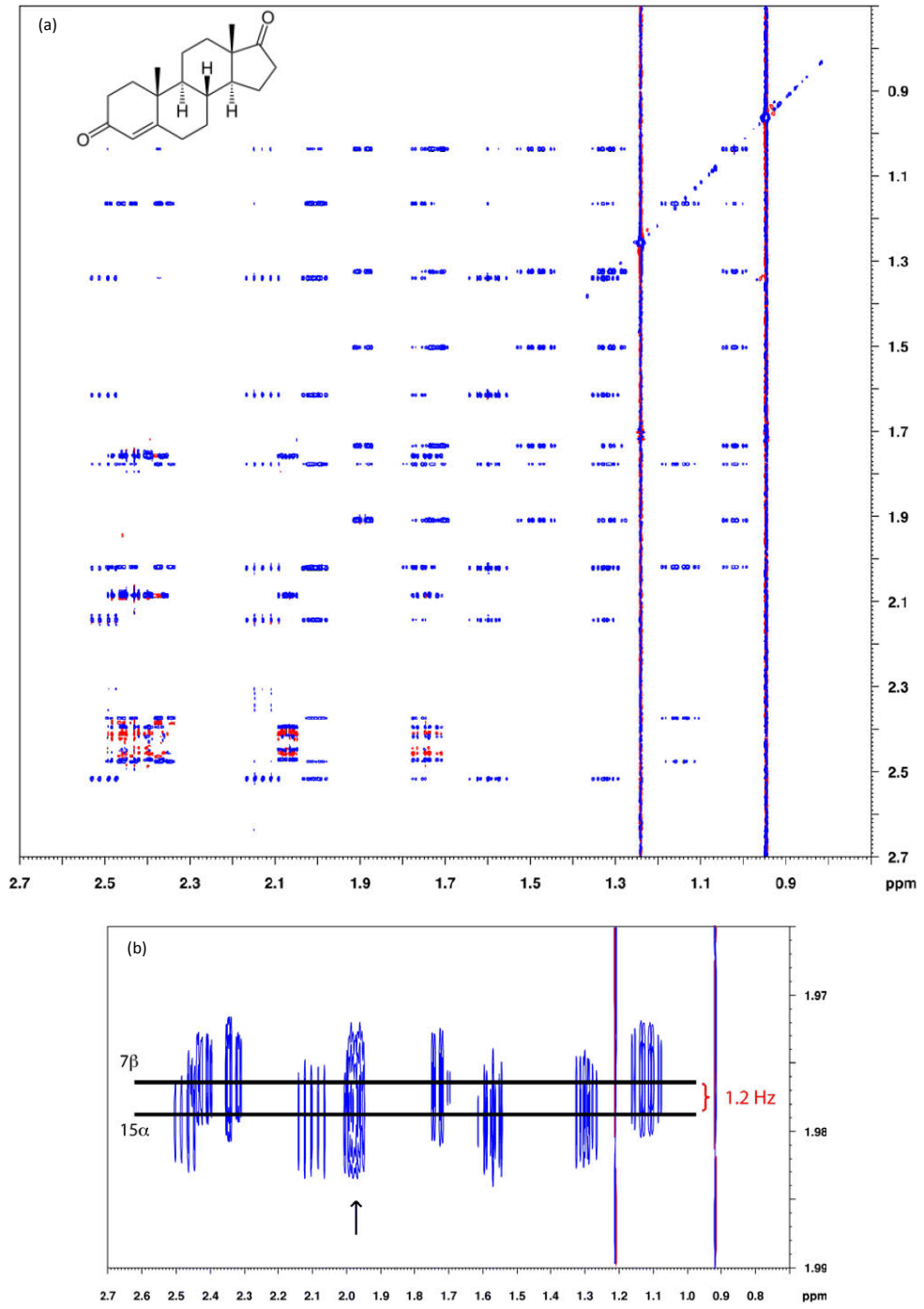

Figure 2.7: BBHD-TOCSY spectrum of 4-androstene-3,17-dione (a) and a zoom (b) on protons 7β and 15α which are separated by 1.2 Hz. The arrow shows the diagonal peaks of protons 7β and 15α.

Morris et al.[19], and later Koivisto[20], proposed another approach to increase the resolution of this experiment. It consists in applying the Zangger-Sterk element during the t_2 time of a pseudo 3D TOCSY experiment. Combined with the covariance[21-23] process, one can obtain a 2D spectrum decoupled in both dimensions. This method is working well, only singlets appear in both dimensions. But coupling information cannot be extracted from this kind of

spectra whereas multiplets are available in the direct dimension of spectra recorded with our approach.

2) 2D BBHD-NOESY

The NOESY experiment[24] brings information about another type of interaction. Spin-spin interactions which take place through electrons are not observed anymore with this experiment but dipolar interactions taking place through space. From this experiment, one can obtain essential data about the tridimensional structure of the studied compound.

a) Principle

This experiment is based on the cross relaxation of spins which follows a dipole-dipole mechanism.

Two spins close enough can experience the Nuclear Overhauser Effect[25]. The first spin creates a local field on spin 2 because of its magnetic moment. This local field is dependent of three parameters. First, the distance r between the two given spins is an important factor because this interaction is inversely proportional to the distance between them raised to the sixth power, in the limit of 5 Å. The second factor is the gyromagnetic ratio γ of the two nuclei. The higher γ is, the more important the magnetic moment is and the more intense the local field is. The third one concerns the orientation of the vector linking spin 1 to spin 2 towards the magnetic field B_0 direction.

The interaction between two nuclei that are not scalarly coupled is defined by four energy levels (Figure 2.8). Six pathways are thus available to switch from one level to another. Four of these pathways are driven by the spin-lattice relaxation and involve the modification of the spin state of one nucleus at a time from α to β and reversely. These transitions are characterized by a relaxation rate noted W_1^X, where X corresponds to the nucleus concerned by the spin state inversion. The last two pathways are driven by cross relaxation; the spin states of both nuclei are inverted at the same time. The relaxation rate is defined by W_2^{12} when $\alpha_1\alpha_2$ becomes $\beta_1\beta_2$, or reversely, and by W_0^{12} when spin states are modified in opposite direction, that is when $\alpha_1\beta_2$ becomes $\beta_1\alpha_2$ (see Figure 2.8).

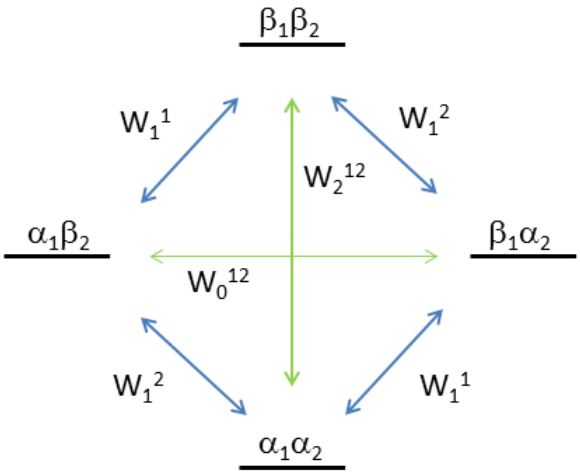

Figure 2.8: Energy levels of two nuclei interacting together and relaxation pathways. Nuclear Overhauser effect occurs when spins are relaxing following the W_0 and W_2 pathways.

At equilibrium, energy level are not equally populated, the stablest one is more populated than the less stable energy level. When a perturbation occurs, the population distribution is modified, spins are located in higher levels. The return to equilibrium can be done by cross relaxation resulting in the transfer of magnetization from one spin to another.

The most common method to observe NOE is to record a 2D NOESY experiment with the pulse sequence shown in Figure 2.9.

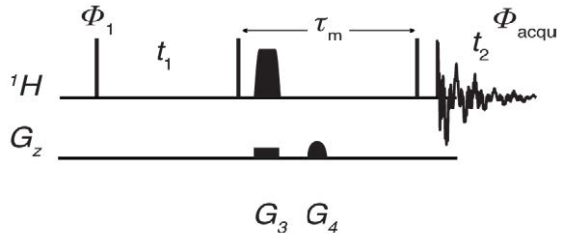

Figure 2.9: Pulse sequence of the ZQ-NOESY experiment

As a 2D experiment (Figure 2.9), after the evolution time, signals are modulated by scalar couplings and chemical shifts. Then starts the mixing time during which magnetization is transferred from one spin to another by cross relaxation. Like during the TOCSY mixing time, the transferred magnetization conserves information about the spin of origin and is responsible for the generation of cross-peaks in the spectrum.

Diagonal peaks come from z-magnetizations that have not been transferred during the mixing time. These peaks are generally of negative sign. Cross-peaks originate from z-magnetizations transferred from one spin to another as a result of cross-relaxation. If the cross-relaxation rate constant is positive i.e. when W_2 takes the advantage on W_0, cross-peaks are of positive sign. If this constant is negative, NOE signals have negative phase. In the case where the cross-relaxation rate constant is equal to zero, no cross-relaxation takes place between close spins so no cross-peaks are observed.

Figure 2.10 shows the NOESY spectrum of strychnine. For this small molecule, diagonal and cross-peaks have opposite signs. It has to be noticed that the intensity of peaks is not constant, some are stronger than others. It is due to the fact that some spins are closer through space than others.

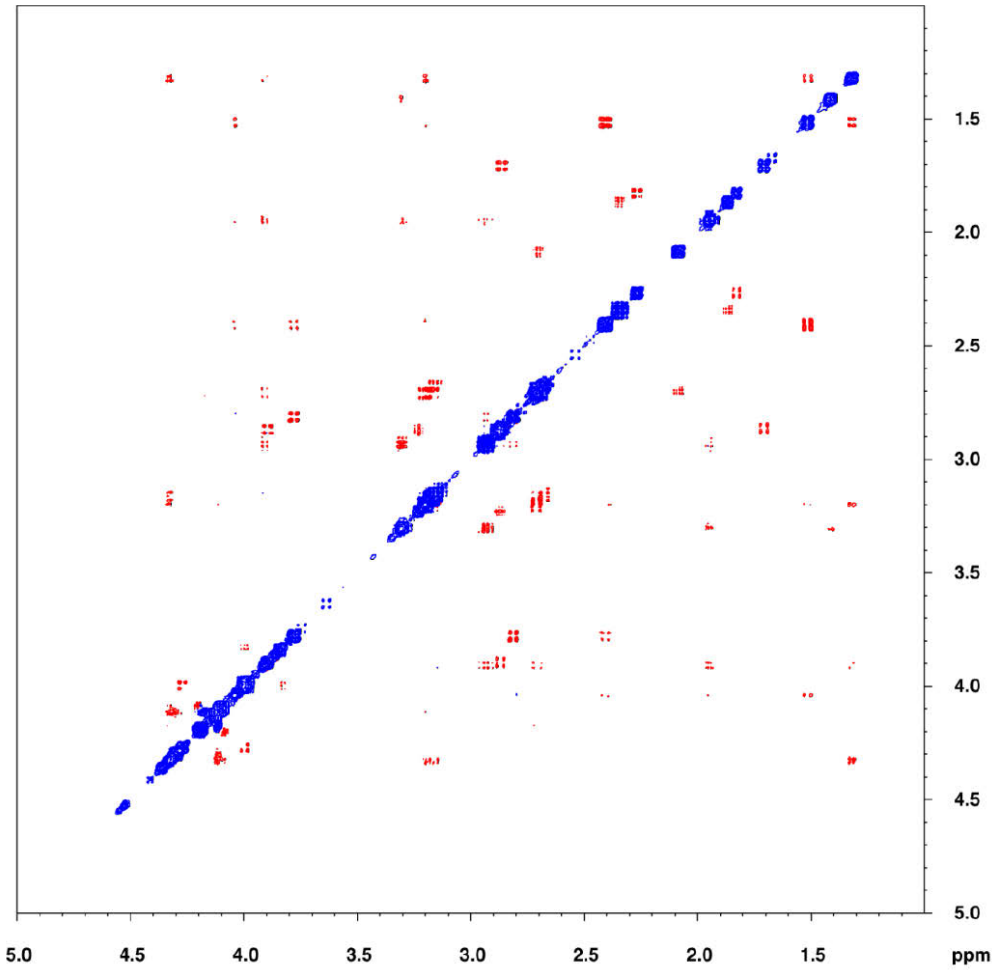

Figure 2.10: NOESY spectrum of strychnine. NOE correlations are shown in red.

b) Decoupling in the F1 dimension

The Zangger-Sterk element can be applied to most of 2D homonuclear experiments[26]. The decoupling motif is introduced into the t_1 evolution time of the NOESY pulse sequence. (Figure 2.11)

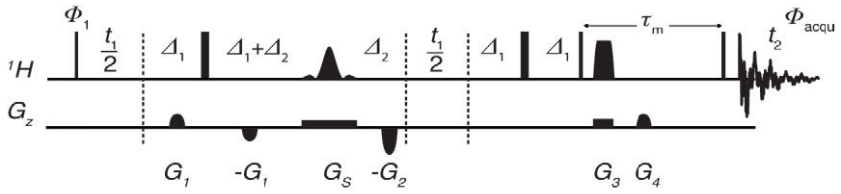

Figure 2.11: Pulse sequence of the BBHD-NOESY experiment

Because of the lack of sensitivity due to the use of the Zangger-Sterk element, the BBHD-NOESY spectrum shown in Figure 2.12 presents a lower signal to noise ratio leading to the observation of t_1 noise masking some signals. This issue will be discussed in Chapter 4. However, the reduction of the multiplicity of signals allows to recover the full intensity of signals. More cross-peaks are therefore visible, for protons at 2.7 ppm for instance, leading to a better documentation of the 3D structure of the studied molecule.

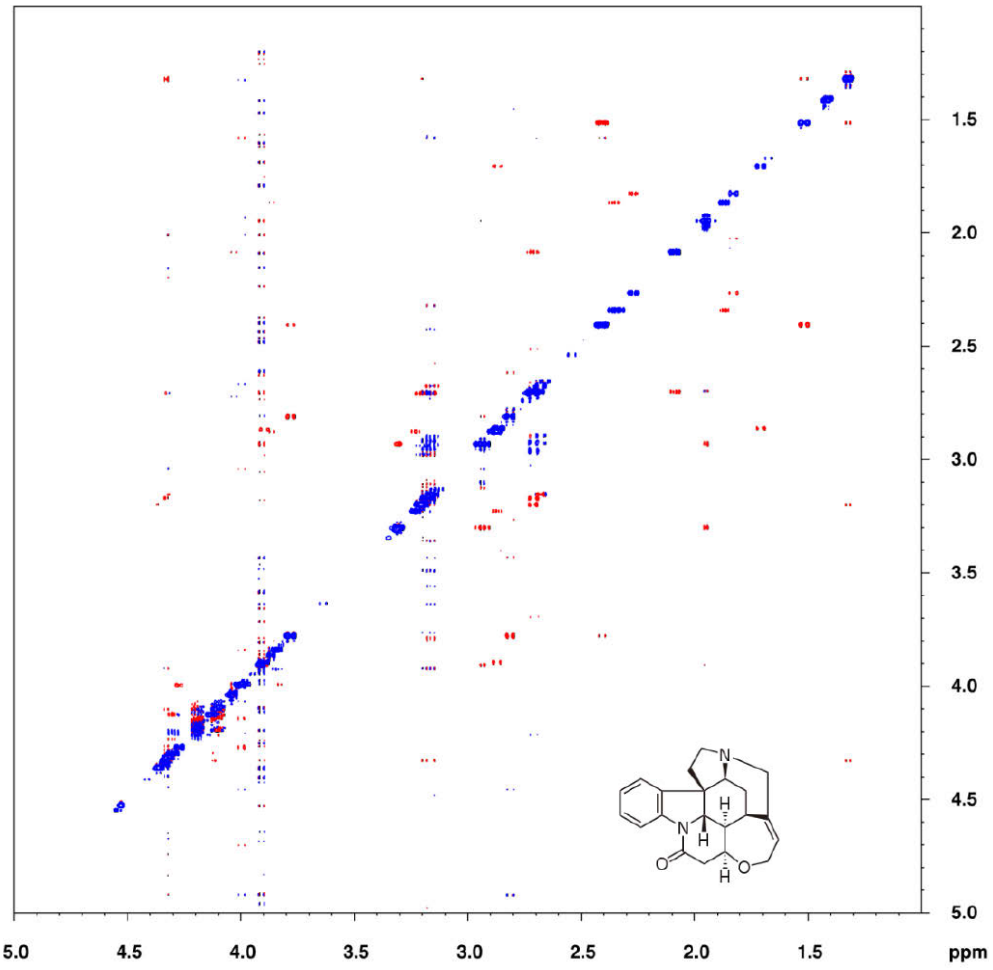

Figure 2.12: BBHD-NOESY spectrum of strychnine. Because of the low sensitivity of the experiment due to the ZS element, t_1 noise is visible and cannot be removed efficiently by symmetrization without introducing wrong correlations in the spectrum. Nevertheless, it is clearly visible that signals are decoupled in the F1 dimension.

3) 2D BBHD-COSY

The introduction of the Zangger-Sterk element in the evolution time of the COrrelation SpectroscopY experiment[11] is not straightforward. Although the COSY spectrum shares the same kind of information with the TOCSY spectrum, this experiment requires another type of magnetization. Indeed, the pulse sequence generates anti-phase magnetization responsible of the cross-correlations. Unfortunately, this type of magnetization is not well supported by the Zangger-Sterk element which creates in-phase magnetization. For this reason, Morris et al.[27] have proposed the Constant Time approach, which can be used with anti-phase signals, for decoupling COSY spectra (Figure 2.13).

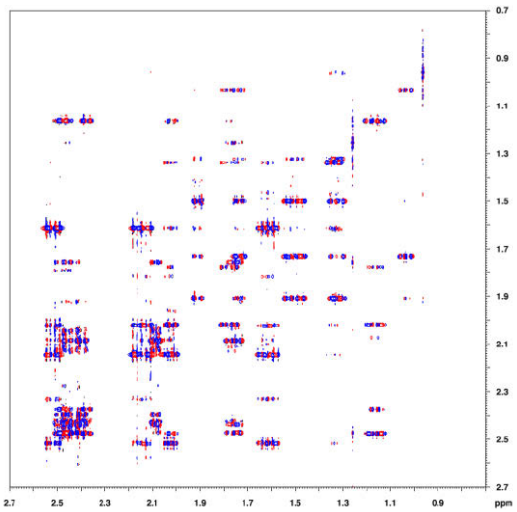

Figure 2.13: CT-COSY spectrum recorded with a 3-quanta filter.

In spite of this difference, it is possible to record a COSY spectrum with the Zangger-Sterk decoupling in the F1 dimension. For this purpose, one needs to slightly modify the pulse sequence shown in figure 2.14.a. By adding a spin-echo[5] before the acquisition time (Figure 2.14.b), scalar couplings can evolve again in order to generate cross-peaks in the spectrum. However, it has to be noted that all coupling information of a molecule cannot be recover from only one spectrum. Indeed, the signal is dependent of the coupling contribution represented by sin 2π J τ. If τ is equal to 1/(4J), the cross-peak corresponding to the signal will appear in the spectrum. Otherwise, if τ is shorter, scalar coupling would not have enough time to evolve and decoupling would cause signal cancellation.

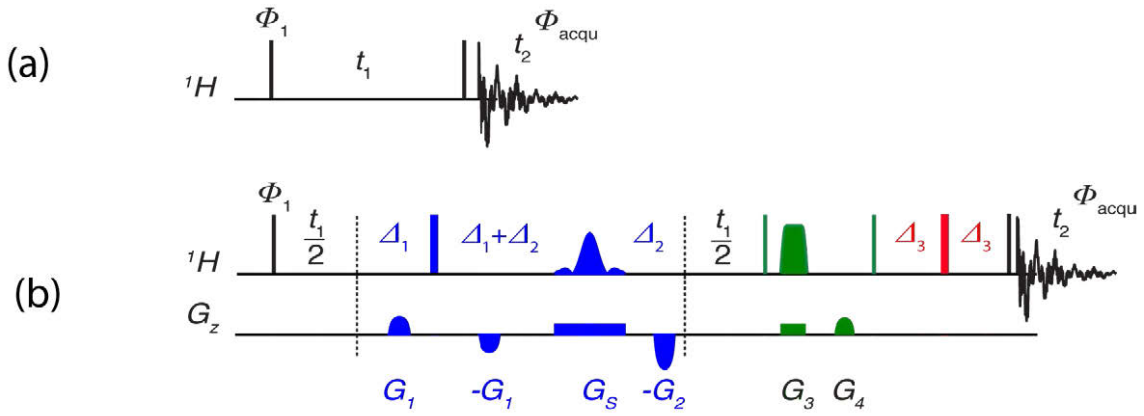

Figure 2.14: Pulse sequences of COSY (a) with decoupling during the t_1 evolution time (b). The Zangger-Sterk element, the modified z-filter and the extra spin-echo are shown in blue, green and red respectively.

One has to record different spectra in order to obtain all the necessary data for the study of a particular molecule. Hereafter is the example of the 4-androstene-3,17-dione. Three different spectra have therefore been acquired in order to cover the range of coupling constant values of this molecule (from 2 to 20 Hz) (Figure 2.15).

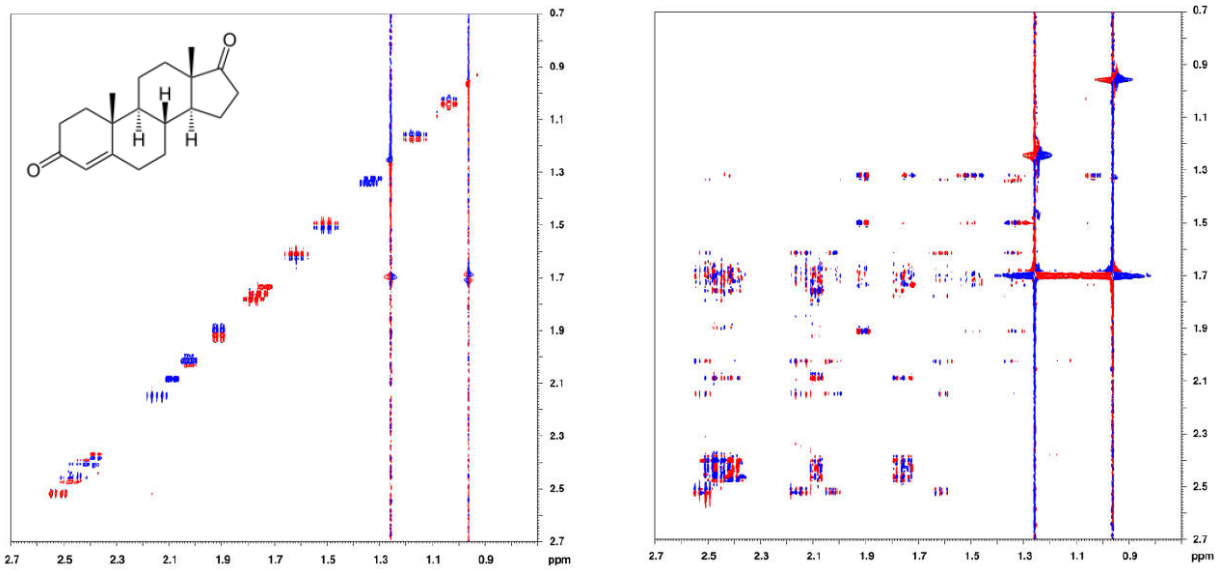

Figure 2.15: COSY spectra of 4-androstene-3,17-dione recorded without (left) and with (right) the extra spin-echo element before the acquisition time. On the left spectrum, no cross-peaks are observable since no anti-phase magnetization is generated by the pulse sequence. On the right spectrum, the addition of the spin-echo element allows the evolution of scalar coupling depending on the coupling constant range value chosen for the delay of the spin-echo (Δ_3 = 1 /4J with J equal to 15Hz for this spectrum). Cross-peaks can therefore be generated and decoupled in F1.

4) Experimental conditions

Two samples were used for the setting up of the BBHD-experiments. These samples were chosen regarding to their complex coupling networks with expression of second-order effects and a high degree of overlapping signals in their 1D proton spectra. Their assignments are presented in Appendix A.

20 mg of 4-androstene-3,17-dione dissolved in 700 µL of $CDCl_3$ in a sealed standard 5 mm NMR tube were used for BBHD-TOCSY and BBHD-COSY experiments. 32 mg of strychnine were dissolved in 700 µL of $CDCl_3$ in a sealed standard 5 mm NMR tube and used for BBHD-NOESY experiments.

Spectra were collected at 298 K on a Bruker 500 MHz spectrometer with a 5 mm DCH ^{13}C-$^{1}H/D$ cryogenic probe equipped with a z-gradient coil.

The parameters used for **Zangger-Sterk element** are identical in all sequences. The selective refocusing pulses applied during the spatial encoding were Rsnob. A compromise between the selectivity of the pulse and the sensitivity of the experiment led to the choice of a 30 ms

selective pulse refocusing a bandwidth of 77.7 Hz. The amplitude of the rectangular encoding gradient G_S depended of the spectral window to cover, corresponding to 0.13 G/cm for the androstenedione sample (to cover 2 ppm) and 0.26 G/cm for the strychnine sample (to cover 4 ppm). The gradients for coherence pathway selection G_1 and G_2 were set to 19.5 G/cm and 39 G/cm respectively. Delays $\Delta 1$ and $\Delta 2$ were set to 1 004 µs and 1 104 µs respectively.

The **z-filters** were calibrated following the instructions of Keeler et al.[17]. A Chirp pulse was used with duration of 40 ms. A second z-filter was used in the case of TOCSY experiment with a second Chirp pulse lasting 30 ms. Pulsed field gradients G3 and G4 had rectangular shapes with amplitudes of 3.25 G/cm and 26 G/cm respectively.

The durations of 90 degree and 180 degree hard pulses were 9.95 µs and 19.80 µs respectively. Recovery delay was set to 2s for both small molecules.

Broadband homodecoupled spectra were sampled according to the States-TPPI quadrature detection mode. Pulses were all along x except the first 90 degree pulse which underwent a two-step phase cycling with detection. Spectra with zero-quantum elimination were recorded with the TPPI quadrature.

For **TOCSY** spectra, two scans of 4096 data points were acquired for each of 512 t_1 increments, with spectral width of 2 ppm in both dimensions. The mixing time was set to 80 ms. The experimental time were 1h 13 min 56s, 43 min 5s and 1h 15 min 36s, for TOCSY, ZQ-TOCSY and BBHD-TOCSY experiments respectively.

NOESY spectra were acquired with a spectral width of 4 ppm in both dimensions and 512 t_1 increments for each of the two scans. The mixing time was set to 400 ms. The experimental time was 1h 2min 6s for the ZQ-NOESY and 2h 2min 29s for the BBHD-NOESY. The number of scans was doubled for the decoupled experiment in order to record a spectrum with a higher sensitivity.

For **COSY** spectra, the spectral window was set to 2 ppm and sampled with two scans and 256 t_1 increments. Parameters of the Constant-Time-COSY experiment have been set for a 3-QF as described by Morris et al.[27]. The additional spin-echo has been set for a scalar coupling of 15 Hz which corresponds to a delay Δ_3 of 16.6 ms. Experimental times were equal to 39 min 7s and 36min 20s respectively for CT-COSY and BBHD-COSY.

All pulse sequences discussed in this chapter are available in Appendix B.

Chapter 3: 1D BroadBand HomoDecoupling

In 1D spectra, proton-proton couplings provide important information about the structure of the analyzed molecule. But because of this splitting induced by scalar couplings, multiplets can be very broad (up to 50Hz) and overlap with other signals. It becomes therefore useful to decouple proton spectra and record pure shift experiments. The main issue related to homonuclear proton decoupling is the impossibility to observe and decouple the same channel with actual NMR spectrometer. Proton decoupling[28-35] had thus been studied for decades by researchers wanting to simplify proton spectra.

In this chapter, a review of the existing methods of proton decoupling will be presented and a new approach will be introduced.

1) Review of proton decoupling methods

There are two types of scalar couplings: homonuclear coupling which exists between nuclei of same nature and heteronuclear coupling between different nuclei. The heteronuclear decoupling is well-known and applied regularly when recording 1D carbon spectra. Proton-carbon ^{1}J couplings are removed by irradiating, in a broadband way, protons frequencies during the acquisition of spectra on the carbon channel. This broadband irradiation cannot be applied in the case of the removal of homonuclear couplings. However, it is possible to selectively irradiate a limited frequency range and to observe the resulting transformations on other signals (Figure 3.1).

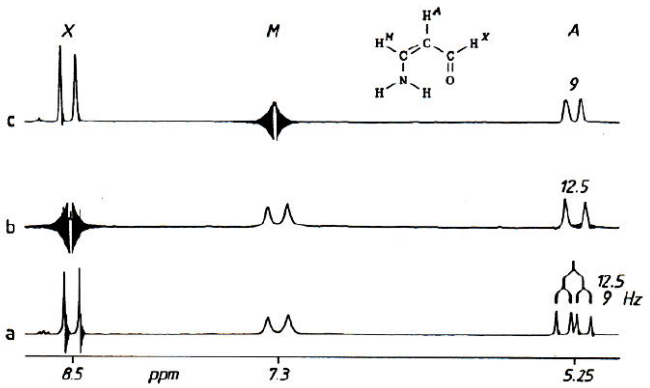

Figure 3.1: Illustration of partial proton decoupling by selective irradiation of signals[36]. (a) classical 1D spectrum, (b) spectrum obtained after selective irradiation of H_X, (c) spectrum recorded with selective irradiation of H_M. The irradiation of H_X leads to the reduction of the multiplicity of the signal of H_A, from doublet of doublets to doublet. The coupling J_{AX} have been removed by saturation. Likewise, the selective irradiation of H_M leads to the elimination of the coupling between H_M and H_A. Protons M and X being not scalarly coupled together, their signals are unaffected during irradiation of one or the other. Only the irradiation of H_A can transform the look of their signals.

a) J-resolved experiment

The first method leading to the obtention of decoupled proton spectra has been the J-resolved spectroscopy[28] developed by Ernst and co-workers in 1976 (Figure 3.2).

Figure 3.2: Pulse sequence of J-resolved experiment

This experiment, based on the spin-echo, is separating chemical shift and scalar coupling information in two distinct dimensions. It is thus possible to analyze one of these parameters without interferences of the second. Chemical shift are expressed in F2 and scalar coupling in F1.

The spectrum is presented as a 2D map where signals are centered at their chemical shift in F2 following a slope of 45 degrees to the F1 dimension (Figure 3.3.A). The projection along the F2 axis of that spectrum leads to the classical 1D proton spectrum where chemical shift and coupling information are mixed together. A particular process of the 2D map is necessary to obtain the 1D spectrum without couplings.

The processing of the 2D spectrum takes place in three steps: shearing, symmetrisation and projection. Signals being tilted, one has to rotate all the signals individually by 45 degrees around their mid-point. Multiplets are then lying along the F1 axis allowing to observe singlets in the F2 projection. The second processing step corresponds to the t_1 noise suppression. Before the shearing of the signals, t_1 noise bands are vertical. With the spectrum tilting, orientations of signals and t_1 artifacts are switched, artifacts are shown with a 45 degree angle whereas signals are parallel and centered in F1 = 0 (Figure 3.3.B). The symmetrisation step leads to the suppression of all non-symmetrical signal or artifact (Figure 3.3.C). This must be carefully applied since it may enhance artifacts that have coincident symmetry, giving them the appearance of genuine signals[37]. Lastly, the multiplet projection along F2 gives a 1D spectrum where only singlets are visible (Figure 3.3.D) while a F1 cross-section gives access to the multiplicity of each signal enabling a direct measurement of coupling constants (Figure 3.3.E).

However, this method has been set aside for years because of two important drawbacks. First, signals are phase-modulated resulting in the presence of signals with phase-twist distorsion. As this modulation is unavoidable, the 2D spectrum is shown in magnitude mode. Unfortunately, the 1D spectrum obtained after projection shows very broad signals (linewidth of 2.8 Hz for androstenedione sample) which decrease the spectral resolution. Moreover, the relative intensity of signals may vary because of this phase-twist distorsion leading to inaccurate integration of signals. The second issue is about strong coupling. Indeed, second-order effects manifest themselves with the apparition of additional peaks around the strongly coupled spins signals. These artifacts can be only limited by recording experiments on higher

field spectrometers. Keeler et al.[38] have enhanced the J-resolved experiment by introducing a double spin-echo. This method leads to the removal of strong coupling artifacts after symmetrisation in order to obtain a proton decoupled proton spectrum free of second-order artifacts.

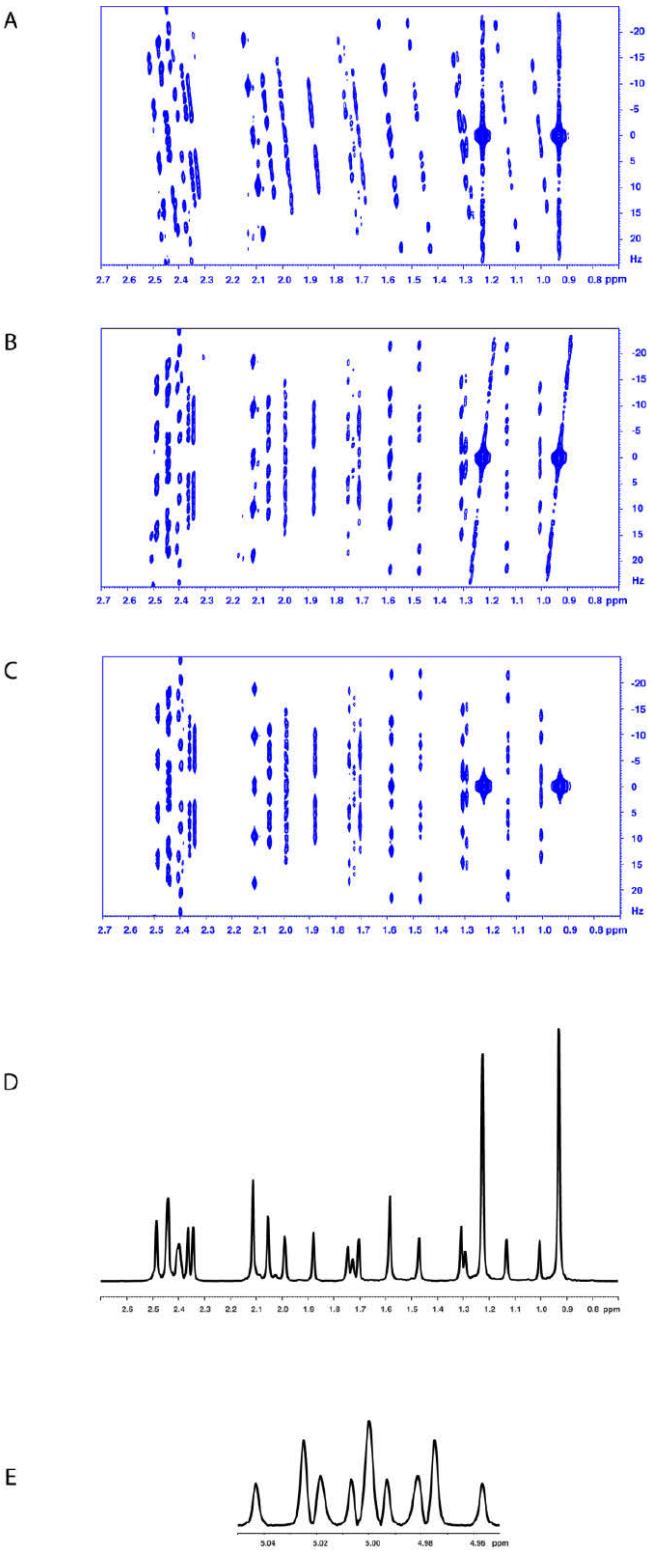

Figure 3.3: Spectra recorded with the J-resolved pulse sequence. (A) J-resolved spectrum of 4-androstene-3,17-dione. (B) J-resolved spectrum after tilting of 45 degrees. (C) J-resolved spectrum after

shearing and symmetrisation. (D) and (E) Projection along F2 and cross-section of the multiplet at 1.54 ppm.

b) Keeler's experiments

Keeler and coworkers have proposed in 2007 two different approaches leading to the obtention of 1D proton decoupled proton spectra.

α) J-spectroscopy experiment

They have developed their own J-spectroscopy experiment[33] using spatial encoding. Their method lies on the combination of two spectra, called J- and anti J-spectra in order to obtain a spectrum with pure absorption signals without phase-distortion.

These two spectra present phase twist lineshapes but if the F1 axis of the anti J-spectrum is reversed and the two spectra added together, the dispersive parts of the phase-twist lineshapes cancel. It is essential that the two spectra have the same intensity; otherwise the suppression of the dispersive component will not be complete. This can only be done using spatial encoding. Indeed, the use of a selective pulse during a z-gradient allows to select the same spins during the acquisition of the spectra and therefore insures an identical intensity. The main drawback is the considerable reduction of the sensitivity of the experiment.

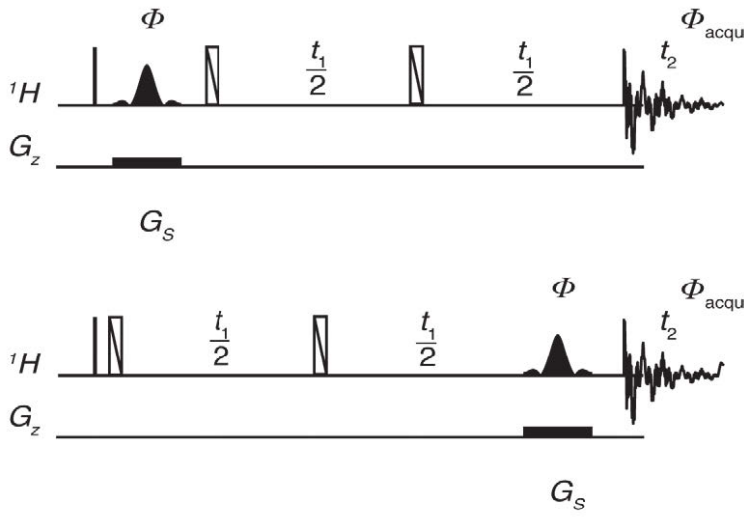

Figure 3.4: Pulse sequences used to record J- and anti J-spectra. The selective pulses are used to select the right coherence transfer pathway. BIP pulses[39] are represented by unfilled rectangles with the diagonal stroke.

The absorption mode J-spectrum (Figure 3.5) recorded with the pulse sequence shown in Figure 3.4 does not exhibit any cross-peaks therefore simplifying the processing steps to get the 1D decoupled spectrum.

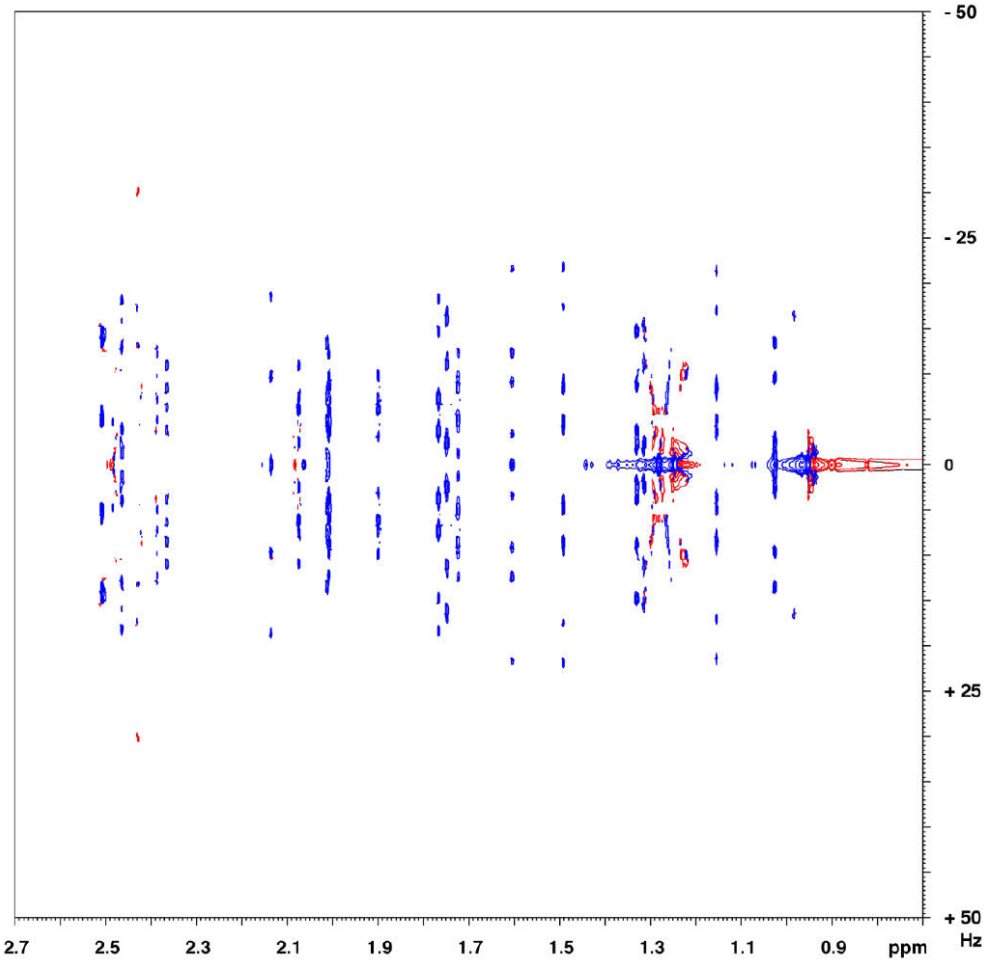

Figure 3.5: 2D spectrum recorded with the J-spectroscopy pulse sequence, after tilting and symmetrization.

This spectrum is processed following the same steps as the J-resolved experiment. Peaks have to be tilted along the F2 dimension and symmetrized before conversion of the 2D spectrum into 1D spectrum.

The good separation of signals in the 2D spectrum is conserved in the 1D spectrum. This experiment has been described as retaining the natural intensities and displaying correct integration of peaks which is, unfortunately, not exactly the case with the spectrum recorded for our test-molecule, as it can be seen in Figure 3.6.

In the case of strongly coupled spins, extra response can be seen in pairs, one peak is positive the other is negative. Because they have opposite signs, these artifacts are cancelled in the projection leading to a 1D homodecoupled spectrum without strong coupling artifacts. The cancellation of these peaks is complete only for modest strong coupling. Some responses are

still appearing in spectra for stronger coupling but do not damage integrals. The five signals with a chemical shift above 2.3 ppm are usually exhibiting a huge decrease in their intensity due to strong coupling artifacts. Here, intensities are approximately correct.

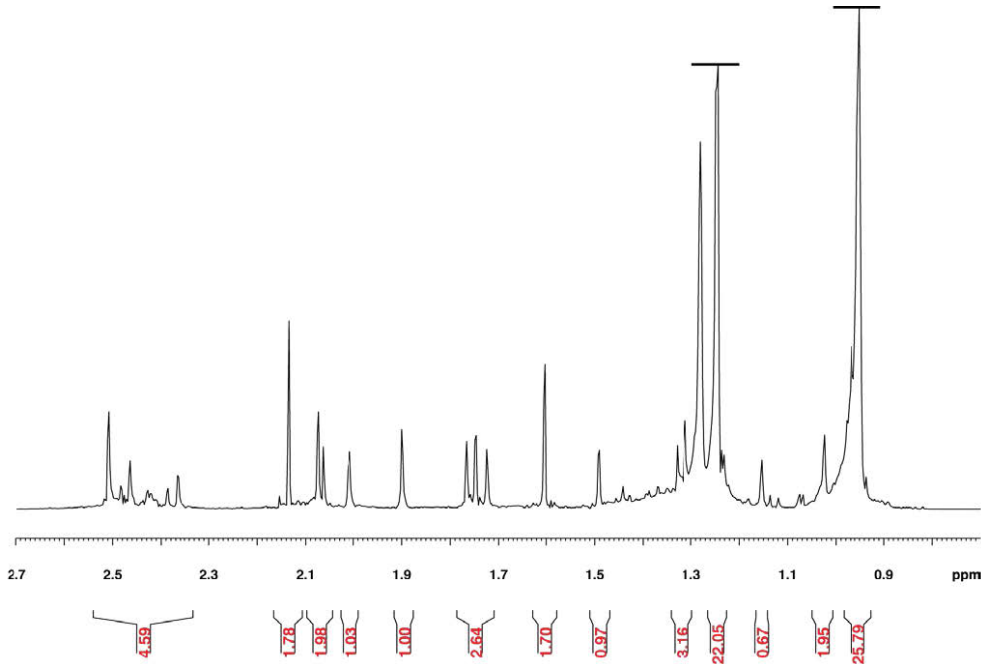

Figure 3.6: 1D decoupled spectrum obtained from J-spectroscopy experiment. Integrals are shown in red.

β) Anti z-COSY experiment

The second experiment developed in the group of Keeler is an alternative to J-resolved spectra and experiments based on the spatial encoding.

The anti z-COSY experiment[34] allows to obtain 1D homodecoupled proton spectra with absorption lineshapes and reliable integration starting from a particular 2D COSY experiment.

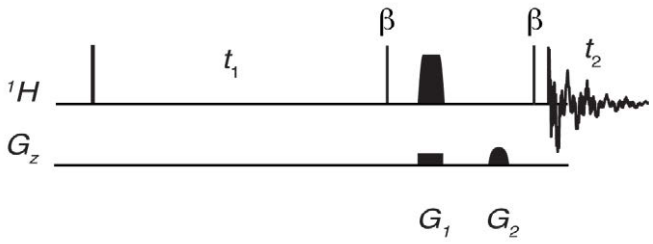

Figure 3.7: Pulse sequence used to record anti z-COSY spectra. Small flip angles pulses are used at the end of t_1 and before detection.

The z-COSY experiment differs from the COSY experiment by its mixing time. Indeed, instead of being composed of one 90 degree pulse, the mixing time of the z-COSY sequence exhibits two small flip angle pulses spaced by a delay. These two pulses have a tip angle β equal to a value between 10 and 20 degrees which is responsible for a reduction of the sensitivity, spins being not totally flipped in the transverse plane.

The anti z-COSY sequence displays, at the beginning of the mixing time, a pulse with an angle equal to β + 180 degrees. Due to this pulse, diagonal peaks are now lying on a line perpendicular to the diagonal. The projection of these multiplets along the diagonal will give only singlets.

The β + 180 degree pulse can be replaced by a β pulse when a modified z-filter is introduced in the mixing time of the pulse sequence (Figure 3.7) leading to the elimination of the ZQ coherence. Peaks have therefore a pure absorption lineshape.

In order to avoid the projection of cross-peaks on the diagonal, a small flip angle pulse is used to limit the intensity of cross-peaks. But β has to be large enough to record diagonal peaks with an acceptable intensity. The spectral width in F1 is also limited to few hundreds of Hertz (Figure 3.8).

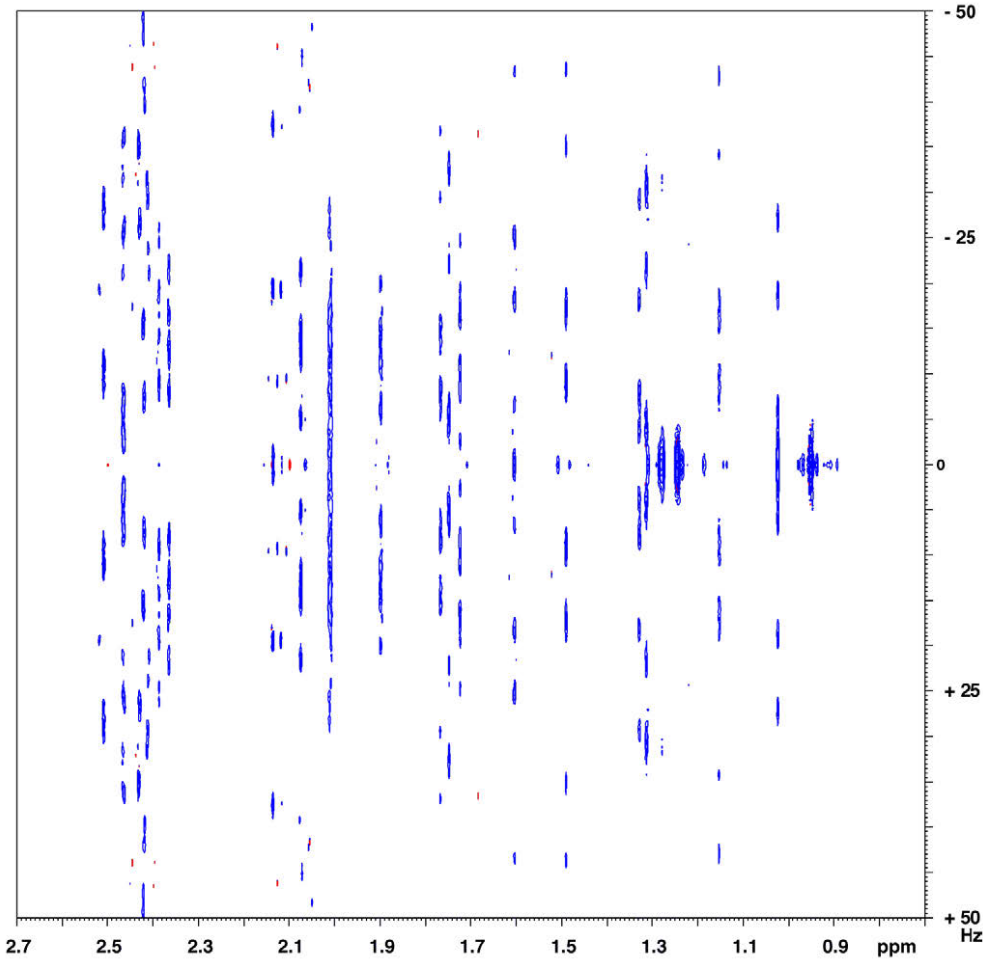

Figure 3.8: Anti z-COSY spectrum of 4-androstene-3,17-dione after peak tilting.

The processing of the 2D spectrum is similar to the processing of J-resolved experiment. First, diagonal signals have to be titled by 45 degrees in order to obtain vertical multiplets. Then, a projection along the F2 dimension is done to get a 1D spectrum exhibiting only absorption singlets (Figure 3.9) whereas a cross-section of the 2D map allows the extraction of coupling constants from each multiplet.

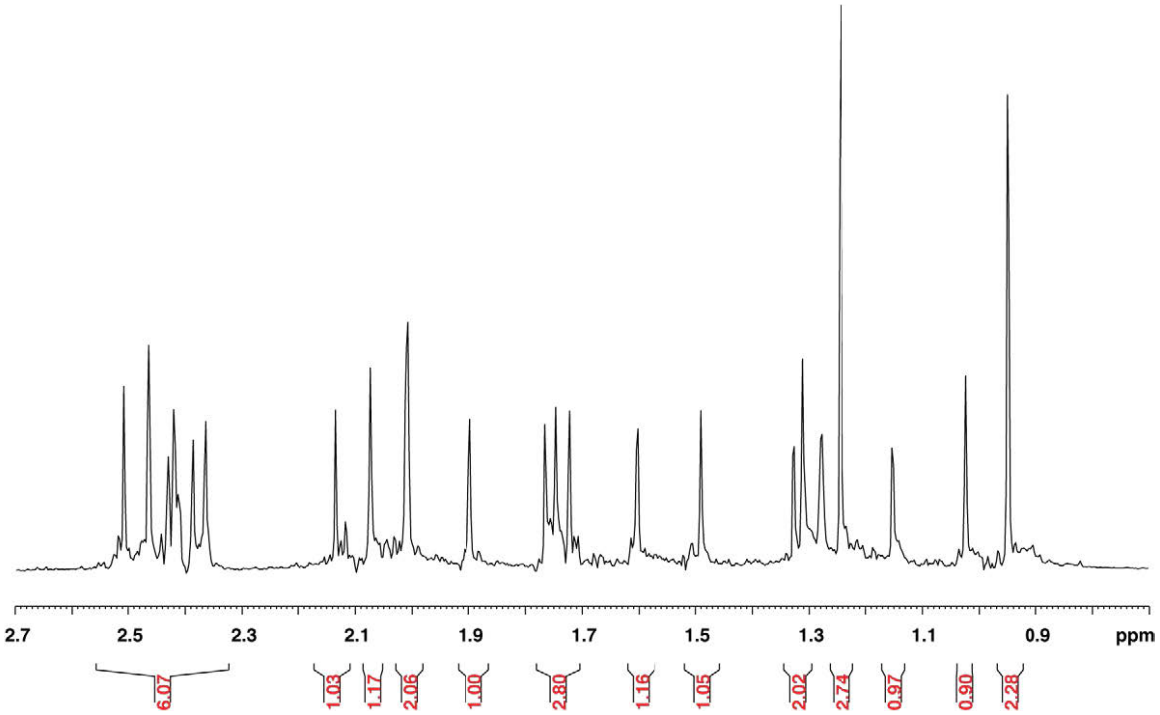

Figure 3.9: 1D proton decoupled proton spectrum obtained from 2D anti z-COSY spectrum. Integrals are shown in red.

This experiment is sensitive to strong coupling artifacts that cannot be suppressed by symmetrisation of the 2D spectrum, extra responses are therefore observed on the corresponding 1D spectrum which is also displaying accurate integrals (Figure 3.9).

c) BIRD experiment

This decoupling method is based on the presence of ^{13}C nuclei in molecules. Indeed, the BIRD experiment[29, 40-41] (Figure 3.10) leads to the proton decoupling by selecting those attached to ^{13}C. Due to its low natural abundance, molecules are containing, depending on the size of the molecule, only one atom of this isotope over all carbon nuclei. It is therefore quite

simple to refocus scalar couplings of proton directly bonded to ^{13}C by inverting all protons linked to ^{12}C and then to observe only the signals of protons attached to ^{13}C.

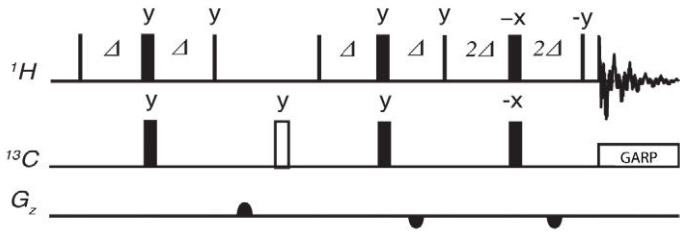

Figure 3.10: Pulse sequence of a BIRD experiment[41]. The INEPT block (the four first pulses) allows the selection of protons bonded to ^{13}C only, and then occurs the decoupling. The white rectangle is alternately used for the suppression of ^{12}C contribution.

Despite of its efficiency and robustness, this method is suffering from two important limitations. Indeed, the decoupling is effective only for protons directly bonded to a carbon isotope with a low natural abundance. The sensitivity of the experiment is limited to 1% of the full signal. This experiment also requires ^{12}C atoms to remove scalar coupling, it cannot be applied to fully enriched ^{13}C samples. The second drawback concerns the decoupling of diastereomeric protons. Indeed, two inequivalent geminal protons being bonded to the same carbon, they cannot be decoupled from one another by using BIRD-based homonuclear decoupling sequences.

d) Zangger-Sterk based experiments

The largest family of homodecoupling methods derives from the experiment of Zangger and Sterk[6] (Figure 3.11).

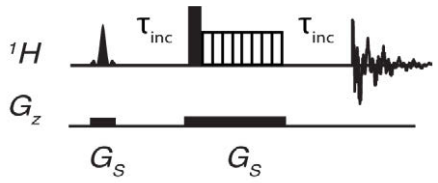

Figure 3.11: Pulse sequence of the experiment developed by Zangger and Sterk in 1997.

In 1997, Zangger and Sterk have proposed a new method using spatial encoding in order to suppress the scalar coupling contribution of each spin of a sample. The decoupling of a spin at time τ can be realized by inverting its coupling partners at the time $\tau/2$.

For this purpose, several spectra are recorded in a 2D manner. Their decoupling element, presented in Chapter 1, is inserted in the middle of an incremented time (Figure 3.11). At the

beginning of the detection period, all scalar coupling have been totally suppressed. The first points of each recorded FID are extracted and assembled into a new FID which is then processed using the usual procedure. This method leads to the obtention of a 1D proton decoupled proton spectrum.

However, this ingenious method presents two drawbacks. Strongly coupled spins are decoupled at the expense of several extra responses called strong coupling artifacts. The 180 degree selective pulse cannot invert one coupling partner without affecting the other at the same time due to their proximity in the spectrum. The second drawback is probably the major one: the sensitivity of this experiment is really low due to spatial encoding. It has been evaluated as 3% of the maximum signal.

This method has been rediscovered recently by two independent NMR groups who modified it to improve its efficiency.

Both have introduced pulsed field gradients to properly suppress signals coming from coupling partners (Figure 3.12).

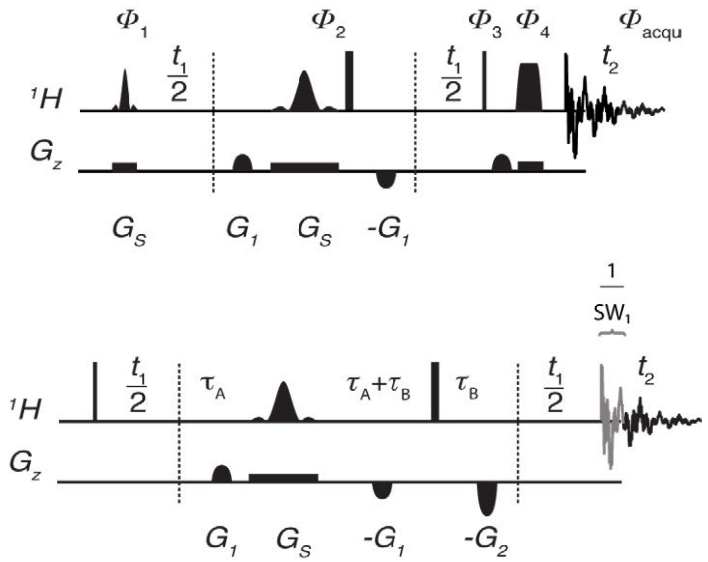

Figure 3.12: Pulse sequence of the δ-resolved experiment of Giraud et al.[9] (2009) (top) and pulse sequence of the pure shift experiment of Morris and coworkers[35] (2010) (bottom).

In the pure shift sequence[35] developed by Morris and coworkers (Figure 3.12.bottom), the selective pulse which is performing the initial spin excitation has been replaced by a 90 degree hard pulse. It allows to reduce the presence of artifacts coming from the imperfection of the slice selective excitation and the problem of diffusion of spins in the sample.

The construction of the new FID has also been modified. The decoupling is effective at the end of the t_1 time. However, the acquisition of the spectrum starts before the end of the evolution time. The acquisition of data chunks, as it was done in the ZS sequence, is now centered at t_1 rather than starting at t_1 allowing to double the width of the chunks.

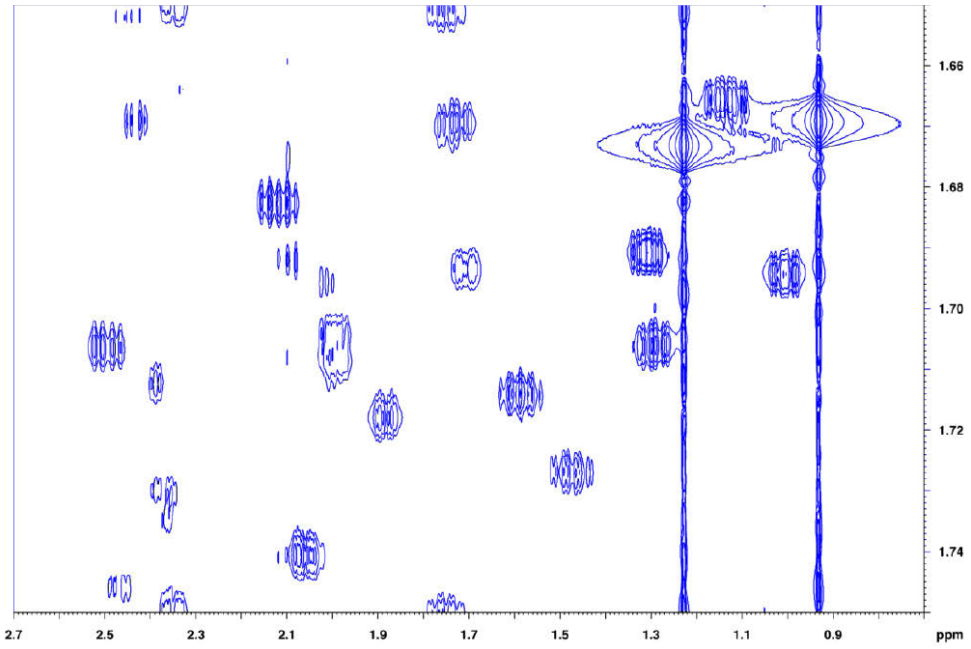

Figure 3.13: 2D pure shift spectrum of 4-androstene-3,17-dione

The 2D pure shift spectrum (Figure 3.13) is then processed using a program that reconstructs the data into a 1D spectrum (Figure 3.14). Because the duration of chunks is reversely proportional to the width of the 2D spectrum in the F1 dimension, it is required to reduce SW_1 to a small value. Only few t_1 increments are recorded making quite short (only few minutes) the acquisition of this spectrum.

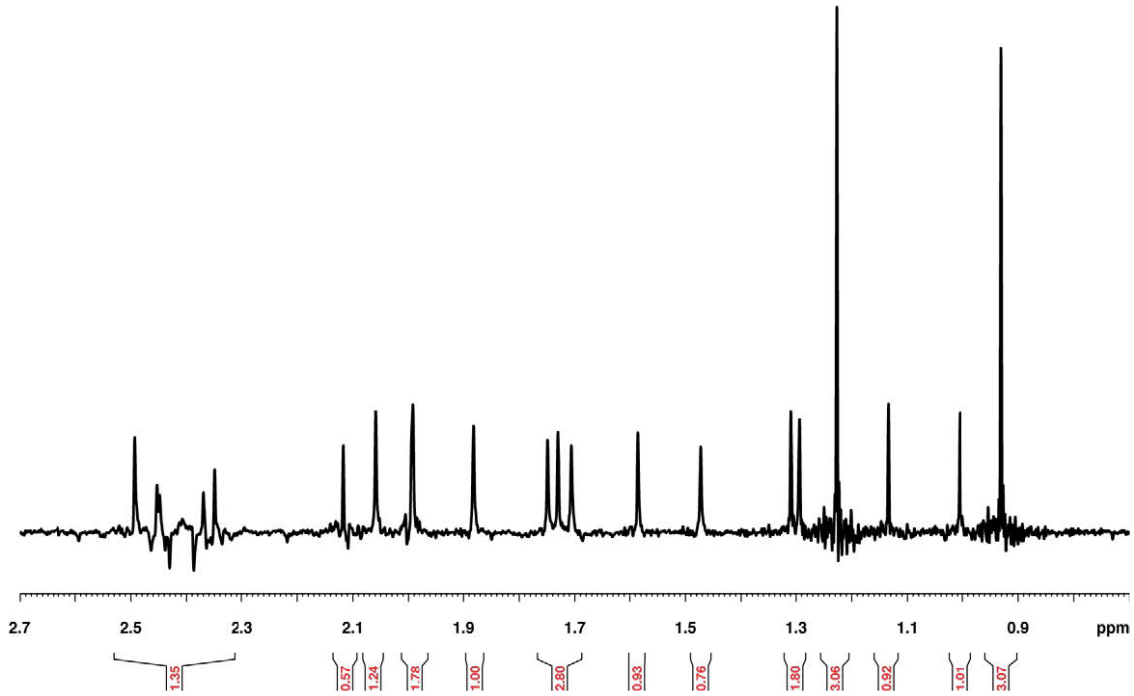

Figure 3.14: 1D pure shift proton spectrum

2) A new decoupling approach

a) ZS-DIAG experiment[42]

Our approach, as most of the methods described in this chapter, is based on the decoupling motif developped by Zangger and Sterk[6] in 1997. Placed in the middle of the t_1 evolution time of the TOCSY experiment[19], it allows to refocus scalar couplings and thus to record signals with singlet lineshape in the indirect dimension of the 2D spectrum.

When the mixing time of the TOCSY contains a spin-lock element, the magnetization of each spin is relayed in all the spin system letting us to trace out the coupling network from proton to proton whatever the distance between them. In the frame of our approach, the mixing time of this 2D experiment only contains the two modified z-filters[17] responsible for the suppression of the ZQ coherence (Figure 3.15). Only diagonal peaks are thus recorded, the spectrum being empty of cross-peaks. We called this experiment the 2D ZS-DIAG experiment[42].

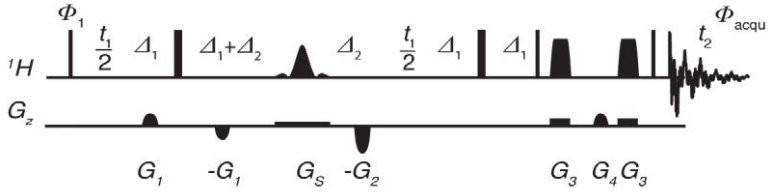

Figure 3.15: Pulse sequence used for the acquisition of 2D ZS-DIAG spectra.

Thanks to the ZS element, recorded diagonal signals are decoupled in the indirect dimension while a complete coupling structure is visible in the directly detected dimension (Figure 3.16). The extraction of cross-sections along F2 leads to the obtention of the trace of each signal with the full multiplicity observable in the classical 1D spectrum.

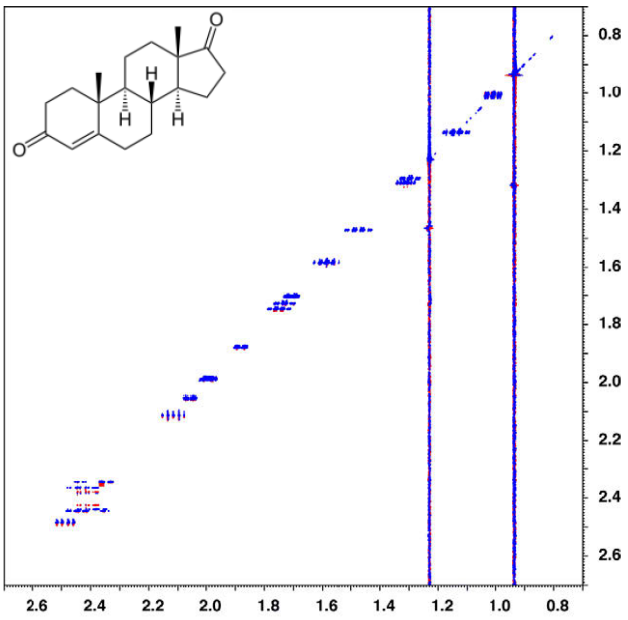

Figure 3.16: 2D ZS-DIAG spectrum of 4-androstene-3,17-dione showing decoupled signals only in F1 .

b) 1D homodecoupled proton spectra[42]

The 2D ZS-DIAG experiment being phase-sensitive, it is vital to properly set the phases of the spectrum prior further post-processing. From this 2D map, it is possible, using a Bruker AU program[43], to extract each signal with a singlet lineshape and to sum them into a 1D spectrum.

This post-processing program works within three steps. First, the diagonal is localized in order to identify the center of each diagonal signal. Then, on each encountered signal, an integration is performed over 50 Hz which is the highest width of a multiplet. There is thus no interference from other signals except in the case of strongly coupled spins. In this case, second-order effects can lead to the overlap of signals of interest with artifacts, leading to an over estimation of the intensity of the concerned signal. Finally, the obtained singlet is added in a 1D spectrum. Figure 3.17 shows how this post-processing is applied to a 2D ZS-DIAG spectrum.

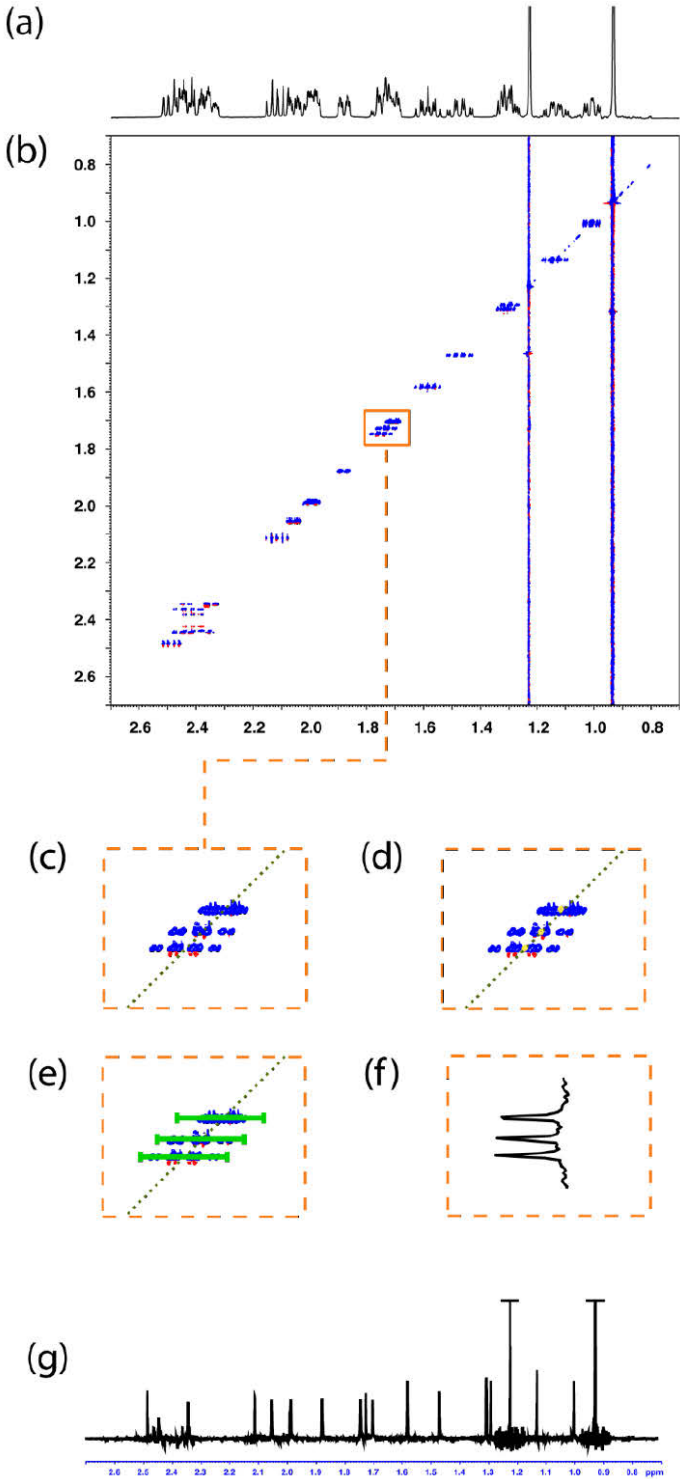

Figure 3.17: Illustration of the processing of the 2D ZS-DIAG experiment leading to the obtention of the corresponding 1D homodecoupled proton spectum. (a) Classical 1D proton spectrum of 4-androstene-3,17-dione. (b) 2D ZS-DIAG spectrum. (c) Expansion of the 2D map on the three signals at 1.7 ppm. The program first identifies the diagonal, represented by the dashed green line, in order to localize the center of each signal, shown by the yellow dots in (d). Each multiplet is integrated over 50 Hz (e). The corresponding singlets of the three signals selected in (c) are shown in (f). This post-processing is done to all signals identified as a diagonal signal. The 1D proton decoupled proton spectrum of 4-androstene-3,17-dione is shown in (g).

No window function is necessary to improve the shape of the signals before the post-processing program is launched since the lineshapes are supposed to be the ones determined by relaxation. As most of 1D proton decoupled proton spectra, integrals are said to be approximately quantitative as it shown in Figure 3.18. Indeed, it is possible that spins relaxed during the pulse sequence. On this account, their integrals may be weaker than integrals obtained with classical spectra recorded with an adequate relaxation delay for quantification. A normalization of the 1D homodecoupled spectrum with a standard 1D spectrum is therefore proposed to recover the real intensities and integrations, especially in the case of strongly coupled spins.

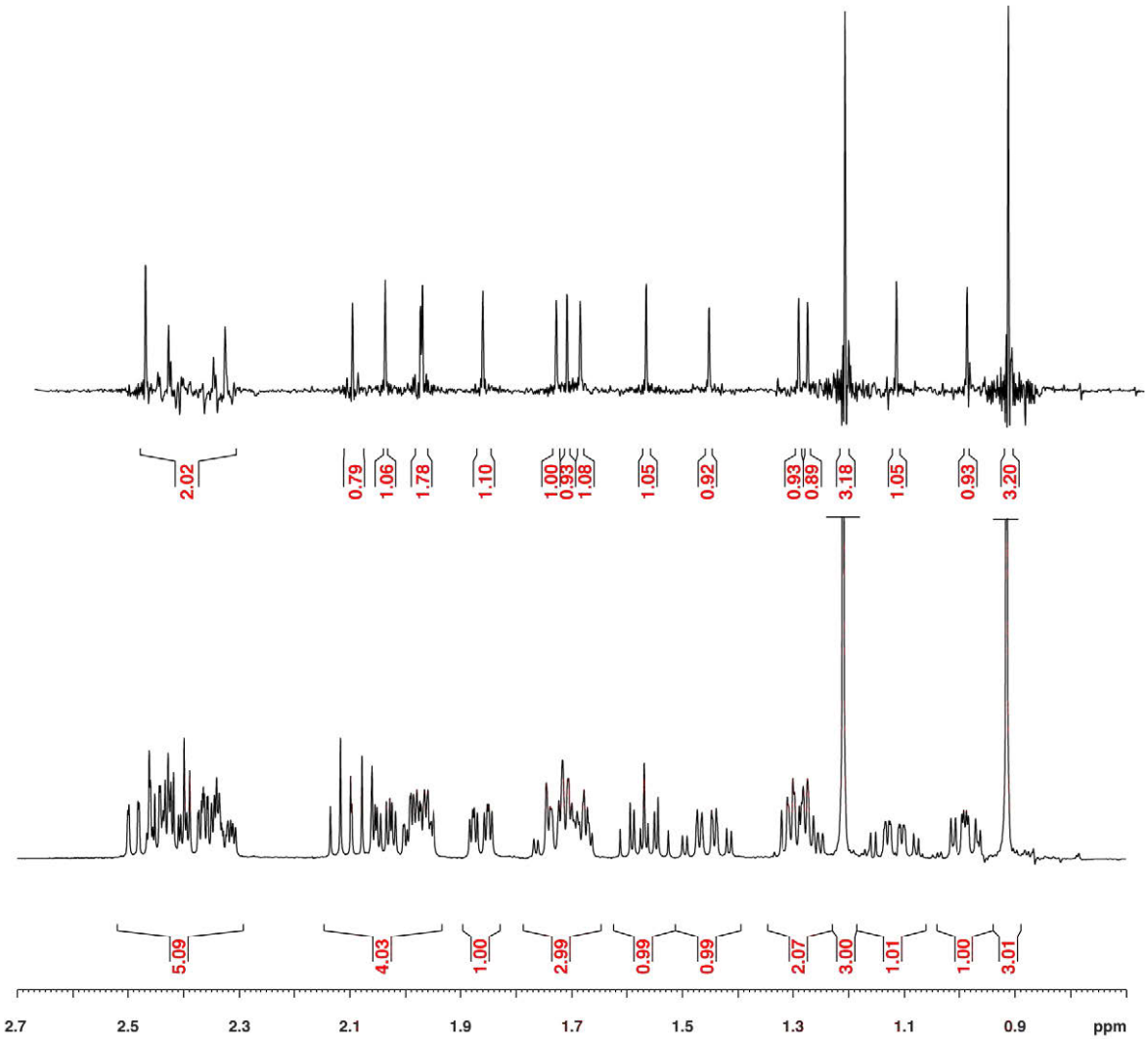

Figure 3.18: 1D standard and homodecoupled spectra of 4-androstene-3,17-dione obtained from the 2D ZS-DIAG. Integrals, shown in red, are said approximately quantitative. Signals at 1.7 ppm are exhibiting integrals in accordance with those found in the standard 1D spectrum. However, signals between 2.3 and 2.5 ppm show reduced integrals due to the presence of strong coupling artifacts.

c) Measurement of ^{1}H-^{1}H coupling constants

From the 2D ZS-DIAG experiment, it is possible to access the 1D homodecoupled proton spectrum but also to analyze the coupling network of the molecule. Indeed, signals from the 2D ZS-DIAG spectrum provide different information. First, the decoupling produces singlets in the F1 dimension leading to the obtention of the decoupled 1D proton spectrum. But it has to be noticed that coupling structures are still available in the directly detected dimension. Thus, by extracting each multiplet and applying a deconvolution process[44-46] to it, coupling constants values can be measured and then spin systems can be traced out.

The figure 3.19 shows the results of this process for the proton H12β of the 4-androstene-3,17-dione. The program written by Dr. Jeannerat extracts a diagonal multiplet from the 2D cross-section. The symmetry of this multiplet is analyzed in order to check if there is no extra peak coming from another signal. Then, the deconvolution process starts. For each step, the highest simplification of the coupling structure is searched. In the case of the proton H12β, the multiplet has a structure of doublet of doublet of doublet. Within the first step of deconvolution, the multiplet is reduced to a doublet of doublet, then a doublet and finally to a singlet. At the end, three different values of coupling constants have been measured (13 Hz corresponding to the coupling between H12β and its geminal partner, 4.1 Hz between H12β and H11β and 2.55 Hz for the coupling of H12β with H11α). As a control of the deconvolution, a synthetic multiplet is reconstructed from these values of coupling constants and is compared to the experimental multiplet. According to a reliability indicator, the processus is validated and another multiplet is analyzed.

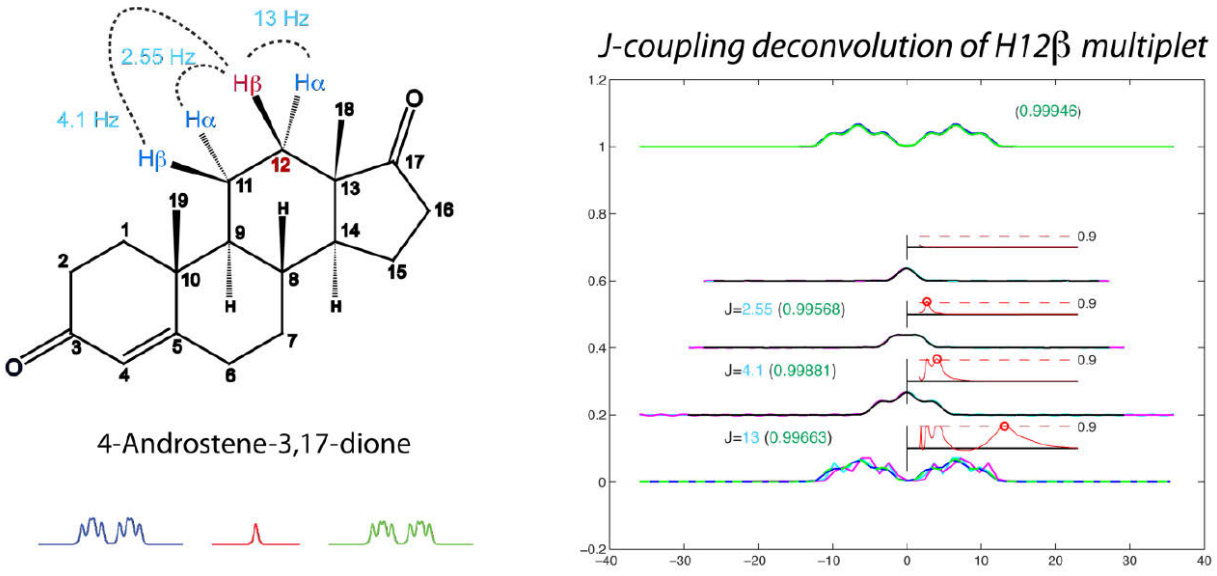

Figure 3.19: Results of the deconvolution process applied to the proton H12β of the 4-androstene-3,17-dione. On the left: the experimental multiplet is shown in blue, the final signal from the 1D homodecoupled spectrum in red and the reconstructed multiplet according to the coupling constants obtained by deconvolution in green. On the right: each step of the simplication processus of the

multiplet H12β.The experimental multiplet (in pink) is symmetrized before the deconvolution (mulitplet in light blue). The value of the coupling constant obtained after each step is in light blue while the reliability indicator and the synthetic mulitplet appear in green.

Coupling constants values can as well be obtained by recording a 2D J-resolved experiment[28]. In this case, chemical shifts information is displayed along the F2 dimension with vertical multiplets while the indirect dimension shows a scale in Hertz for the direct measurement of coupling constant values (Figure 3.20). This experiment requires an important number of points in the F1 dimension in order to obtain an acceptable resolution for the clean determination of coupling constants.

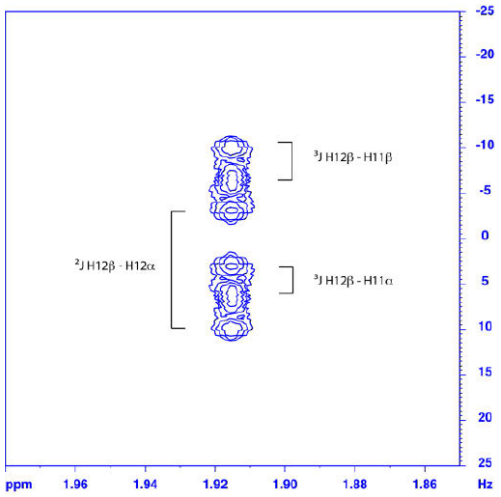

Figure 3.20: Zoom on the spectral region of the J-resolved experiment, after 45 degree rotation, showing the proton H12β of 4-androstene-3,17-dione in $CDCl_3$.

No special care is required for the automated determination of coupling constants with the presented method since high-resolution multiplets are already available in the F2 dimension of the ZS-DIAG experiment.

d) Analysis of second-order effects

Second-order effects concern only spins which share a scalar coupling described as strong coupling. Two spins are said strongly coupled when the difference between their chemical shifts is less than 10 times the value of the coupling constant shared by these two spins. Therefore, the spin system is no longer considered as being of first-order. Additional signals appear in the spectrum at chemical shifts depending on the coupling constant between the two given spins. Thus, these additional responses or strong coupling artifacts may be located at +/- J/2 around the main signals, with positive or negative phases (Figure 3.21).

Second-order effects are sometimes expressed in a symmetric way in the 2D spectrum. So they cannot be removed by spectral symmetrization. Magnetization responsible for these artifacts coming from magnetization of the strongly coupled spins, the intensity of the main signals can be severely reduced in favor of the intensity of artifacts in function of the strength of the coupling and the bandwidth of the soft pulse. Only the usage of a pulse, the selectivity of which has been maximized, can lead to the elimination of these extra peaks.

Strong coupling artifacts can be superimposed to signals of interest. An identification step of these responses has been added to the processing of the 2D ZS-DIAG spectrum in order to limit the impact of these artifacts on the main or adjacent signals. This identification is based on the fact that strong coupling artifacts do not appear like real diagonal signals, i.e. symmetric on the diagonal of the spectrum. They are thus easily localized and treated differently during the next step of the processing.

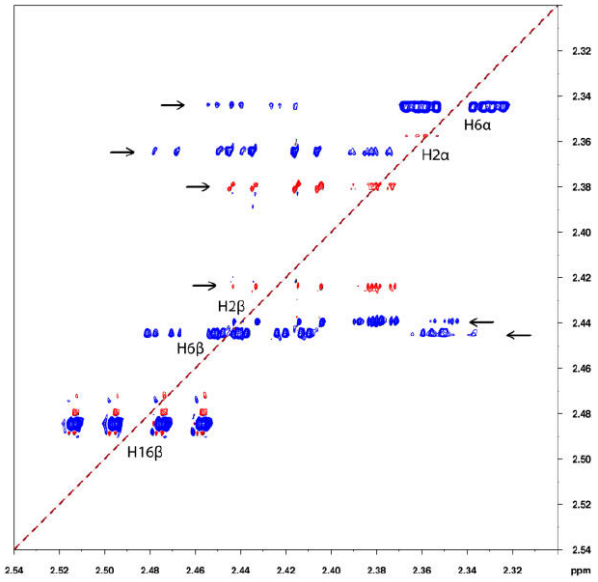

Figure 3.21: Expansion of a 2D ZS-DIAG spectrum showing strong coupling artifacts. Only diagonal peaks are supposed to appear in this spectrum. Extra signals, with positive or negative phase, are identified here as strong coupling artifacts. Their intensity is sometimes higher than the main signal which hardly appears on the diagonal because of the roof effect. The diagonal and artifacts are highlighted by red dashed line and black arrows, respectively.

3) Resolution enhancement by spectral aliasing

The resolution corresponds to the capacity to separate two adjacent signals and is thus characterized by the minimum gap between two signals so that the valley separating them is a fraction of the intensity of the concerned signals. In 2D NMR, the resolution is always maximal in the direct dimension but depends on the number of points acquired and so on the time granted to the acquisition of the spectrum for the indirect dimension.

There are two ways to increase the resolution of a 2D spectrum. The first one has been seen in Chapter 2 (Figure 2.5) and consists in increasing the number of points acquired in the indirect dimension of the spectrum. The major drawback of this simple method is the drastic increase of the experimental time. Indeed, the acquisition of a spectrum of 10 ppm over 10 ppm with 8k and 128 points, in F2 and F1 respectively, takes only 13 minutes whereas the increase of the number of points from 128 to 1k requires an experimental time eight fold longer. The second option is to apply spectral aliasing[47-50].

To understand the theory of spectral aliasing we need to go back to the FID and the different techniques of sampling of the NMR signal.

a) Nyquist condition and its violation

An NMR signal appears as a wave decaying with time because of relaxation processes. This wave is characteristic of a given frequency of resonance. The detection of an NMR signal consists in sampling this Free Induction Decay by a given number of data points. The Nyquist theorem states that for a good sampling of this wave, we need to sample it with regular interval and a sampling rate of at least twice the frequency of the wave of interest. Because the FID contains all the frequencies of resonance of a molecule, the sampling rate has to be twice the highest frequency contained in the FID. It means that the dwell time DW which is the interval between two data points is defined by:

$$DW = \frac{1}{2\,fmax}$$

With fmax the Nyquist frequency or the highest frequency to be sampled.

For obtaining a 2D spectrum with good resolution, we need to record it with a huge number of t_1 increments that takes time. When recorded with only few hundreds of increments, resonances with frequencies different of only few Hertz do not have enough time to be resolved. Their signals are thus overlapped in the spectrum.

For reaching the resolution where these resonances are distinguished, without increasing the number of data points in the F1 dimension, we need to increase the dwell time. The problem is that, by doing so, the Nyquist condition is not fulfilled. If the dwell time is increased, the acquisition time is increased by the same factor. The two frequencies have now enough time to distinguish themselves and to be resolved in the spectrum.

The dwell time is linked to the highest frequency to sample and so to the spectral width SW by the following relation:

$$DW = \frac{1}{2\,SW}$$

Increasing the dwell time means reducing the spectral width. For example, DW is equal to 100 µs for a spectrum of 10 ppm in both dimensions and is increased to 500 µs when SW is

reduced to 2 ppm. The violation of the Nyquist condition implies that all signals existing outside of the boundaries of the spectral width will be folded back into the spectrum. The signal will be identical as if the Nyquist condition was fulfilled but its frequency will be different depending on how far the real frequency from the edge of the spectral width is.

This phenomenon can arise only in the F1 dimension that is why we are interested in applying it to our experiments.

b) 2D aliased experiments

Spectral aliasing can be applied to all experiments with more than one dimension. In the group of Dr. Jeannerat, spectral aliasing has been successfully combined to heteronuclear experiment such as HSQC[51]. In this case, aliasing leads to a better separation of proton-carbon correlations in the carbon dimension (Figure 3.22). One can then determine precisely the chemical shift of each carbon based on the comparison between a normal HSQC and an aliased one. HSQC recorded with a full window in the carbon dimension gives chemical shift information with a limited precision. Only values without any decimal digit can be trusted. A contrario, HSQC spectra recorded with a spectral width in F1 reduced to 10 ppm[52] shows values of chemical shifts with a higher precision but with ambiguities on the figures of tens and hundreds. To recover the complete value of carbon chemical shifts, one has to compare values obtained with both spectra.

As it can be seen in Figure 3.22, spectral aliasing allows an enhancement of the resolution of a factor depending on the reduction of the width in the F1 dimension. At 35 ppm in the carbon dimension and 1.8 ppm in the proton dimension, it is difficult to determine how many signals are superimposed. The analysis of the corresponding 10 ppm spectrum presents two different signals at 5.20 and 5.70 ppm. The combination of both spectra leads to the real values of chemical shifts: 35.20 and 35.70 ppm for the two carbon signals.

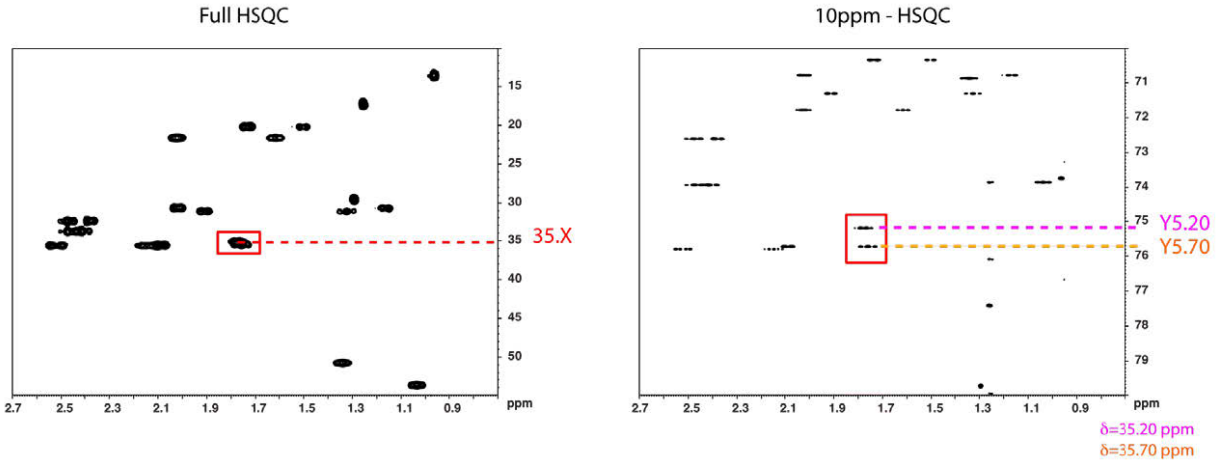

Figure 3.22: Comparison of a full and a 10 ppm HSQC for the determination of the carbon chemical shifts. Both spectra are used for determining precisely values of chemical shifts.

Spectral aliasing can be combined with our ZS-DIAG experiment. Indeed, because there are only diagonal peaks in the spectrum, the spectral window in F1 can be reduced to a smaller value without risking to introduce more overlaps. The recorded spectrum would be as if the diagonal spectrum with a spectral width of 10 ppm is cut in several stripes of the same width, let's say 1 ppm. Then all these stripes are superimposed and stretched to the size of a 10 ppm spectrum (Figure 3.23).

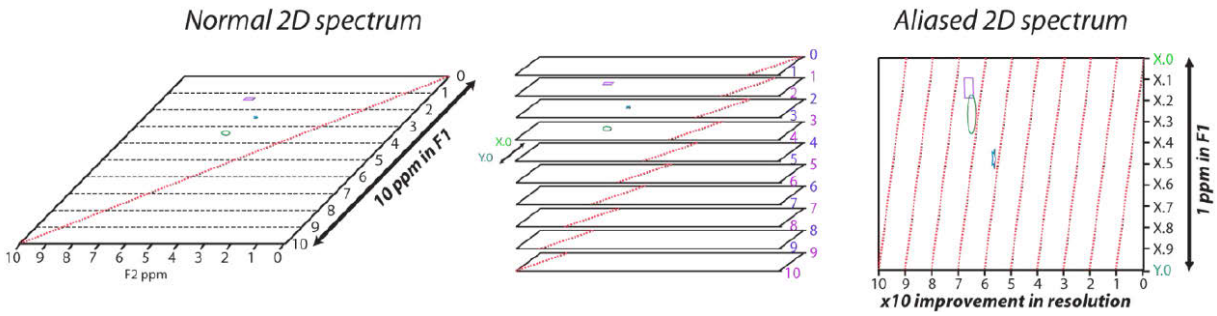

Figure 3.23: Principle of spectral aliasing in homonuclear spectra[12].

The ZS-DIAG signals are following the diagonal of the spectrum which is folded several times depending on the reduction factor of the spectral window. There are no ambiguities about the real chemical shift of each signal since it is a homonuclear experiment aliased in F1. The enhancement of the resolution in the aliased dimension helps to better define the chemical shifts of signals (figure 3.24) as it has been the case previously with the combination of the full and 10 ppm HSQC[52].

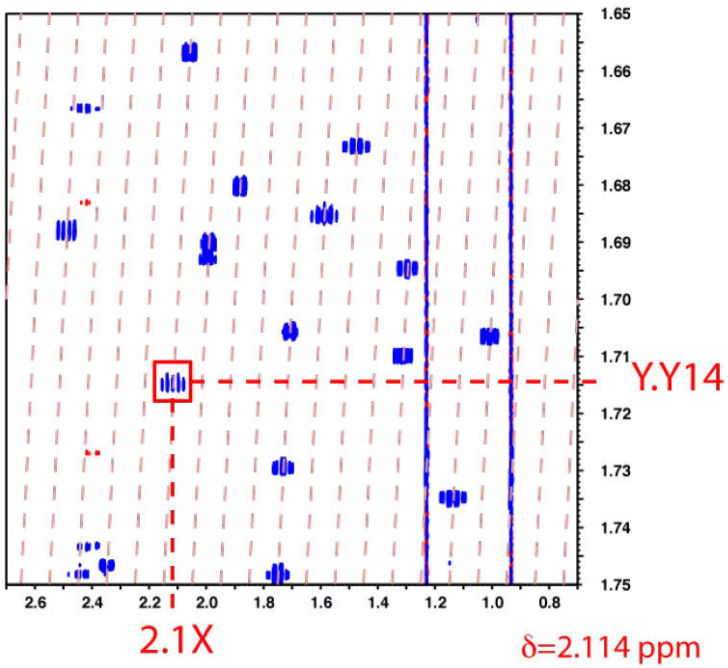

Figure 3.24: Determination of chemical shifts with ZS-DIAG experiment aliased in F1. The exact proton chemical shift can be access within the same spectrum.

Our special processing leading to the obtention of 1D homodecoupled proton spectra is well working whether the F1 dimension of 2D ZS-DIAG spectra is full or aliased (Figure 3.25). All signals can be found in the final 1D spectrum since the treatment of the data is following the diagonal of the 2D spectrum. However, the choice of the quadrature detection is really important. The acquisition of ZS-DIAG spectra can be done with TPPI, States or States-TPPI. But the sampling of the FID will be executed in different manner and will lead to a different type of folding. It is advisable to distinguish TPPI and QF quadrature that lead to a folding phenomenon from States, States-TPPI and Echo-Anti-Echo quadrature detection which lead to spectral aliasing. As it is shown in the figure 3.26, the folding of the diagonal is different. When recorded with TPPI, the diagonal is folded with a W motif which can increase the degree of overlap in the spectrum instead of spreading the signals. It has to be noted that, in this case, the processing program cannot find the right position of signals that makes the signals appear at wrong chemical shifts in the 1D homodecoupled proton spectrum. That is why it is necessary to use the States-TPPI quadrature detection for the acquisition of aliased version of ZS-DIAG experiments.

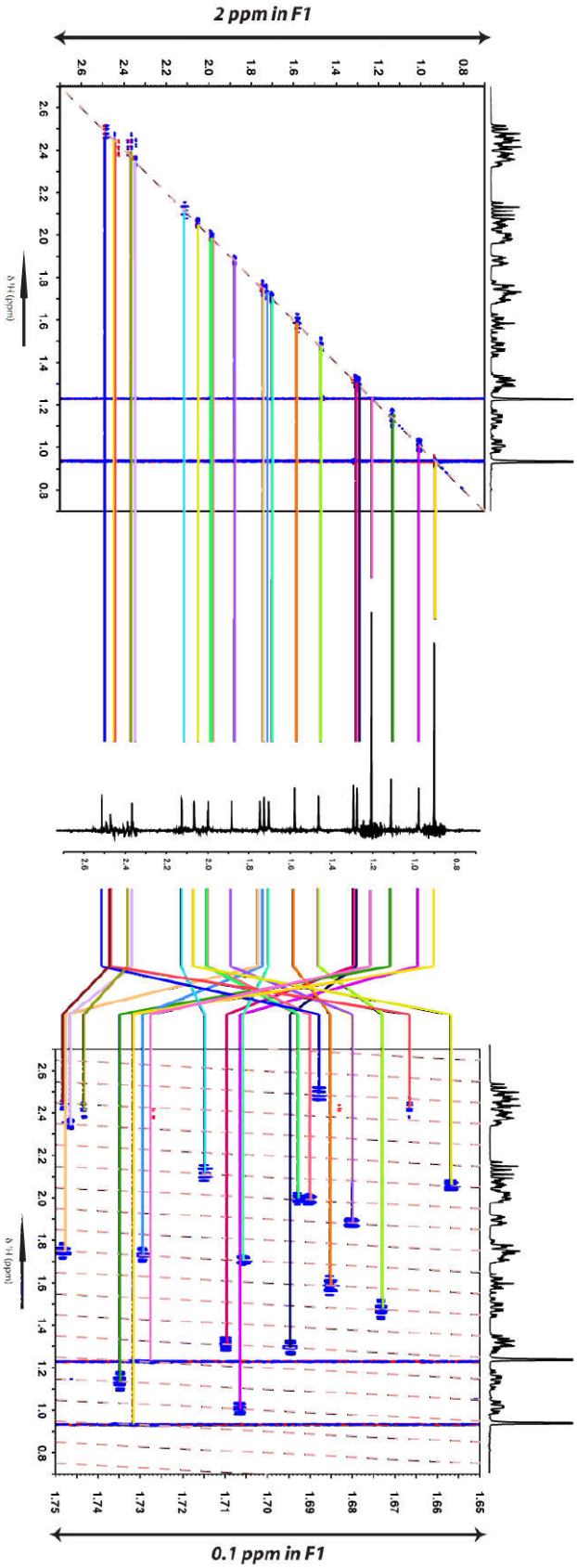

Figure 3.25: Full and aliased ZS-DIAG spectra can be processed into 1D homodecoupled proton spectra.

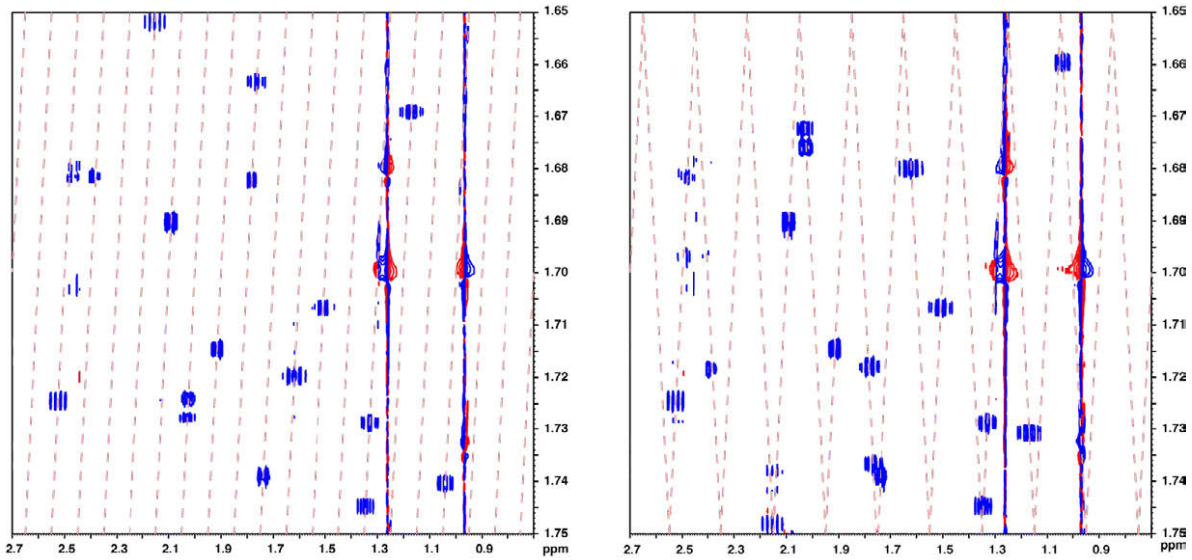

Figure 3.26: Illustration of the spectral aliasing with States-TPPI (left) and spectral folding with TPPI (right) for the 2D ZS-DIAG experiment. The diagonals are not following the same scheme of folding which can lead to the introduction of new signal overlaps in the case of TPPI.

In the case of our 2D ZS-DIAG experiment, the spectral window in F1 can be reduced from 10 to 0.1 ppm. It allows a resolution enhancement of two orders of magnitude. Because the spectral window is smaller, less data points are required for obtaining the same resolution as a full spectrum. It means therefore that less time is required for the acquisition of an aliased spectrum. It also supposed that if less points are needed for recording resolved spectra, it is possible to increase the number of t_1 points in order to access the top-resolution. Spectra have been recorded with different spectral windows and number of t_1 increments. To access top-resolution, only 64 points are required for a SW of 0.1 ppm (Figure 3.27).

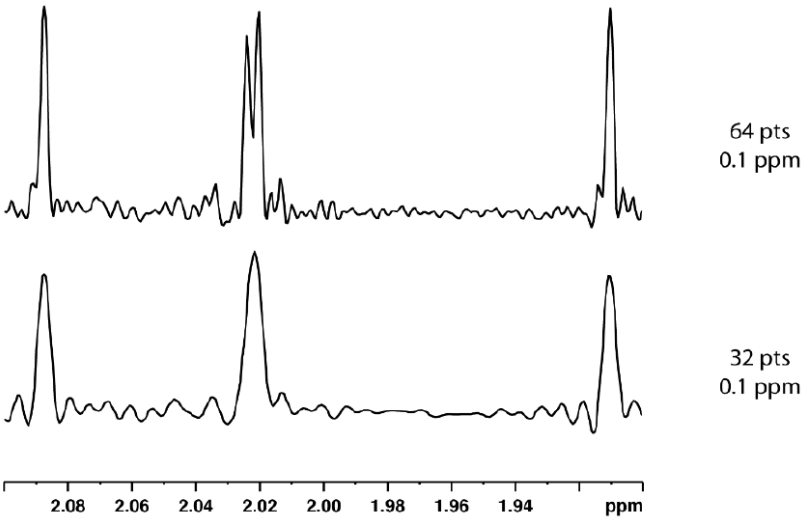

Figure 3.27: Comparison of expansions of 1D homodecoupled spectra with different numbers of points for a spectral width of 50 Hz in the F1 dimension. The two signals in the middle are resolved only when the spectrum is recorded with at least 64 points for a spectral window of 0.1 ppm in the F1 dimension.

The figure 3.27 illustrates the limit for reaching the top resolution. It is of course possible to reduce more the spectral width in F1 in order to save more experimental time. Indeed, recording a full spectrum with high resolution would take more than 11 hours while reducing the spectral width from 10 to 0.1 ppm enables to record the spectrum in only 7 minutes with the same resolution. However, there is a limitation to the reduction of SW1. If this spectral window is smaller than the signal width, each multiplet risks to be folded in the spectrum and to generate multiple peaks instead of a unique singlet in the 1D homodecoupled spectrum.

4) Experimental conditions

All spectra were recorded at 298K on a Bruker 500 MHz spectrometer with a 5 mm DCH ^{13}C-$^{1}H/D$ cryogenic probe equipped with a z-gradient coil. The sample used was containing 20 mg of 4-androstene-3,17-dione dissolved in 700 µL of $CDCl_3$ in a sealed NMR tube.

J-resolved experiment was recorded in 1h 2min 21s using spectral widths of 10 and 0.1 ppm in F2 and F1 respectively. The sampling was done using the QF quadrature mode with 128 t_1 increments and four scans per increment.

For the **Anti z-COSY** spectrum, two scans of 8164 points were acquired for each 256 increments, with spectral widths of 10 and 0.2 ppm, respectively for the direct and indirect dimensions. The sampling was done according to the States quadrature detection mode in 34 min 59s. The flip angle of the second and third pulses was set to 20 degrees, a compromise between sensitivity and suppression of artifacts. The zero-quantum coherence eliminated was applied using a Chirp pulse of 40 ms during a z-gradient of 3.25 G/ cm, and a purge gradient of 50% of the maximal amplitude.

Keeler's **J-spectroscopy experiment** has been acquired in 1h 4min 39s with a spectral window in the indirect dimension set to 0.2 ppm and sampled with Echo-Anti-echo quadrature with 4 scans and 256 increments. BIP pulses of 100 µs were used for reducing artifacts associated with imperfect refocusing. The Zangger-Sterk element was using a 30 ms Rsnob pulse during a z-gradient of 0.65 G/cm.

Morris **Pure Shift** spectrum was acquired in 3 min 19 s with spectral widths of 10 and 0.1 ppm, 32 increments and two scans sampled using QF mode. A 30ms Rsnob pulse was used during a gradient of 0.65 G/cm. 32 chunks of 20 ms were concatenated before FT to obtain pure shift spectra.

For the **ZS-DIAG** experiment, the Zangger-Sterk element and z-filters were identical as described in Chapter 2. Two sets of parameters have been used for recording normal and aliased spectra. For the full spectrum, with a spectral window of 2 ppm in both dimensions, 512 t_1 increments and two scans were acquired in 1h 35min. For the aliased spectrum, SW_1 was reduced to 0.1 ppm. 64 increments were recorded in 7 min 23s. These experiments have to be recorded with a special attention to the stability of the spectrometer. Indeed, a default of regulation of the temperature during acquisition may generate convection of the solution especially when low-viscosity solvents are used. This may severely degrade the quality of spectra.

The pulse sequence of the 2D ZS-DIAG experiment discussed in this chapter is available in Appendix C.

Chapter 4: Sensitivity Enhancement by Frequency Modulation

1) Sensitivity of homodecoupled proton experiments

The experiments described in this manuscript are homonuclear experiments applied to the most abundant nucleus which has the best magnetogyric ratio. However, the sensitivity of experiments based on the Zangger-Sterk element[6] is a real problem. Because of spatial encoding, only few spins contribute to the signals. Indeed, the sensitivity is determined by the ratio between the refocusing bandwidth of the selective pulse and the spectral window covered by the spatial encoding gradient. These two parameters can be adjusted to record spectra with acceptable signal-to-noise ratio.

a) Impact of the amplitude of the spatial encoding gradient

The amplitude of the spatial encoding gradient determines the range of frequencies that will appear in the spectrum. If the gradient is set to zero, only the frequencies selected by the soft pulse will be observable. When its amplitude is increased, the range of frequencies is larger so more peaks can be observed (Figure 4.1). But the higher the spatial encoding gradient is, the less sensitive the experiment will be.

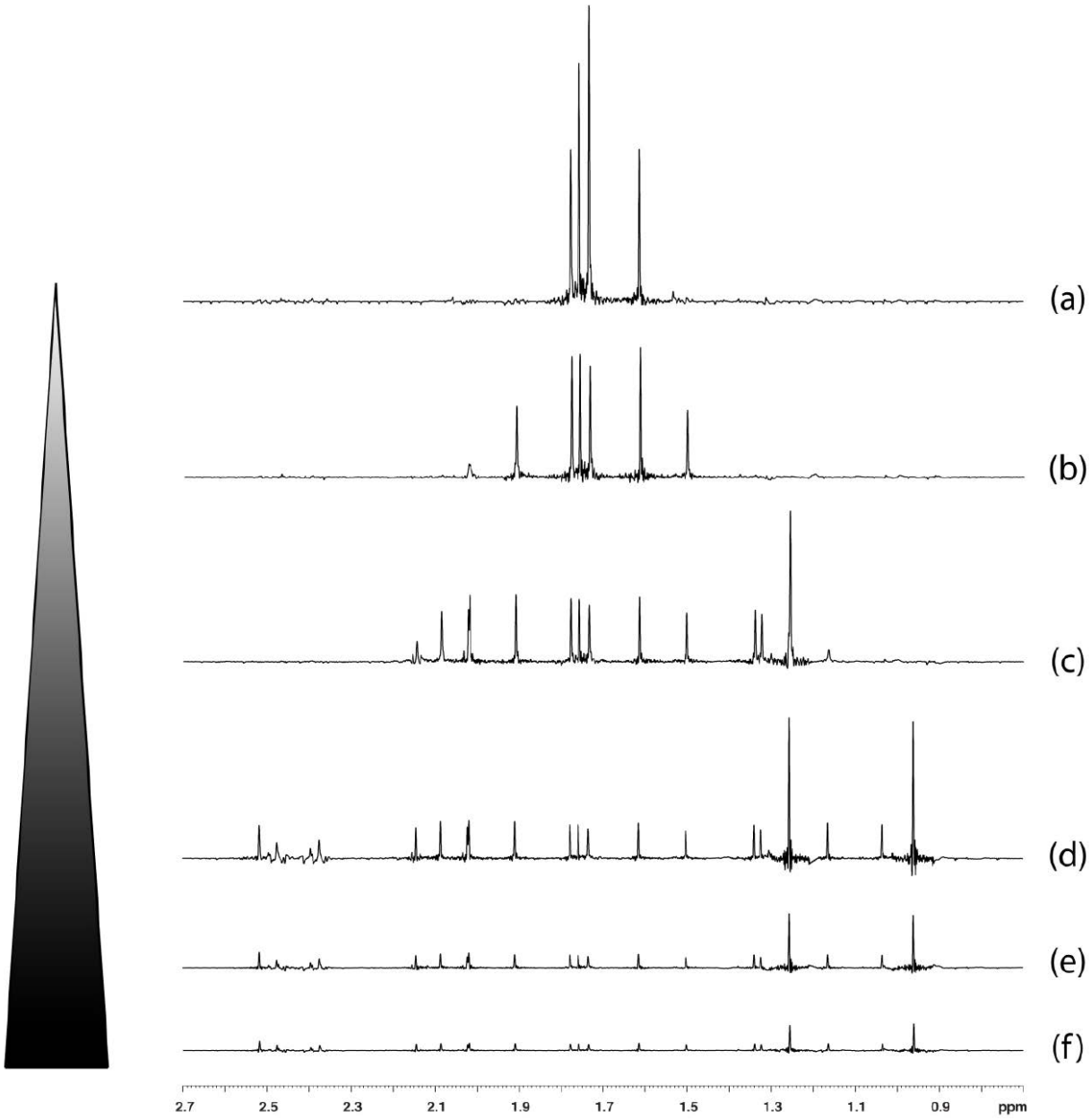

Figure 4.1: 1D homodecoupled proton spectra recorded with a 30 ms Rsnob pulse and different values of gradient: (a) 0, (b) 0.05, (c) 0.1, (d) 0.2, (e) 0.3 and (f) 1% of the maximal amplitude of the z-gradient.

Because of the slice selection caused by the spatial encoding gradient, one usually records what is called band-selective experiment. In this case, the spectral window is reduced to the minimum as well as the amplitude of the gradient in order to have all desired signal with more intensity.

b) Impact of the selectivity of the soft pulse

The selectivity of the soft pulse determines how thin the slices are and so how many spins are responsible for the signals. The thinner the slices are, the fewer the number of spins are selected; and thus lower the intensity of signals is.

A ZS-DIAG spectrum recorded with a 30 ms Rsnob pulse and a spatial encoding gradient shows only singlets instead of multiplets in the decoupled dimension. But it also shows some artifacts due to the selection of coupling partners or to second-order effects (Figure 4.2). A solution to limit the presence of these kinds of artifacts in the spectra is to maximize the selectivity of the soft pulse used in the decoupling element, that is increase the duration of the selective pulse. A 120 ms Rsnob pulse refocuses a bandwidth of 19.4 Hz which reduces a lot the intensity of the potential artifacts. But increasing the duration of the soft pulse from 30 to 120 ms reduces the sensitivity by a factor four. The advantage of using a 120 ms pulse instead of 30 ms is that the selectivity of the pulse is higher so there is less risk to select two partners of coupling at the same time and therefore less recoupling or strong coupling artifacts (Figure 4.2).

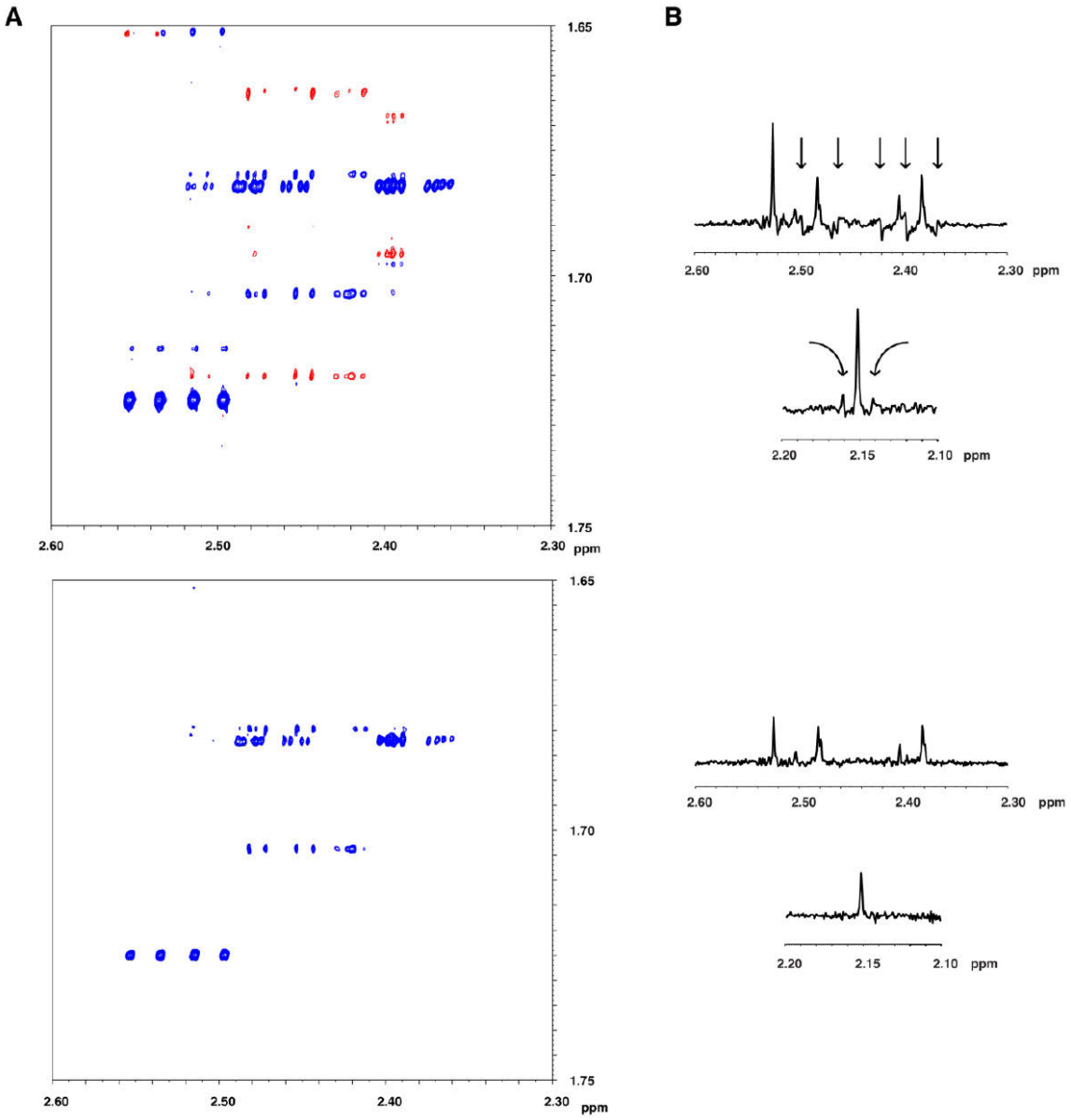

Figure 4.2: Artifacts due to the lack of selectivity of the soft pulse. A) Zoom on a region of the 2D aliased map where strongly coupled spins signals of the 4-androstene-3,17-dione are located. The upper spectrum recorded with a 30 ms Rsnob pulse refocusing a bandwidth of 77.7 Hz shows negative artifacts due to second-order effects. The lower spectrum has been recorded with a more selective pulse (120 ms, 19.4 Hz) and therefore does not present artifacts. B) 1D homodecoupled spectra corresponding to the 2D spectra shown in (a). Artifacts are highlighted with arrows. The second trace shows a signal outside of the window from 2.3 to 2.6 ppm feeling similar effects.

Once we know the factors responsible for the sensitivity loss, we can propose a method to solve this important issue. The first step is to find the best shape of soft pulse to use in the Zangger-Sterk decoupling element. Then, we propose to apply a multiple-site irradiation instead of only one centered at the carrier frequency. The last step consists in finding the combination of modulation to avoid the generation of artifacts and record a spectrum with the highest possible signal-to-noise ratio.

2) Selective Pulse Choice

The choice of the selective pulse is really important since it will impact on the sensitivity and the quality of the experiment. This pulse has to act on few spins only and not on the whole spins of the sample in order to remove the interactions between the selected spins and their coupling partners. If the coupling partners feel the effect of the selective pulse, the decoupling cannot occur.

Different selective 180 degree pulses have been tested with our ZS-DIAG experiment. It concerns pulses with universal applications which means pulses able to trigger an excitation, an inversion or a refocusing of spins. Within the frame of the Zangger-Sterk decoupling element, this pulse has to selectively refocus spins. It is essential to use a pulse as short as possible in order to avoid spin relaxation during the pulse, but also a pulse carrying out a good refocusing within the desired selectivity. The excitation profile of the pulse should be as rectangular as possible leading to the selection of spins in the refocusing bandwidth without acting on spins outside of this bandwidth.

For this purpose, the acquisition parameters of the experiment and the selectivity of the pulse have been kept constant. It has to be noted that pulses have different shapes. Their duration can therefore vary for the same refocusing bandwidth. For example, a pulse with a Gaussian shape can be shorter than a Rsnob pulse refocusing both 77.7 Hz.

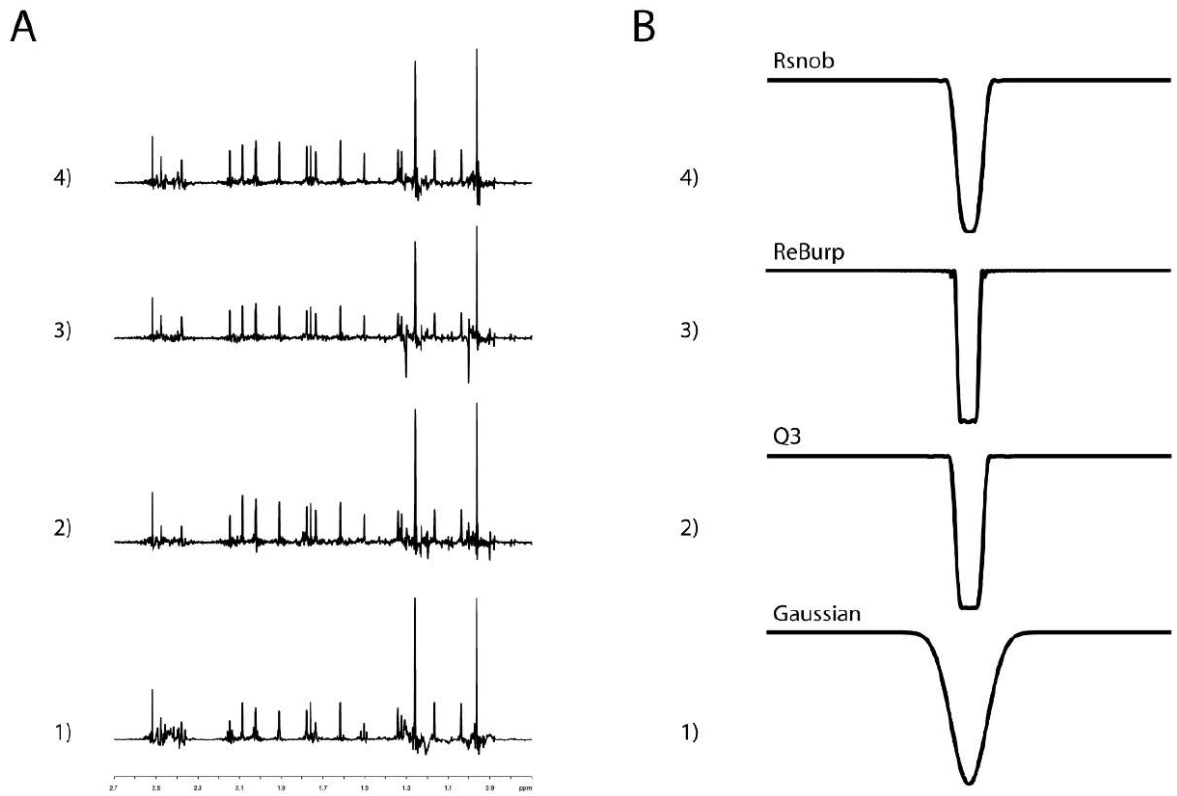

Figure 4.3: A) Homodecoupled 1D proton spectra recorded with different shaped pulse refocusing 77.7 Hz: 1) 11.3 ms Gaussian pulse, 2) 43.9 ms Gaussian Cascades Q3 pulse, 3) 74.8 ms ReBurp pulse and 4) 30 ms Rsnob pulse. B) Excitation profil of each pulse.

The simplest selective pulse has a Gaussian shape[53]. This pulse is used by the coworkers of Zangger[54] and Parella[55]. Indeed, Gaussian pulses do not need to last long for having a good selectivity (12 ms for a selectivity of 73.5 Hz) which is a good compromise between pulse selectivity and sensitivity. However, the excitation profile of this pulse is not optimum. Transition regions are quite large resulting in the presence of artifacts in the decoupled spectrum (Figure 4.3.A.1 and B.1).

Other more elaborated pulses have been developed over years. The use of clusters of Gaussian pulses, represented here by the Gaussian cascades Q3 pulse[56], increases the performances of the Gaussian pulse. The excitation profile of the Q3 pulse is rectangular and the spectrum does show lower intensity artifacts (Figure 4.3.A.2 and B.2).

The two last pulses belong to the BURP pulses[57] (Band-selective Uniform Response Pure-phase pulses) and to the SNOB pulses[58] (Selective excitation fOr Biochemical applications pulses). The spectrum recorded with a ReBurp pulse of 75 ms is of comparable quality as the spectrum recorded with a 30ms Rsnob pulse (Figure 4.3.A.3 and A.4). Only the signal-to-noise ratio is different. For the same selectivity and a shorter duration, the Rsnob soft pulse allows to record a spectrum with less artifacts and a better signal-to-noise ratio than other tested pulses. Rsnob pulses are therefore a good choice leading to the refocusing of scalar couplings when applied with the Zangger-Sterk decoupling element. These pulses will be used in our method of sensitivity enhancement.

3) Frequency Modulation

Our technique of sensitivity enhancement for proton decoupling experiments consists in the phase modulation of the selective pulse. The generated selective pulse irradiates the sample at different frequencies. Thus, instead of having only one offset for an irradiation in the middle of the spectrum, this pulse is covering the frequency range at different points.

This technique has already been used in the Jeannerat group to increase the sensitivity of HSQC experiments with samples of ^{13}C labeled cholesterol[59-60]. Parella and coworkers[55] have also applied the frequency modulation to their experiments by generating pulses according to the frequencies of resonance of their samples, to avoid the selection of coupled paired spins. In this manuscript, a more general method[42] will be presented.

a) Frequency-modulated pulse

The generation of the selective pulse is quite simple. One just has to precisely determine the offsets of irradiation and input them in a list of frequencies. This file is then used in the Shape Tool command of Topspin where it is asked to choose the pulse shape, the number of points (in order to have the better definition of the pulse) and its duration. Once the pulse is created, one has to determine its power. Indeed, pulses are characterized by three parameters: the shape, the duration and the power.

First, the power of standard pulse without modulation has to be calculated according to the hard 90 degree pulse used. The longer a selective pulse is compared to the 90 degree pulse, the lower the power of the selective pulse is. For example, with our 500 MHz spectrometer, the 90 degree pulse is defined by a duration of 9.95 µs and a power level of 2.80 dB. A Rsnob pulse of 30 ms has a power level of 52.96 dB.

A new attenuation factor is then added to the power determined previously depending on the number of frequencies used to generate the selective pulse, so the modulations will be applied with the correct power level. This attenuation factor is calculated using the following relation:

$$\text{Attenuation factor} = -20\ \text{Log}_{10}\,(\text{number of modulations})$$

The more a selective pulse is frequency modulated, the more its power should be increased. A Rsnob pulse of 30 ms with 10 frequencies of irradiation will have a power of 32.96 dB (with an attenuation power of – 20 dB).

Two kinds of modulations have been tested in order to obtain the best possible signal-to-noise ratio while limitating the generation of artifacts in the spectrum. These methods have been set up with a 30ms Rsnob pulse before increasing the selectivity of the pulse.

b) Equidistant frequency modulation

Our first method of modulation of the selective pulse consists in allocating irradiation sites over the proton frequency range using a constant interval[60]. Thus, the entire spectrum can be covered in the same way as it is shown in Figure 4.4. For generating a pulse modulated 10 times with a 500 MHz spectrometer, the frequencies interval for irradiation sites is 500 Hz.

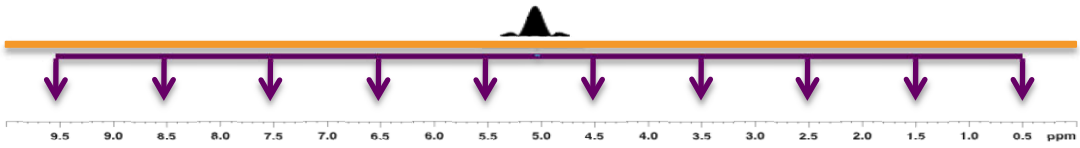

Figure 4.4: Equidistant frequency modulation. The irradiation sites are separated by a constant distance over the entire range of proton frequencies.

In order to monitor the evolution of the signal-to-noise ratio, 20 different selective pulses having a 30 ms duration have been generated with an increasing number of modulations. Figure 4.5 presents 12 of the 20 corresponding 1D homodecoupled proton spectra.

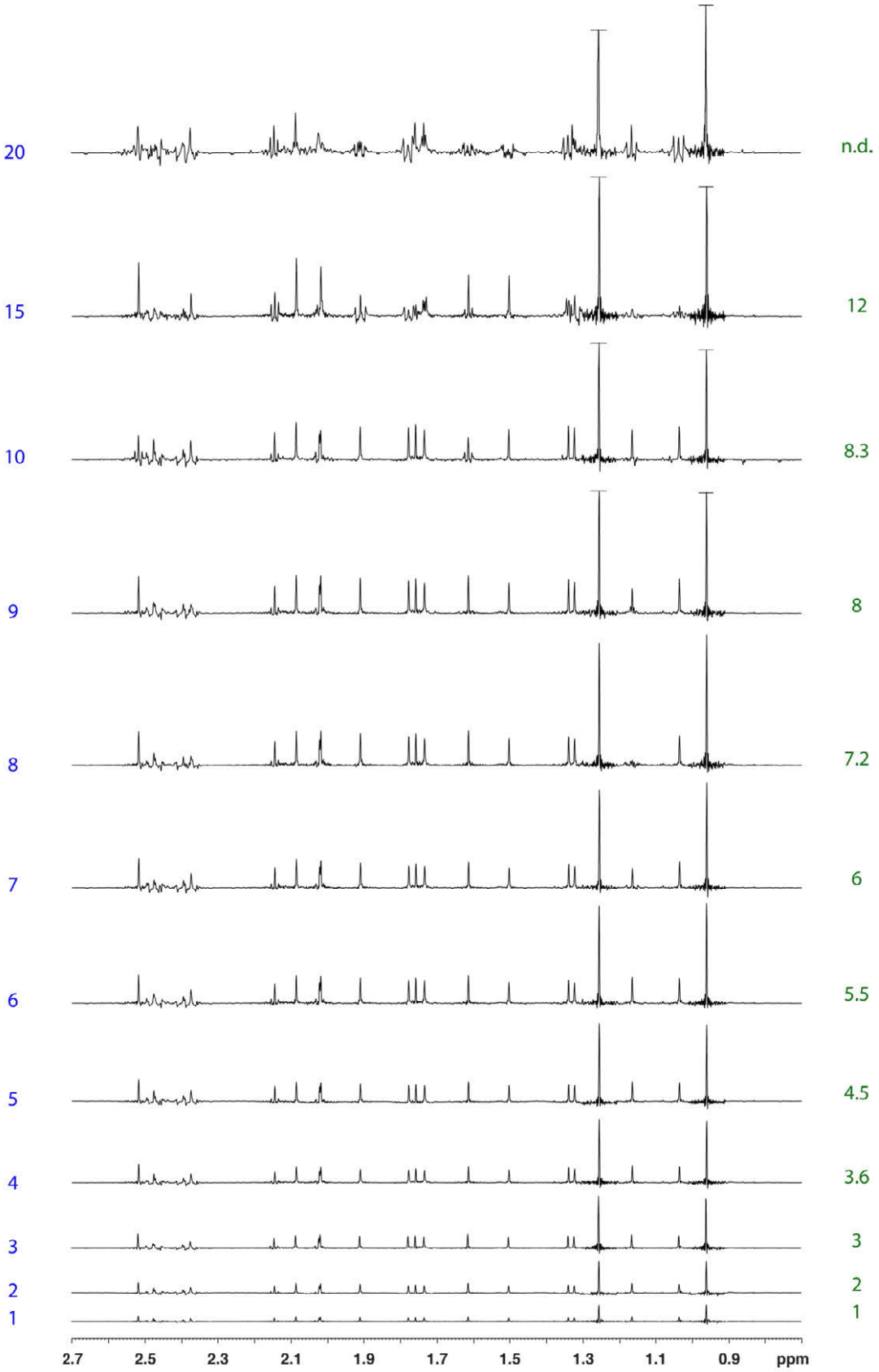

Figure 4.5: 1D homodecoupled proton spectra obtained from 2D ZS-DIAG experiments recorded using frequency-modulated selective pulses. The number of frequencies used for the modulation and the sensitivity enhancement factor are shown in blue and in green respectively. The higher the modulation level of the selective pulse is, the better the sensitivity improvement. Till 10 frequencies of irradiation,

spectra are considered as being of good quality; all signals are decoupled and appear in the spectra with a minimum of recoupling artifacts. Beyond 10 modulations, it becomes difficult to differentiate real signals from artifacts, the intensity of main signals being highly decreased at the benefit of the recoupling artifacts.

The analysis of these spectra confirms the efficiency of the modulation. Indeed, it is clearly visible that the intensity of signals is improved when increasing the number of frequencies. No multiplets are observed, the modulation of the selective pulse does not disrupt the Zangger-Sterk element action.

However, it is difficult to quantify in a precise manner the enhancement of the sensitivity of this experiment. Generally, the sensitivity of an experiment is determined by the calculation of the signal-to-noise ratio of the recorded spectrum. Astonishingly, some variations of this ratio have been observed. Indeed, the sensitivity of our experiment increases linearly from 1 to 4 modulations then varies from one spectrum to another. This can be explained by the fact that the frequency modulation of the selective pulse accidentally introduces artifacts by selecting pairs of coupled spins reducing the amplitude of main signals.

It has also been observed that some artifacts are located in noise regions. Our test-molecule has got two methyles giving really intense signals as singlets. It is common to observe wiggles at the bottom of intense signals like methyles. These wiggles appear in spectra along the F2 dimension as signals of the residual protonated part of highly concentrated solvent like D_2O. Due to the reduced size of the spectral width in F1, these perturbations of the signal are folded over the entire spectrum leading to an increase of the noise intensity (Figure 4.6) and therefore leading to the calculation of a signal-to-noise ratio lower than expected.

The enhancement of the sensitivity has been evaluated as follows.

The spectrum recorded with a non-modulated pulse is used as reference and is noted 1. Its intensity is then compared to each spectrum obtained with frequency modulation. A ratio is determined by adjusting the intensity of signals of the reference spectrum to the target spectrum. A value of the sensitivity enhancement is therefore obtained. These sensitivity improvement factors are shown in Figure 4.5.

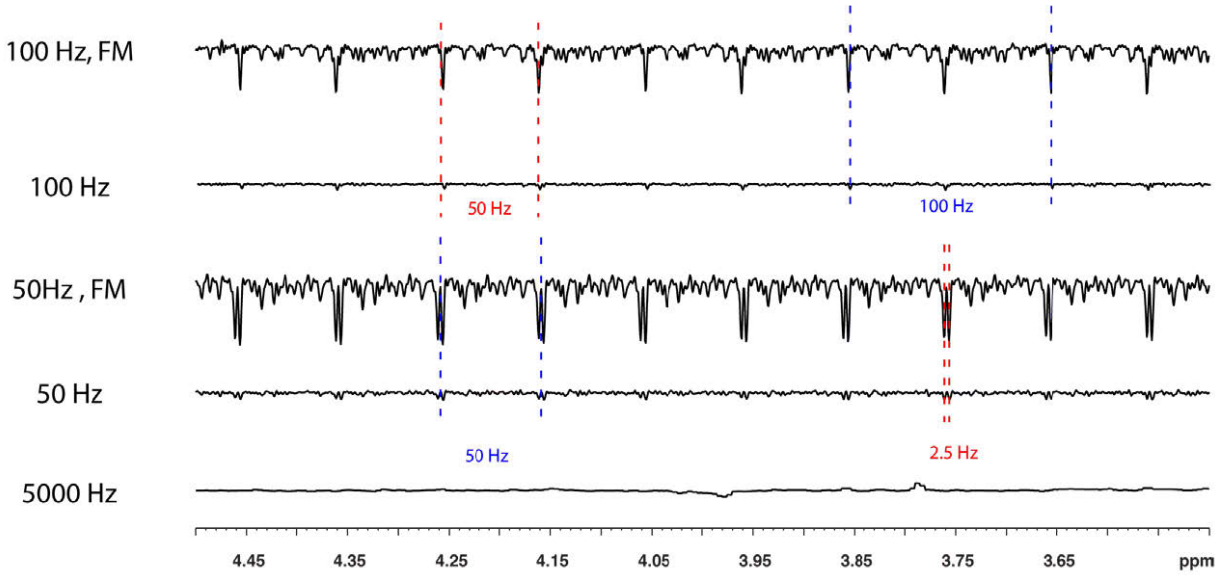

Figure 4.6: Expansions of noise regions of 1D homodecoupled spectra of 4-androstene-3,17-dione recorded with and without spectral aliasing in F1 and with and without frequency-modulation (FM) of the selective pulse. Noise artifacts are generated by the folding of the bottom of the two methyles of the molecule. When the spectral width is reduced to 0.1 ppm, i.e. 50Hz at 500 MHz, signals of these two CH_3 are separated by 2.5Hz in F1 (shown in red). Artifacts are thus appearing as a doublet with 2.5 Hz between the two lines. These artifacts are then repeated every 50 Hz because of aliasing and have a higher intensity with pulse modulation. With a SW_1 equal to 0.2 ppm, the two methyle groups are separated by around 50Hz in the 2D map and therefore appear in the 1D spectrum as singlets 50 Hz apart.

As said above, some artifacts due to the selection of scalarly coupled spins can occur in the spectrum. These artifacts appear on both sides of the main signal and are separated by the scalar coupling constant characteristic of the two coupled spins that have been selected at the same time. Increasing the number of modulations increases the risk of selecting these two spins. So the number of spins, of the whole sample, responsible for these signals is higher, leading to more intense signals. But the main signal and the artifacts are coming from the same magnetization. So the increase of the intensity of the recoupling artifacts leads to the decrease of the intensity of the main signal. Therefore, the higher the pulse is modulated, the more the main signal is disappearing at the benefit of the recoupling artifacts.

Artifacts are appearing because the soft pulse is selecting a large range of frequencies for the refocusing of the J-coupling contribution. Some of these artifacts can be removed by increasing the selectivity of the soft pulse, i.e. by reducing the refocusing bandwidth of this pulse. The selectivity of the soft pulse has therefore been increased from 77.7 to 19.4 Hz. It has been shown in Figure 4.2 that using a 120 ms Rsnob instead of a 30 ms Rsnob removes some artifacts that are already present in the spectrum before introducing the modulation.

Because the bandwidth of the selective pulse has been reduced by a 4 factor, one can imagine that the number of irradiation sites can be raised by the same factor. The highest level of modulation of a 30 ms pulse, without introducing artifacts, being equal to 10, the pulse of 120 ms should be modulated by 40 different frequencies without any problem. But it is shown in

Figure 4.7 that spectra recorded with a 120 ms modulated Rsnob pulse present important recoupling artifacts beyond 20 modulations.

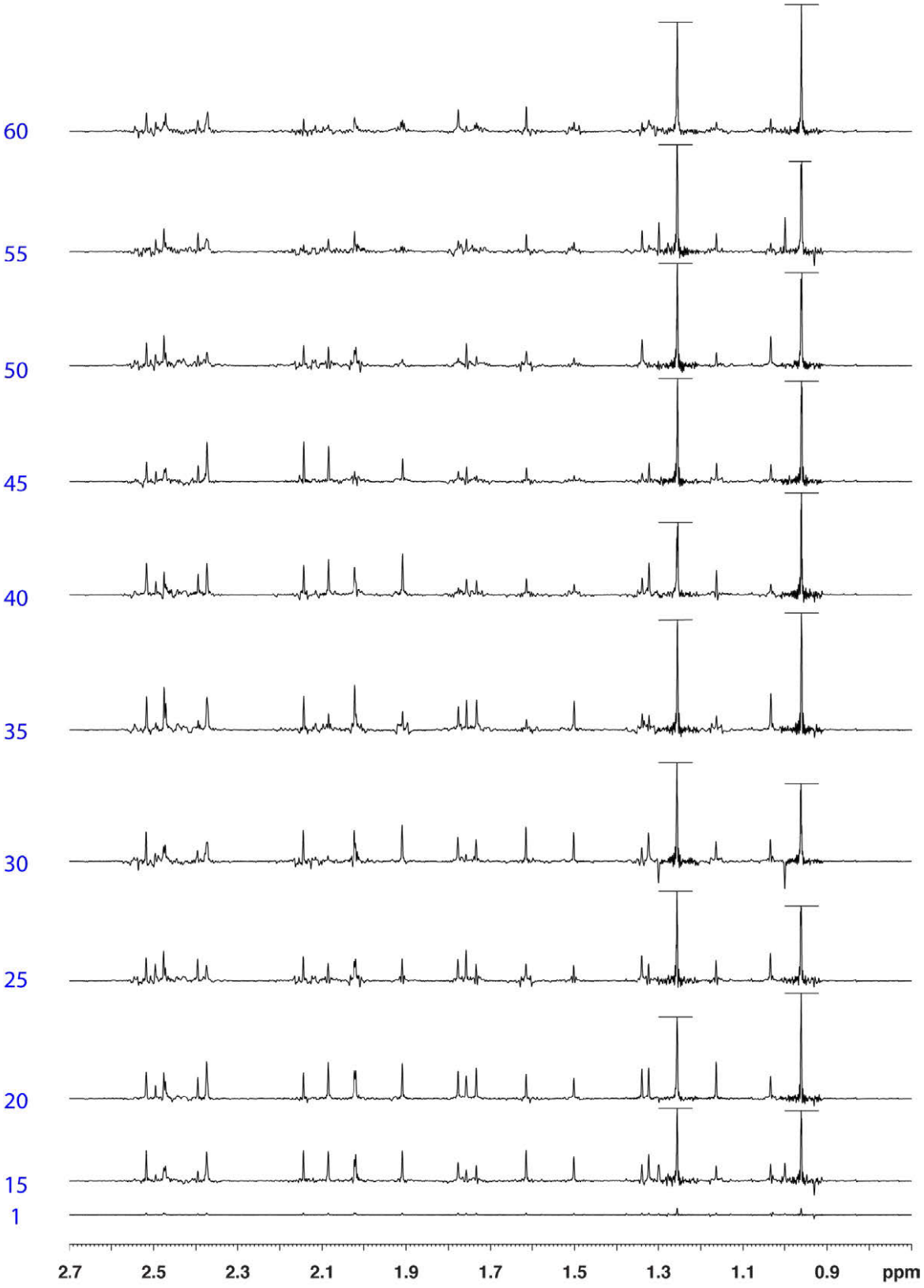

Figure 4.7: 1D homodecoupled spectra recorded with 120 ms Rsnob pulse modulated from 1 to 60 times.

c) Non-equidistant frequency-modulation (nemo)[42]

In order to minimize the generation of recoupling artifacts, Parella and coworkers[55] have proposed to create pulses according to the sample to analyze. The frequencies selected are determined by the resonances of the studied molecule avoiding the simultaneous selection of scalarly coupled spins.

A more general approach is proposed here with the introduction of the non-equidistant modulation[42] of the selective pulse. Instead of irradiating at constant interval, the gap between frequencies is progressively incremented. Figure 4.8 shows the differences between a non-modulated pulse, an equally-spaced modulated pulse and a non-equidistant modulated pulse.

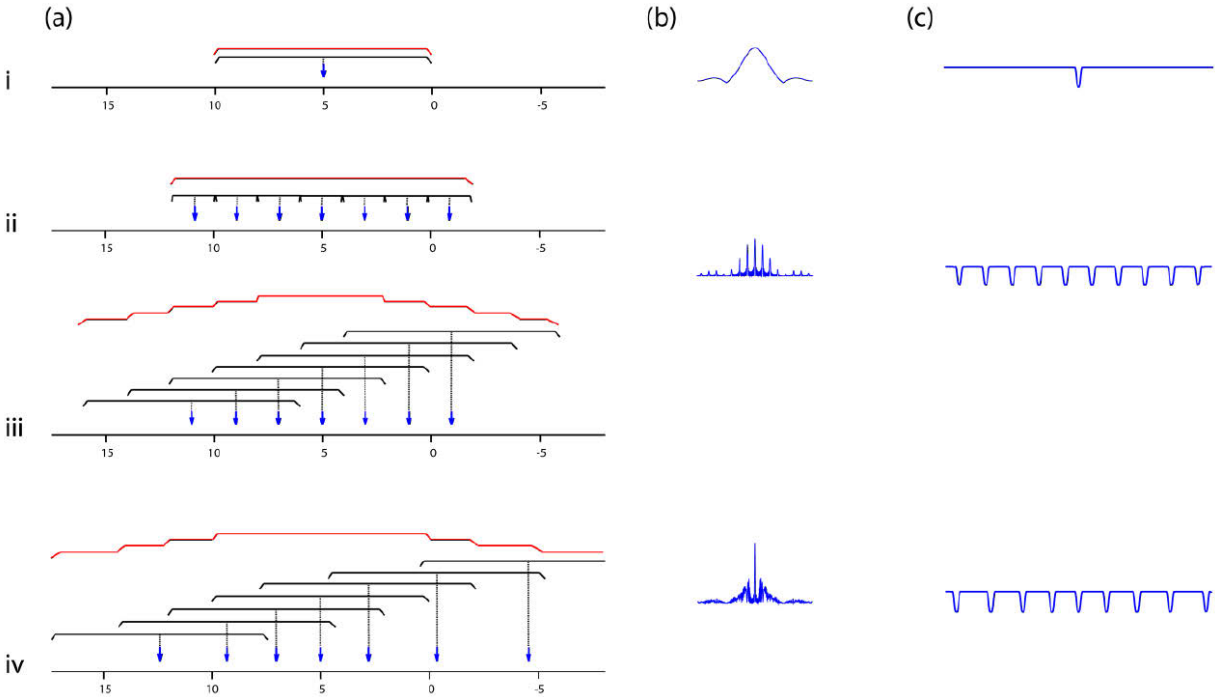

Figure 4.8: (a) Illustration of the repartition of frequencies, shown by blue arrows, and gradient amplitude, shown by the black lines, (b) shape of the soft pulse and (c) excitation profiles. From (i) to (iv) are represented pulses without, with equidistant and non-equidistant modulation. The amplitude of the spatial encoding gradient has an impact on the coverage of the full range of proton frequencies. To guarantee a homogeneous excitation, the amplitude of the gradient is increased to cover each irradiation site in the same way. (i) A simple Rsnob pulse is used in combination with a gradient covering 10 ppm. (ii) The Rsnob pulse is modulated and the gradient adapted to the gap between frequencies. A single coverage of the spectrum is performed. (iii) The encoding gradient is increased to cover 10 ppm. (iv) A nemo-pulse is used. The gradient is homogeneous over a 10 ppm window (shown by the red line).

It is possible to modulate the pulse using one or two different blocks of frequencies covering more than the range of 0 to 10 ppm. Indeed, the consequence of the incrementing of the gap between frequencies is the extension of the spectrum's coverage. It compels to increase the strength of the spatial encoding gradient to ensure the complete coverage of frequencies. So, instead of setting the gradient to the size of the gap between frequencies, it has to be increased at least to the size of the biggest gap. In order to guarantee the homogeneity of the excitation over the active volume of the sample, the spatial encoding gradient is increased to cover at least a range of 10 ppm. Thus, the edges of the active volume are experiencing the

same strength of gradient (and the same excitation profile) as the middle of the sample; the intensity of signals is therefore not influenced by the position of the spins in the sample (Figure 4.8.a).

With nemo-pulses, accidental irradiations of pairs of coupled spins can still occur. There is a higher probability to select coupling partners. But their contribution is reduced to a small part of the signal. Recoupling artifacts are thus really less intense than main signals. They are detected at a level close to the level of the noise because they are averaged over the whole sample.

The sensitivity enhancement is limited to a factor around 20, which is already a good improvement (Figure 4.9.a). This can be explained by the fact that the closer the frequencies are, the higher the risk of selecting two partners of coupling is. But the high number of irradiation sites allows to minimize the recoupling artifacts meaning that only a part of the modulation is contributing to the real improvement of the signal intensity. However, when the density of frequencies is reaching the limit of frequency differentiation (Figure 4.9.b), the nemo-pulse is not working at its maximum and some recoupling artifacts can reappear in the spectrum.

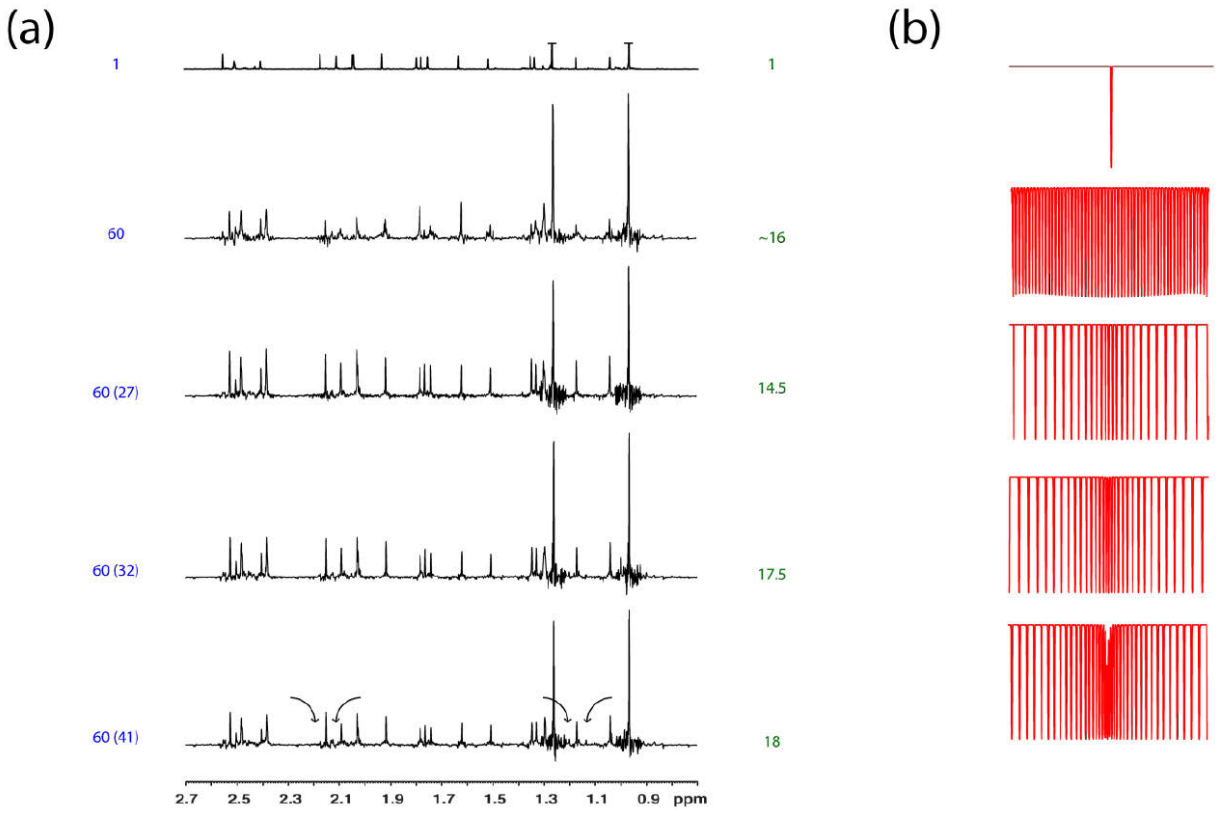

Figure 4.9: (a) 1D decoupled spectra recorded with a 60-nemo-Rsnob of 120 ms. The density of irradiation sites inside the range of 0-10 ppm is progressively increased, from 27 to 41 frequencies. The closer the frequencies are, the higher the probability to simultaneously select coupling partners is. The sensitivity enhancement is limited to 20. (b) Excitation profiles of the 60-nemo-pulses used, only frequencies within the 0-10 ppm range are shown. When the frequency density is too high, lines of the profile can merge reducing the efficiency of the pulse and therefore reintroducing some recoupling artifacts (shown by arrows in the spectrum 60(41)).

4) Applications to 2D experiments

By applying the frequency-modulation of pulses, the sensitivity of experiments using the Zangger-Sterk element is increased by a factor depending on the number of frequencies used to modulate the pulse. It has been shown in this chapter that the frequency-modulation can be applied to experiments leading to 1D homodecoupled proton spectra but also to 2D spectra such as 2D TOCSY or 2D HSQC. Thanks to this artifact free modulation, good quality spectra with a sufficient signal-to-noise ratio can be recorded, even with samples containing small amount of molecules, while keeping a reasonable number of scans and thus without increasing too much the total duration of the acquisition (Figure 4.10).

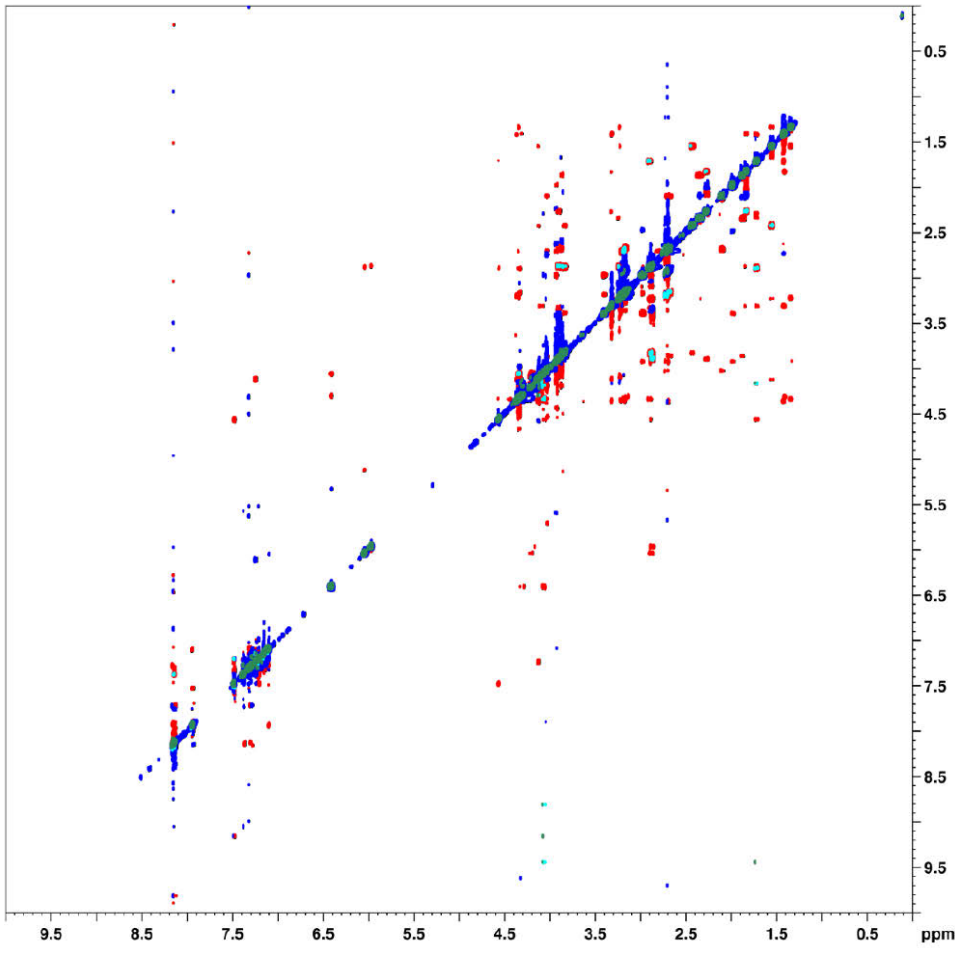

Figure 4.10: 2D BBHD-NOESY spectra of strychnine acquired with a standard Rsnob pulse (in green and light blue) and a frequency-modulated selective pulse (in blue and red). Spectra are shown at the same intensity level. It is clear that the sensitivity of the BBHD-NOESY experiment is greatly enhanced by the use of a frequency-modulated selective pulse.

Moreover, it is possible to apply spectral aliasing to 2D experiments such as 2D TOCSY[12]. Indeed, if the spectral width in F1 is carefully chosen, the spectrum will show signals with a low risk of signal overlap. Thus, a 2D TOCSY spectrum could be quickly recorded with high-resolution and an acceptable sensitivity for experiments using the spatial encoding methodology. With this aliased spectrum, the coupling network of the analysed molecule can still be traced out (Figure 4.11).

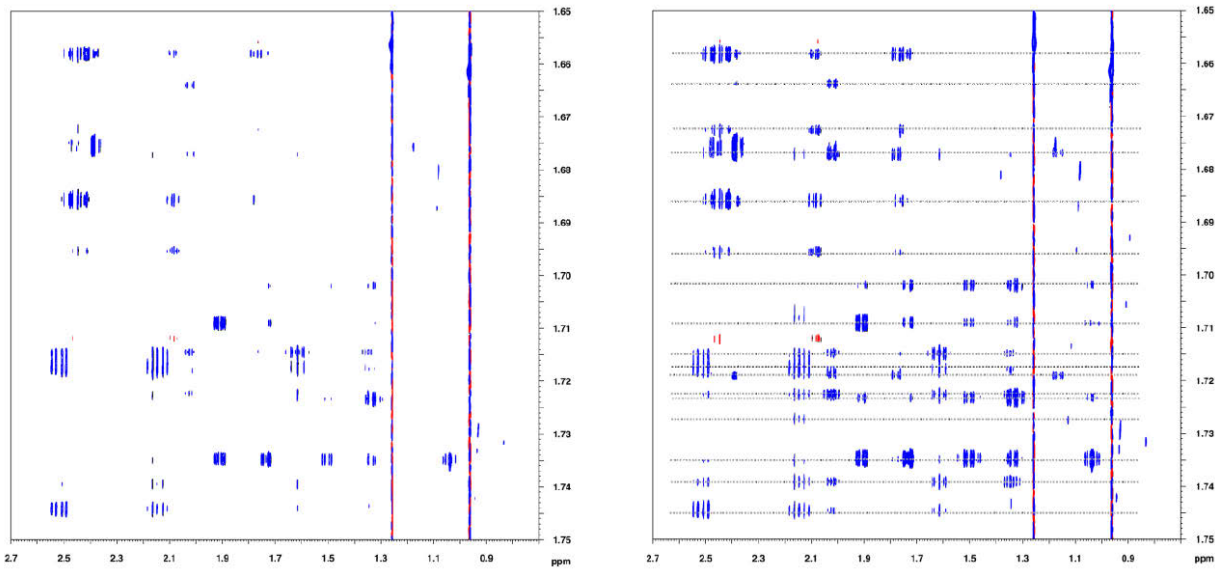

Figure 4.11: 2D BBHD-TOCSY spectra acquired with a F1 spectral width set to 0.1 ppm and a standard Rsnob pulse (left) or a frequency-modulated selective pulse (right). Spectra are shown at the same intensity level. Dotted lines are highlighting spins systems.

5) Experimental conditions

All experiments were performed on a Bruker 500 MHz spectrometer equipped with a DCH helium-cooled probe using a sample containing 20 mg of 4-androstene-3,17-dione dissolved in 700 µL of $CDCl_3$ sealed in a standard 5 mm NMR tube.

The parameters of 2D ZS-DIAG experiments were as follows. The Zangger-Sterk element and z-filters were identical as described in Chapter 2. The Rsnob pulse lasted 30 ms or 120 ms. The spatial encoding gradient was set to cover 10 ppm, i. e. 0.65 G/cm. The spectral window in the indirect dimension was set to 50 Hz and sampled using the States-TPPI quadrature mode with 64 increments and two scans per increment. The spectral window in F2 was set to 10 ppm, with the carrier frequency at 5 ppm, and recorded with 8196 points. The total acquisition time was 7 min and 23 s with a recovery delay of 2 s.

For the **equidistant modulations**, the list of frequencies was determined dividing the spectral window in F2, 10 ppm, by a factor equal to the number of modulations.

For the **non-equidistant modulations**, the first frequency of the list was set at the carrier frequency. The width of the gap was determined by dividing the full F2 width by the number of modulations and again by a factor between 0.25 and 0.75 to adjust the frequency density of the pulse. The increment was equal to a tenth of the gap separating the two first frequencies. The list of frequencies was obtained by adding on one side and substracting on the other side of the carrier frequency the increasingly incremented gap. This gap is minimal at the carrier frequency and increased more and more when reaching the edge of the spectrum. Hereafter is the example for the obtention of a 10 modulated pulse; the gap g is equal to 1 ppm and the increment i to 0.1 ppm.

Number of modulations	10	8	6	4	2	1	3	5	7	9
Incremented gap	g+8i	g+6i	g+4i	g+2i	g	0	g+i	g+3i	g+5i	g+7i
in ppm	1,8	1,6	1,4	1,2	1,0	0,0	-1,1	-1,3	-1,5	-1,7
in Hz	900,23	800,21	700,18	600,16	500,13	0,00	-550,14	-650,17	-750,20	-850,22
Frequency in Hz	6001,04	5100,81	4300,60	3600,42	3000,26	2500,13	1949,99	1299,82	549,62	-300,60
Frequency with regards to O1	3500,91	2600,68	1800,47	1100,29	500,13	0,00	-550,14	-1200,31	-1950,51	-2800,73

The processing of the spectra consisted in the standard double FT without window function. 1D homodecoupled proton spectra were obtained after launching our AU program.

These experiments have to be recorded with a special attention to the stability of the spectrometer. Indeed, a default of regulation of the temperature during acquisition may generate convection of the solution especially when low-viscosity solvents are used. This may severely jeopardize the quality of spectra.

Conclusion

Although, the Nuclear Magnetic Resonance is a method of choice in the fields of chemistry and structural biology, it is not always obvious to extract clear information about the structure of molecules in solution.

Various methods have been developed for decades in order to simplify the interpretation of collected data such as the 2D NMR, the enrichment of molecules with isotopes, visible or not depending the nucleus observed, experiments allowing the analysis of all kinds of spin interactions, direct or indirect, and lately, the development of experiments leading to the removal of some of these interactions like scalar couplings. New methods, always more powerful and successful, are needed; some methods are even rediscovered years after their initial development.

In our case, the development of a new pulse sequence element, called the Zangger-Sterk element, has been a huge breakthrough for the methodology of the homonuclear decoupling. Scalar coupling is the source of important structural information: it allows to trace out the sequence of atoms in a molecule and to determine the bond angles. But it is sometimes necessary to eliminate the contribution of scalar coupling. This new element has been introduced in several pulse sequences such as 2D TOCSY, 2D NOESY, 2D HSQC, … leading to the obtention of spectra where signals have only singlet lineshapes.

This element has also been used to record 1D homodecoupled spectra. Although different methods have been proposed to obtain 1D proton decoupled proton spectra, the method presented in this manuscript established an interesting alternative. Thank to spectral aliasing, a 2D map is quickly recorded without sacrificing the spectral resolution. A simple processing converts this two-dimensional spectrum into a 1D spectrum where scalar coupling information has been eliminated. So, only singlets are recorded leading the simplification of the study of complex mixtures by NMR.

The main aim of our method is to remove the contribution of scalar interactions. But it is also interesting to keep this information in spectra. The presence of complete coupling structures in the direct dimension of 2D BBHD spectra allows the extraction of all coupling constants values leading to a complete characterization of molecules.

The terms “experiments based on Zangger-Sterk element” being synonyms of low sensitivity experiments, a solution has been proposed. The introduction of the frequency-modulation of selective pulses enables an enhancement of the sensitivity of experiments using this decoupling element by one order of magnitude, without any kind of penalty.

The method presented in this manuscript allows us to record one- and two-dimensional spectra with high-resolution, reasonable experimental time and free of recoupling artifacts. This semi-quantitative method is effective and can therefore be applied to other experiments based on spatial encoding.

It is not possible to conclude about our approach without comparing it with other homodecoupling methods. These methods have been developed through years, each one trying to bring a solution to an issue of the previous method. Different parameters have to be evaluated (Table C.1).

First, each experiment leads to the acquisition of good quality spectra with high-resolution but it requires a specific number of scans, t_1 increments and thus different experimental time. It has been shown that, thanks to the spectral aliasing, the acquisition of a 2D ZS-DIAG spectrum takes less than 8 min with 2 scans and 64 increments whereas recording a J-resolved spectrum or an anti z-COSY experiment takes more than 30 min. Our experiment is thus competitive with others, shorter as the pure shift experiment of Morris.

The second parameter to evaluate concerns the aspect of peaks in spectra. Whereas J-resolved experiments lead to very broad signals, linewidths of peaks obtained from other experiments are determined by relaxation when the resolution is sufficient. These experiments can be considered as approximately quantitative. After normalization with a 1D spectrum, 1D homodecoupled spectra recorded with the 2D ZS-DIAG pulse sequence and with or without frequency-modulation present correct integration of peaks.

Last, but not least, important advances have been made about the sensitivity of experiments in the last decade. J-resolved and anti z-COSY spectra are displaying better signal-to-noise ratio than experiments based on the Zangger-Sterk element. Because of spatial encoding, only few spins are contributing to the signals, the sensitivity is therefore low. The use of frequency-modulated selective pulses allows an improvement of signal-to-noise ratio by one order of magnitude. Pure shift and ZS-DIAG experiment are leading to similar 1D proton decoupled proton spectra. Only the processing could make a difference. Recently, Morris and coworkers have published a variation of their pure shift experiment, called PSYCHE[61], where the Zangger-Sterk element is replaced by two concatenated Chirp pulses. This experiment presents advantages of a spectrum recorded with a highly selective pulse (no artifacts of selectivity or recoupling are observable) and the ones of a spectrum recorded with a lower selective pulse (which means a better sensitivity). Thanks to the frequency-modulation of the selective pulse, the 2D ZS-DIAG shows a better signal-to-noise ratio when the nemo is used at its maximal capacity.

	J-resolved	Anti z-COSY	J-spectroscopy	Pure Shift	ZS-DIAG
Experimental time	Long	Long	Long	Short (Few mins)	Short (Few mins)
Linewidth	Broad and distorted	~	Broad	Good	Good
Integration	-	~Quantitative	-	~Quantitative	~Quantitative
Strong coupling	Possible suppression of extra responses	Extra responses	Limited extra responses	Extra responses depending on selectivity	Extra responses depending on selectivity
Sensitivity	++	+ depends on β	Low	Low, enhancement by nemo	Low, enhancement by nemo
Extraction of coupling constants	Yes, direct measurement	Yes, from cross-sections	Yes, direct measurement	No	Yes, automatic

Table C.1: Comparison of important parameters of the different approaches giving access to 1D homodecoupled proton spectra.

Appendix

A- Assignments

A-1 4-androstene-3,17-dione

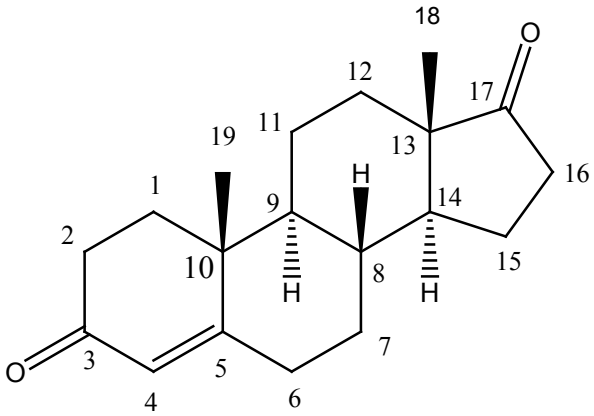

Proton	Multiplicity	Integration	Chemical Shift (ppm)	Coupling Constant (Hz)
1α	ddd	1H	1.676	14.55, 13.47, 4.71
1β	ddd	1H	2.006	13.47, 5.01, 3.19
2α	ddd	1H	2.314	16.94, 4.71, 3.19
2β	ddd	1H	2.386	16.94, 14.55, 5.01
4	s	1H	5.7	-
6α	ddd	1H	2.298	14.77, 4.24, 2.46
6β	ddd	1H	2.397	14.77, 13.90, 5.25
7α	ddd	1H	1.084	13.90, 12.84, 11.76, 4.24
7β	dddd	1H	1.940	12.84, 5.25, 3.65, 2.46
8β	dddd	1H	1.699	11.76, 10.88, 10.69, 3.65
9α	ddd	1H	0.956	12.47, 10.69, 4.24
11α	dddd	1H	1.650	13.79, 4.26, 4.24, 2.77
11β	dddd	1H	1.422	13.79, 13.29, 12.47, 4.16
12α	ddd	1H	1.240	13.29, 13.10, 4.26,
12β	ddd	1H	1.822	13.10, 4.16, 2.77
14α	ddd	1H	1.260	12.79, 10.88, 5.82
15α	ddd	1H	1.943	12.42, 8.98, 5.82
15β	dddd	1H	1.537	12.79, 12.42, 9.15, 8.89
16α	ddd	1H	2.059	19.32, 9.15, 8.98
16β	dd	1H	2.432	19.32, 8.89
18	s	3H	1.177	-
19	s	3H	0.883	-

A-2 Strychnine

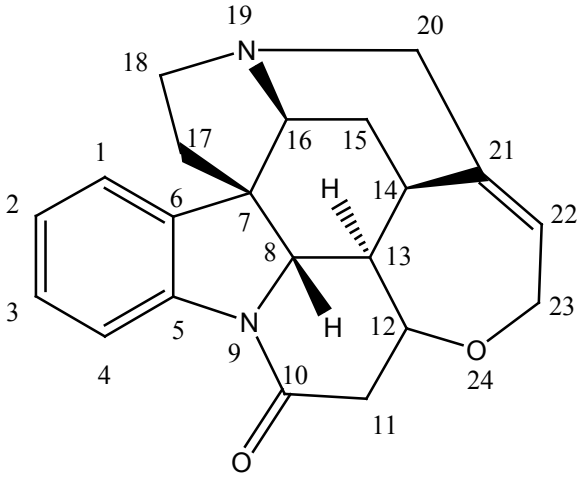

Proton	Multiplicity	Integration	Chemical Shift (ppm)
1	d	1H	7.19
2	t	1H	7.11
3	t	1H	7.27
4	d	1H	8.10
8	d	1H	3.88
11α	dd	1H	3.15
11β	dd	1H	2.68
12	dt	1H	4.30
13	dt	1H	1.30
14	m	1H	3.17
15α	d	1H	1.49
15β	dt	1H	2.38
16	m	1H	4.01
17α	m	1H	1.92
17β	m	1H	1.92
18α	m	1H	1.92
18β	ddd	1H	2.90
20α	d	1H	2.78
20β	dd	1H	3.75
22	dd	1H	5.95
23α	dd	1H	4.08
23β	dd	1H	4.17

B- Pulse sequences of 2D BBHD experiments

B-1 BBHD-TOCSY

```
;bbhd_tocsy.ac

;avance-version (07/12/14)

;Homonuclear Hartmann-Hahn transfer using DIPSI2 sequence for mixing
;phase sensitive
;with homodecoupling during t1 based Zangger-Sterk method
;with spatial encoding
;with ZQ elimination

;"Elimination of zero-quantum interference in two-dimensional NMR spectra'
;Michael J. Thrippleton and James Keeler
;Angew.Chem.Int.Ed. 2003, 42, 3938-3941

#include <Avance.incl>
#include <Delay.incl>
#include <Grad.incl>


"d0=3u"
"p2=p1*2"
"p22=p32"
"p27=500u"
"d27=500u"
"d13=4u"
"d18=d13+p27+d27"
"d11=30m"
"d12=20u"

"in0=inf1/2"

"d7=500u"
"d6=d7"


1 ze
2 d11
3 d1
  d12 pl1:f1
  p1 ph1
  d0
  d13 UNBLKGRAD
  p27:gp3
  d27
  p2 ph6
  d13
  p27:gp3*-1
```

```
  d27
  3u
  100u pl0:f1
  (center (p22:gp4) (p32:sp29 ph7):f1)
  100u pl1:f1
  d13
  p27:gp7*-1
  d27
  d0
  p2 ph5
  3u
  d18
  p1 ph2                    ; mixing time
  5u pl0:f1
  300u gron0
  p11:sp1:f1 ph4
  100u groff
  5u pl10:f1
                            ;DIPSI-2
4 p6*3.556 ph23
  p6*4.556 ph25
  p6*3.222 ph23
  p6*3.167 ph25
  p6*0.333 ph23
  p6*2.722 ph25
  p6*4.167 ph23
  p6*2.944 ph25
  p6*4.111 ph23

  p6*3.556 ph25
  p6*4.556 ph23
  p6*3.222 ph25
  p6*3.167 ph23
  p6*0.333 ph25
  p6*2.722 ph23
  p6*4.167 ph25
  p6*2.944 ph23
  p6*4.111 ph25

  p6*3.556 ph25
  p6*4.556 ph23
  p6*3.222 ph25
  p6*3.167 ph23
  p6*0.333 ph25
  p6*2.722 ph23
  p6*4.167 ph25
  p6*2.944 ph23
  p6*4.111 ph25

  p6*3.556 ph23
  p6*4.556 ph25
  p6*3.222 ph23
  p6*3.167 ph25
  p6*0.333 ph23
  p6*2.722 ph25
```

```
  p6*4.167 ph23
  p6*2.944 ph25
  p6*4.111 ph23
  lo to 4 times l1
                              ;end of DIPSI-2
  5u pl0:f1
  d6 gron5
  300u gron0
  p12:sp2:f1 ph4
  100u groff
  d7
  5u pl1:f1
  d13 BLKGRAD
  p1 ph3                      ;end of mixing time

  go=2 ph31

  d11 mc #0 to 2 F1PH (ip1, id0)
exit

ph1=0 2          ;hard pulse 90
ph2=0 0          ;hard pulse 90 before DIPSI2
ph3=0 0          ;hard pulse 90 after DIPSI2
ph4=0            ;sweep pulse
ph5=0 0          ;hard pulse 180
ph6=0 0          ;hard pulse 180
ph7=0 0          ;selective pulse 180
ph23=3           ;pulse in DIPSI2
ph25=1           ;pulse in DIPSI2
ph31=0 2

;pl0 : zero power (120 dB)
;pl1 : zero power (120 dB)
;pl2 : high power
;pl10: DIPSI-2 power
;p1  : 90 degree high power pulse
;p6  : 90 degree low power pulse
;p11 : duration of first sweep
;p12 : duration of second sweep
;d0  : incremented delay
;d1  : relaxation delay
;d6  : duration of homospoil
;d7  : recovery delay
;d9  : TOCSY mixing time
;sp1 : strength for first sweep
;sp2 : strength for second sweep
;gpz0: gradient strength for ZQ suppression
;gpz5: gradient strength for homospoil
;l1  : loop for DIPSI cycle
;in0 : 1/(2 * SW) = DW
;nd0 : 2
;NS  : 2 * n
;DS  : 8
;td1 : number of t1 increments
;MC2 : TPPI, States-TPPI, States
```

B-2 BBHD-NOESY

```
;noesygpzs.ac

;2D homonuclear correlation via dipolar coupling
;dipolar coupling may be due to noe or chemical exchange
;with gradient/rf spoil pulse in  mixing time
;with homodecoupling during t1 based on zg_gsel_1.ac
;with spatial encoding
;with zero-quantum elimination based on Thrippleton-Keeler's method

;M. J. Thrippleton & J. Keeler
;Angew. Chem. Int. Ed. 42, 3938-3941 (2003)

;$CLASS=HighRes
;$DIM=2D
;$TYPE=
;$SUBTYPE=
;$COMMENT=

#include <Avance.incl>
#include <Grad.incl>
#include <Delay.incl>

"p2=p1*2"
"p22=p30"
"p27=500u"
"p31=5m"

"d11=30m"
"d12=20u"
"d13=4u"
"d16=200u"
"d18=d13+p27+d27"
"d27=500u"

"in0=inf1/2"

"d0=in0/4-p1*2/3.1416"

"DELTA=in0/4-p1*2/3.1416"
"DELTA1=d8*0.5-p16-d16"
"DELTA2=d8*0.5-p16*2-d16*3-p32-34u"

"acqt0=-p1*2/3.1416"

1 ze
2 d11
3 d12 pl1:f1
  d1
  50u UNBLKGRAD
  p1 ph1
  d0
  d13
  p27:gp3
```

```
  d27
  p2 ph6
  d13
  p27:gp3*-1
  d27
  DELTA
  d18
  100u pl0:f1
  (center (p22:gp4) (p30:sp30 ph7):f1)
  100u pl1:f1
  d13
  p27:gp5*-1
  d27
  d0
  d18
  p2 ph5
  d18
  DELTA
  p1 ph2
  DELTA1
  p16:gp2
  d16
  3u
  p2 ph8
  3u
  p16:gp2*-1
  d16
  DELTA2
  10u gron0
  (p32:sp29 ph4):f1
  20u groff
  d16 pl1:f1
  p31:gp6
  d16
  4u BLKGRAD
  p1 ph3
  go=2 ph31
  d11 mc #0 to 2 F1PH(ip1, id0)
exit

ph1=0 2         ;first pulse 90
ph2=0 0 2 2     ;second pulse 90
ph3=0           ;third pulse 90
ph4=0           ;z-filter
ph5=0           ;second pulse 180 (ZS)
ph6=0           ;first pulse 180 (ZS)
ph7=0           ;selective pulse 180 (ZS)
ph8=0           ;pulse 180 in the middle of mixing time
ph31=0 2 2 0

;pl1 : f1 channel - power level for pulse (default)
;sp29 : f1 channel - power for adiabatic shaped pulse (Chirp for z-filter)
;sp30 : f1 channel - power for selective pulse (Rsnob for ZS)
;p1 : f1 channel - 90 degree high power pulse
;p2 : f1 channel - 180 degree high power pulse
```

```
;p16 : homospoil/gradient pulse
;p22 : f1 channel - power for spatial encoding gradient
;p30 : f1 channel - 180 degree selective pulse (Rsnob)
;p32 : shaped pulse (chirp)
;d1 : relaxation delay ; 1-5 * T1
;d8 : mixing time
;d11 : delay for disk I/O
;d12 : delay for power switching
;d16 : delay for homospoil/gradient recovery
;inf1 : 1/SW = 2 * DW
;in0 : 1/SW = 2 * DW
;NS : 2 * n
;DS : 4
;td1 : number of experiments
;FnMODE : States-TPPI, TPPI, States or QSEQ

;use gradient ratio :   gp 0 : gp 1
;                       ca. 10 :   40

;for z-only gradients :
;gpz0 : ca. 10%
;gpz6 : 40%

;use gradient files :
;gpnam1 : SMSQ10.100
;gpnam2 : SMSQ10.100
;gpnam3 : SMSQ10.100
;gpnam4 : RECT.1
;gpnam5 : SMSQ10.100
;gpnam6 : SMSQ10.100

;for sweepwidth of adiabatic shape and ajusting gpz0
;see supplementary material of M. J. Thrippleton & J. Keeler
;Angew. Chem. Int. Ed. 42, 3938-3941 (2003)
```

B-3 BBHD-COSY

```
;mjt_zcosy_hd4.ac
;based on zcosy of Keeler&Thrippleton
;2D homonuclear shift correlation
;with zero-quantum elimination
;with homodecoupling during t1
;with spatial encoding
;
;$CLASS=HighRes
;$DIM=2D
;$TYPE=
;$SUBTYPE=
;$COMMENT=


#include <Avance.incl>
#include <Grad.incl>
#include <Delay.incl>

"in0=inf1/2"
"p3=1.0*p1"

"d5=500u"
"p2=p1*2"
"p22=p32"
"p27=500u"
"d27=500u"
"d13=4u"
"d12=20u"
"d18=d13+p27+d27"
"DELTA=1s/2*(cnst1*2)"

1 ze
2 d1
  d12 pl1:f1
  50u UNBLKGRAD
3 p1 ph1
  d0

  d13
  p27:gp3
  d27
  p2 ph6
  d13
  p27:gp3*-1
  d27
  100u pl0:f1
  (center (p22:gp4) (p32:sp29 ph7):f1)
  100u pl1:f1
  d13
  p27:gp7*-1
  d27
  d0
  p3 ph2
```

```
  3u pl0:f1
  300u gron0
  p11:sp1:f1 ph4
  d5 gron5
  100u groff
  50u BLKGRAD
  d12 pl1:f1

  p3 ph3
  DELTA
  p2 ph5
  DELTA
  p3 ph3

  go=2 ph31

  d1 mc #0 to 2 F1PH(ip1,id0)
exit


ph1=0 2
ph2=0
ph3=0
ph4=0
ph5=0 0             ;hard pulse 180
ph6=0 0             ;hard pulse 180
ph7=0 0             ;selective pulse 180
ph31=0 2

;pl0 : zero power (120 dB)
;pl1 : f1 channel - power level for pulse (default)
;p1 : f1 channel -  90 degree high power pulse
;p11 : duration of sweep
;d0 : incremented delay (2D)
;d1 : relaxation delay; 1-5 * T1
;d2 : longitudinal period
;d5 : duration of homospoil
;sp1 : strength of sweep
;gpz0 : gradient strength for ZQ suppression
;gpz5 : gradient strength for homospoil
;inf1: 1/SW = 2 * DW
;in0: 1/(1 * SW) = 2 * DW
;nd0: 1
;NS: 2 * n
;DS: 16
;td1: number of experiments
;FnMODE: States-TPPI, TPPI, States or QSEQ


;Processing

;PHC0(F1): 90
;PHC1(F1): -180
;FCOR(F1): 1
```

C- Pulse sequences for 1D BBHD experiments

C-1 2D ZS-DIAG

```
;djres.ac
;based on mjt_tocsyg_gd_hd

;avance-version (07/12/14)

;Homonuclear Hartmann-Hahn transfer using DIPSI2 sequence for mixing
;phase sensitive
;with homodecoupling during t1 based on zg_gsel_1.ac
;with spatial encoding
;with ZQ elimination

;"Elimination of zero-quantum interference in two-dimensional NMR spectra'
;Michael J. Thrippleton and James Keeler
;Angew.Chem.Int.Ed. 2003, 42, 3938-3941

#include <Avance.incl>
#include <Delay.incl>
#include <Grad.incl>


"d0=3u"
"p2=p1*2"
"p22=p32"
"p27=500u"
"d27=500u"
"d13=50u"
"d18=d13+p27+d27"
"d11=30m"
"d12=20u"

"in0=inf1/2"

"d7=500u"
"d6=d7"


1 ze
2 d11
3 d12 pl1:f1
  d1
  p1 ph1
  d0
  d13 UNBLKGRAD
  p27:gp3
  d27
  p2 ph6
  d13
  p27:gp3*-1
  d27
  3u
```

```
  100u pl0:f1
  (center (p22:gp4) (p32:sp29 ph7):f1)
  100u pl1:f1
  d13
  p27:gp7*-1
  d27
  d0
  p2 ph5
  d18
  3u
  p1 ph2
  5u pl0:f1
  300u gron0
  p11:sp1:f1 ph4
  100u groff
  d6 gron5
  300u gron0
  p12:sp2:f1 ph4
  100u groff
  d7
  5u  pl1:f1
  d13 BLKGRAD
  p1 ph3

  go=2 ph31

  d11 mc #0 to 2 F1PH (ip1, id0)
exit


ph1=0 2          ;hard pulse 90
ph2=0 0          ;hard pulse 90 before DIPSI2
ph3=0 0          ;hard pulse 90 after DIPSI2
ph4=0            ;sweep pulse
ph5=0 0          ;hard pulse 180
ph6=0 0          ;hard pulse 180
ph7=0 0          ;selective pulse 180
ph23=3           ;pulse in DIPSI2
ph25=1           ;pulse in DIPSI2
ph31=0 2


;pl0 : zero power (120 dB)
;pl1 : zero power (120 dB)
;pl2 : high power
;pl10: DIPSI-2 power
;p1  : 90 degree high power pulse
;p6  : 90 degree low power pulse
;p11 : duration of first sweep
;p12 : duration of second sweep
;d0  : incremented delay
;d1  : relaxation delay
;d6  : duration of homospoil
;d7  : recovery delay
;d9  : TOCSY mixing time
```

;sp1 : strength for first sweep
;sp2 : strength for second sweep
;gpz0: gradient strength for ZQ suppression
;gpz5: gradient strength for homospoil
;l1 : loop for DIPSI cycle
;in0 : 1/(2 * SW) = DW
;nd0 : 2
;NS : 2 * n
;DS : 8
;td1 : number of t_1 increments
;MC2 : States-TPPI

Bibliography

1) F. Bloch, W. W. Hansen, M. Packard, *Phys. Rev*. 69 (**1946**) 127.
2) E. M. Purcell, H. C. Torry, R. V. Pound, *Phys. Rev*. 69 (**1946**) 37-38.
3) R. N. Bracewell, *The Fourier Transform and its applications*, McGRaw-Hill (**1965**).
4) M. Karplus, *J. Am. Chem. Soc*. 85 (**1963**) 2870-2871.
5) E. L. Hahn, *Phys. Rev*. 80 (**1950**) 580-594.
6) K. Zangger, H. Sterk, *J. Magn. Reson*. 124 (**1997**) 486-489.
7) M. Nilsson, G. A. Morris, *Chem. Commun* (**2007**) 933-935.
8) N. Giraud, L. Béguin, J. Courtieu, D. Merlet, *Angew. Chem. Int. Ed*. 49 (**2010**) 3481-3484.
9) N. Giraud, M. Joos, J. Courtieu, D. Merlet, *Magn. Reson. Chem*, 47 (**2009**) 300-306.
10) E. E. Kwan, S. G. Huang, Eur. *J. Org. Chem.* (**2008**) 2671-2688.
11) W. P. Aue, E. Bartholdi, R. R. Ernst*, J. Chem Phys.* 64 (**1976**) 2229-2246.
12) A. Cotte, M. Foroozandeh, D. Jeannerat, *CHIMIA* 66 (**2012**) 764-769.
13) L. Braunschweiler, R. R. Ernst*, J. Magn. Reson*. 53 (**1983**) 521-528.
14) M. H. Levitt, R. Freeman, T. Frenkiel, *J. Magn. Reson*. 47 (**1982**) 328-330.
15) A. J. Shaka, C. J. Lee, A. Pines, *J. Magn. Reson*. 77 (**1988**) 274-293.
16) N. E. Jacobsen, *NMR spectroscopy explained: simplified theory, applications and examples for organic chemistry and structural biology*, John Wiley & Sons (**2007**).
17) M. J. Thrippleton, J. Keeler, *Angew. Chem. Int. Ed*. 42 (**2003**) 3938-3941.
18) J.-M. Böhlen, M. Rey, G. Bodenhausen, *J. Magn. Reson*. 84 (**1989**) 191-197.
19) G. A. Morris, J. A. Aguilar, R. Evans, S. Haiber, M. Nilsson*, J. Am. Chem. Soc*. 132 (**2010**) 12770-12772.
20) J. J. Koivisto, *Chem. Commun*. 49 (**2013**) 96-98.
21) R. Brüschweiler, F. L. Zhang*, J. Chem. Phys*. 120 (**2004**) 5253-5260.
22) R. Brüschweiler, *J. Chem. Phys*. 121 (**2004**) 409-414.
23) D. A. Snyder, R. Brüschweiler, *Multidimensional correlation spectroscopy by covariance NMR in Encyclopedia* of R. K. Harris, R. E. Wasylishen, Eds., John Wiley & Sons, Chichester (**2009**).
24) A. Kumar, R. R. Ernst, K. Wütrich, *Biochem. Biophys. Res. Commun*. 95 (**1980**) 1-6.
25) A. W. Overhauser, *Phys. Rev*. 92 (**1953**) 411-415.
26) J. A. Aguilar, A. A. Colbourne, J. Cassani, M. Nilsson, G. A. Morris, *Angew. Chem. Int. Ed.* 51 (**2012**) 6460-6463.
27) J. A. Aguilar, A. A. Colbourne, J. Cassani, M. Nilsson, G. A. Morris, *Angew. Chem. Int. Ed.* 51 (**2012**) 6460-6463.
28) W. P. Aue, J. Karhan, R. R. Ernst*, J. Chem. Phys*. 64 (**1976**) 4226-4227.
29) J. R. Garbow, D. P. Weitekamp, A. Pines, *Chem. Phys. Lett*. 93 (**1982**) 504-509.
30) M. Woodley, R. Freeman, *J. Magn. Res. Ser. A* 109 (**1994**) 103-112.
31) S. Simova, H. Sengstschmid, R. Freeman, *J. Magn. Reson.* 124 (**1997**) 104-121.
32) P. Mutzenhardt, F. Guenneau, D. Canet, *J. Magn. Reson*. 141 (**1999**) 312-321.
33) A. J. Pell, J. Keeler, *J. Magn. Reson*. 189 (**2007**) 293-299.
34) A. J. Pell, R. A. E. Edden, J. Keeler, *Magn. Reson. Chem*. 45 (**2007**) 296-316.
35) J. A. Aguilar, S. Faulkner, M. Nilsson, G. A Morris, *Angew. Chem. Int. Ed*. 49 (**2010**) 3901-3903.
36) M. K. Denk, *CHEM 2070 Structure and Spectroscopy*, University of Guelph (**2005**)

37) T. W. Claridge, *High-resolution NMR techniques in organic chemistry*, Tetrahedron Organic Chemistry, Vol. 27, second edition, Elsevier.
38) M. J. Thrippleton, R. A. E. Edden, J. Keeler*, J. Magn. Reson*. 174 (**2005**) 97-109.
39) M. A. Smith, H. Hu, A. J. Shaka, *J. Magn. Reson*. 151 (**2001**) 269-283.
40) J. A. Aguilar, M. Nilsson, G. A. Morris, *Angew. Chem. Int. Ed*. 50 (**2011**) 9716-9717.
41) A. Lupulescu, G. L. Olsen, L. Frydman, *J. Magn. Reson*. 218 (**2012**) 141-146.
42) A. Cotte, D. Jeannerat, *Angew. Chem. Int. Ed.* 54 (**2015**) 6016-6018.
43) TopSpin, Bruker.
44) P. Huber, G. Bodenhausen, *J. Magn. Reson. Ser. A* 102 (**1993**) 81-89.
45) D. Jeannerat, G. Bodenhausen, *J. Magn. Reson*. 141 (**1999**) 133-140.
46) D. Jeannerat*, J. Magn. Reson.* 186 (**2007**) 112-122.
47) U. Eggenberger, P. Pfländer, G. Bodenhausen, *J. Magn. Reson*. 77 (**1988**) 192-196.
48) P. Schmieder, S. Zimmer, H. Kessler, *Magn. Reson. Chem*. 29 (**1991**) 375-380.
49) G. Bayiha Ba Njock, D. E. Pegnyemb, T. A. Bartholomeusz, P. Christen, B. Vitorge, J.-M. Nuzillard, R. Shivapurkar, M. Foroozandeh, D. Jeannerat, *CHIMIA* 64 (**2010**) 235-240.
50) D. Jeannerat, *Encyclopedia of Magnetic Resonance*, G. A. Morris (editor) John Wiley & Sons (**2011**)
51) G. Bodenhausen, D. J. Ruben, *Chem. Phys. Lett* 69 (**1980**) 185-189.
52) B. Vitorge, S. Bieri, M. Humam, P. Christen, K. Hostettmann, O. Muñoz, S. Loss, D. Jeannerat, *Chem. Commun* (**2009**) 950-952.
53) C. Bauer, R. Freeman, T. Frenkiel, J. Keeler, A. J. Shaka, *J. Magn. Reson*. 58 (**1984**) 442-457.
54) N. Helge-Meyer, K. Zangger, *Angew. Chem. Int. Ed*. 52 (**2013**) 7143-7146.
55) L. Castañar, P. Nolis, A. Virgili, T. Parella*, Chem. Eur. J*. 19 (**2013**) 15472-
56) L. Emsley, G. Bodenhausen*, J. Magn. Reson*. 97 (**1992**) 135-148.
57) H. Geen, R. Freeman, *J. Magn. Reson*. 93 (**1991**) 93-141.
58) Ē. Kupče, J. Boyd, I. D. Campbell, *J. Magn. Reson. Ser. B* 106 (**1995**) 300-303.
59) M. Foroozandeh, P. Giraudeau, D. Jeannerat, *Chem. Phys. Chem*. 12 (**2011**) 2409-2411.
60) F. Foroozandeh, P. Giraudeau, D. Jeannerat, *Magn. Reson. Chem*. 51 (**2013**) 808-814.
61) M. Foroozandeh, R. W. Adams, N. J. Meharry, D. Jeannerat, N. Nilsson, G. A. Morris, Angew. Chem. Int. Ed. 53 (**2014**) 6990-6992.